

**EVALUATION OF PHARMACOSTATISTICAL MODEL
COMPONENTS USING A NONLINEAR MIXED-EFFECT
APPROACH**

A DISSERTATION SUBMITTED TO THE FACULTY OF THE UNIVERSITY
OF MINNESOTA BY

MUTAZ JABER

IN PARTIAL FULFILLMENT OF THE REQUIREMENTS FOR THE DEGREE
OF DOCTOR OF PHILOSOPHY

Advisor: Dr. Richard C. Brundage
Co-advisor: Dr. Mahmoud Al-Kofahi

December 2022

Mutaz M. Jaber © 2022

Acknowledgment

Many have influenced my thinking in pharmacometrics during my journey and I would like to start with my advisor and friend, Dr. Richard C. Brundage. Dick has made an enormous contribution to my thinking and skills on both the scientific and personal level. He believed in me when almost no one did. His patience with me was enormous during discussions and all the time. I was lucky not only because I got the honor to be his student but also to be the last one. I'm thankful our path crossed. I wish you (Dick) and Nancy a wonderful and fun retirement. I would like to thank Dr. Mahmoud Al-Kofahi, my co-advisor, for his endless support and motivation during my studies. Mahmoud's input was exceptional on a different levels. I'd also like to thank Dr. Kyriakie Sarafoglou for her contribution to my skills and all the work we did together. She influenced my thinking on the clinical side and motivated the implementation of pharmacometric methods in clinical practice.

I'm very thankful to my committee member, Dr. Angela Birnbaum for her feedback and the fun discussion in her classes, Dr. Kyle T. Baron for his inputs and the development of the invaluable tool "mrgsolve" that is used extensively in this work, and Dr. Tiefeng Jiang for his contribution to my statistical background. I was lucky to take statistics courses with him.

I'm thankful for my family: Mom, Dana Obeidat, Dad, Mohammad B. Jaber, and

my brothers, Muhannad, Majed and Malek for their unconditional support during my Ph.D. studying abroad. I'm also thankful for my life partner, love and wife Batool for her endless support during this period and our baby boy, Sinan. I'm also thankful for my in-laws, Khaled Obeidat and Rawdah Obeidat for their support and motivation during my studies. Nancy Blessing was always there for support and love and a huge thanks goes to her.

I would like to thank Dr. Malek Okour, who told me about pharmacometrics and introduced me to the field. Also, Dr. Mera Ababneh for her guidance during my PharmD and post-PharmD. Many thanks go to my co-authors and friends, Dr. Takuto Takahashi, Dr. Burrhan Yaman, Dr. Mark N. Kristen, Dr. Pam Jacobson, Dr. Shen Cheng, Abderahman Saqr, and many others. Special thanks go to the whole department of Experimental and Clinical pharmacology for everything...

Dedication

To my parents, Dana Obeidat and Mohammad B. Jaber

To my love and partner, Batool and our baby Sinan

For my beloved family; Muhannad, Majed, and Malek

Abstract

A nonlinear mixed-effect population pharmacokinetic (PPK) approach is a pharmacostatistical concept used to study pharmacokinetic (PK) and/or pharmacodynamic (PD) variability at the population level. PPK quantifies the typical PK and/or PD population parameters values (central tendency measures) and the magnitude of variability among individuals (measures of dispersion). Types of data used in PPK are collected from either a well-controlled clinical trial or routine care (observational studies). In terms of samples collected, this method can handle dense and limited (sparse) data given a sufficient number of subjects, and assuming the recorded samples were withdrawn at times to allow PK/PD parameter estimation. In a nonlinear mixed-effects modeling (NLMEM) approach of PK and PD data, two levels of random effects are generally modeled: between-subject variability (BSV) and residual unexplained variability (RUV). In the study described in chapter 3, the goal was to investigate the extent to which PK and RUV model misspecification, errors in recording dosing and sampling times, and variability in drug content uniformity contribute to the estimated magnitude of RUV and PK parameter bias. We found the contribution of dose and dosing time misspecifications have negligible effects on RUV but result in higher bias in PK parameter estimates. Inaccurate documentation of sampling time results in biased RUV and increases with the magnitude of perturbations. Combined perturbation scenarios in the studied sources will propagate the variability and accumulate in RUV magnitude and result in bias of PK parameter

estimates. This work provides insight into the potential contributions of many factors that comprise RUV and bias in PK parameters.

In chapter 4 we describe a study designed to evaluate the impact of deviations in recorded time in NLMEM settings. An assumption that clinical data are recorded without any error is optimistically made. While some study personnel will record the actual times when there is a deviation others record the nominal time. Therefore, we investigate including an additional random effect on the independent variable time and quantitate the bias in estimated parameters; and determine the sensitivity of the magnitude of deviation between actual and recorded times on parameter estimation bias. Hence, we report that adding a random quantity to the recorded time will lead to reducing the bias and imprecision in PK estimates compared to assuming the recorded time is absolute.

In chapter 5, we take a closer look at diagnosing pharmacostatistical models. Specifically, both traditional weighted residuals (WRES) and conditional weighted residuals (CWRES) are common metrics to graphically evaluate model acceptability in population analyses. Limited by the lower limit of quantification (LLOQ) of analytical techniques, it is not uncommon to have concentrations reported as below the LLOQ (BLQ) in PK studies. Although various approaches have been proposed to accommodate BLQ data, M3 method currently appears to be most common. That being said, NONMEM excluded the calculation of all WRES/CWRES for each subject with BLQ data due to a concern that the residuals for that subject might be biased. Our aim was to conduct a simulation study to investigate the extent to which weighted residual calculations in subjects having some BLQ data might be biased when using the M3 method. We conclude that bias in CWRES and WRES can be detected but is small and unlikely to impact decisions made based on weighted residual-based diagnostic plots when the M3 method with MDVRES is performed to

accommodate BLQ observations in the scenarios we studied.

Another important pharmacostatistical component is structural PK model, and in chapter 6, we evaluate absorption models. Absorption processes are complex but rarely have sufficient data to capture parameters of a mechanistic model. Typically, a single absorption model (e.g., first-order, mixed-order, lag, or distributive delay model), is assumed to apply to all individuals with the expectation that random effects will accommodate individual differences. However, distinct absorption profiles may coexist in a given dataset. Thus, we propose that individualized absorption models should be considered when multiple absorption profiles are evident in a population analysis.

Machine learning is gaining wider attention in clinical pharmacology and pharmacometrics as computational capacity increases. Methods for machine learning use statistical algorithms and methods that are capable of doing automated learning from existing data to uncover patterns. Therefore, we wish to evaluate an exercise in chapter 7 to train a deep neural network to automatically prespecify absorption models.

Finally, the knowledge provided in this thesis will bring us closer to use pharmacometrics methodology to individualize patient care by understanding the sources of variability and embrace model individualization concept.

Contents

Acknowledgment	i
Dedication	iii
Abstract	iv
1 Introduction	1
1.1 Overview	2
1.2 Estimation methods	7
1.3 Thesis Remarks	11
2 Sources of Variability	17
2.1 Overview	17
2.2 Assay Variability	18
2.3 Manufacturing	19
2.4 Dosing times	20
2.5 Sampling times	21
2.6 Model misspecification	22
3 Investigating The Contribution of Residual Unexplained Variability Components in a Nonlinear-Mixed Effect Approach	23
3.1 Overview	24

3.2	Introduction	25
3.3	Methods	26
3.3.1	Literature review	26
3.3.2	Pharmacostatistical model	27
3.3.3	Sample collection design	27
3.3.4	Perturbations to the Model	27
3.3.5	Software and Evaluation	29
3.4	Results	31
3.4.1	Literature Review	31
3.4.2	MP	31
3.4.3	CTEP	32
3.4.4	TEP	32
3.4.5	Combined perturbations	32
3.5	Discussion	34
3.6	Tables	39
3.7	Figures	41
4	The impact of unrecorded time deviation in nonlinear mixed-effect analyses	47
4.1	Overview	48
4.2	Introduction	49
4.3	Methods	50
4.3.1	Notation	50
4.3.2	Simulation methods	52
4.4	Results	56
4.4.1	Part I: Berkson error (κ) model	56
4.4.2	Part II: Magnitude difference between recorded and actual time	57
4.5	Discussion	58

4.6	Tables	62
4.7	Figures	64
5	Evaluation of bias in weighted residual calculations when handling below the limit of quantification data	73
5.1	Overview	74
5.2	Perspective	75
5.3	Conclusions	80
5.4	Tables	81
5.5	Figures	82
6	Individualized Absorption Models in Population Pharmacokinetic Analyses	83
6.1	Overview	84
6.2	Perspective	85
6.3	Conclusion	90
6.4	Tables	91
6.5	Figures	92
7	Application of Deep Neural Networks in Pharmacokinetic Analysis	93
7.1	Overview	94
7.2	Introduction	95
7.3	Methods	98
7.3.1	Observed Data and Visual Assignment	98
7.3.2	Estimation of Pharmacokinetic Model	98
7.3.3	Simulation of Training Profiles	99
7.3.4	Deep Learning Algorithm	100
7.3.5	Evaluation	101
7.4	Results	101

7.5	Discussion	102
7.6	Conclusions	105
7.7	Tables	106
7.8	Figures	109
8	Summary and final thoughts	114
	References	118
	Appendix	129
A	Investigating The Contribution of Residual Unexplained Variability Components in a Nonlinear-Mixed Effect Approach	130
A.1	Literature review	131
B	The impact of unrecorded time deviation in nonlinear mixed-effect analyses	166
C	Evaluation of Bias in Weighted Residual Calculations	251
D	Individualized absorption models	260
E	Application of Deep Neural Networks in Pharmacokinetic Analysis	262

List of Tables

3.1	Pharmacokinetic parameter values with corresponding between-subject variability reported as coefficient of variation.	39
3.2	Median RUV magnitude for combined sources based on different sample collection designs.	40
4.1	Pharmacokinetic parameter values with corresponding between-subject variability reported as coefficient of variation.	62
4.2	True simulated deviation and estimated deviation using kappa model stratified on the affected percentage in the experimental unit.	63
5.1	Bias calculations on population and individual levels	81
6.1	Comparison of key analysis metrics	91
7.1	Population-level pharmacokinetic estimates and the between-subject variability (% CV) from the re-analysis used in the simulation.	106
7.2	Collection of data with associated overall accuracy and loss value	107
7.3	Confusion matrix presents the classification of the external patient data	108

List of Figures

3.1	Contribution of Manufacturing perturbation on RUV and PK parameters; left-hand panel present relative bias; right-hand panel present the relative mean squared error. The Greek symbol Omega present between-subject variability magnitude	41
3.2	Contribution of inaccurate documentation of PK sampling time on RUV and PK parameters; left-hand panel present relative bias; right-hand panel present the relative mean squared error. The Greek symbol Omega present between-subject variability magnitude	42
3.3	Contribution of inaccurate documentation of dosing time on RUV and PK parameters; left-hand panel present relative bias; right-hand panel present the relative mean squared error. The Greek symbol Omega present between-subject variability magnitude	43
3.4	Contribution of residual model misspecification on RUV and PK parameters; left-hand panel present absolute bias; right-hand panel present the relative mean squared error. The Greek symbol Omega present between-subject variability magnitude	44
3.5	Contribution of structural PK model misspecification on RUV and PK parameters; left-hand panel present absolute bias; right-hand panel present the relative mean squared error. The Greek symbol Omega present between-subject variability magnitude	45

3.6	Contribution of combined perturbations on RUV and PK parameters; left-hand panel present relative bias; right-hand panel present the relative mean squared error. The Greek symbol Omega present between-subject variability magnitude	46
4.1	Comparison of the relative bias (yaxis) for the null model (red) and kappa model (blue) stratified on study design and percentage of error. Error magnitudes are shown on the x-axis. Panel A present 100% of samples are affected by error; Panel B present 50% of samples are affected by error; Panel C 20% of samples are affected by error. . . .	64
4.2	Comparison of the relative bias (yaxis) for the null model (red) and kappa model (blue) stratified on study design and percentage of error. Error magnitudes are shown on the x-axis. Panel A present 100% of samples are affected by error; Panel B present 50% of samples are affected by error; Panel C 20% of samples are affected by error. . . .	65
4.3	Comparison of the relative bias (yaxis) for the null model (red) and kappa model (blue) stratified on study design and percentage of error. Error magnitudes are shown on the x-axis. Panel A present 100% of samples are affected by error; Panel B present 50% of samples are affected by error; Panel C 20% of samples are affected by error. . . .	66
4.4	Comparison of the relative root mean squared error (yaxis) for the null model (red) and kappa model (blue) stratified on study design and percentage of error. Error magnitudes are shown on the x-axis. Panel A present 100% of samples are affected by error; Panel B present 50% of samples are affected by error; Panel C 20% of samples are affected by error.	67

4.5	Comparison of the relative bias (yaxis) for the null model (red) and kappa model (blue) stratified on study design and percentage of error. Error magnitudes are shown on the x-axis. Panel A present 100% of samples are affected by error; Panel B present 50% of samples are affected by error; Panel C 20% of samples are affected by error. . . .	68
4.6	Comparison of the relative bias (yaxis) for the null model (red) and kappa model (blue) stratified on study design and percentage of error. Error magnitudes are shown on the x-axis. Panel A present 100% of samples are affected by error; Panel B present 50% of samples are affected by error; Panel C 20% of samples are affected by error. . . .	69
4.7	True simulated deviation (x axis) and estimated deviation using kappa model (y -axis) stratified on the affected percentage in the experimental unit and colored by study design.	70
4.8	The magnitude difference (delta) between the actual time and recorded time. Panel (A) present the relative bias; Panel (B) present the root mean squared error.	71
4.9	The magnitude difference (delta) between the actual time and recorded time. Panel (A) present the relative bias; Panel (B) present the root mean squared error.	72
5.1	Weighted residuals for both the SUBSET and the M3 data in both scenarios. Upper panels present CWRES; Lower panels present WRES. Left panels present scenario 1; Right panels present scenario 2. The absolute values of the WRES and CWRES less than 0.1 units in all plots were censored to improve clarity.	82

6.1	Observed concentration-time profile for three representative subjects, each demonstrating a different absorption shape: first order process (green), an Erlang absorption process (red), and shoulder model for simultaneous distributed-delay and first-order processes (blue).	92
7.1	Observed concentration-time profiles for three representative shapes. (red) presents the first-order process; (blue) presents the Erlang process; (black) presents the mixed first-order and Erlang processes.	109
7.2	Pharmacokinetic structural models of the three absorption profiles. (A) First-order absorption; (B) Erlang absorption process; (C) Mixed first-order and Erlang absorption.	110
7.3	Overview of deep neural network algorithm structure.	111
7.4	The output of the developed DNN with three examples from the external cortisol data.	112
7.5	Probability counts for DNN model prediction. Dark blue presents the correct classification; Light blue presents the incorrect classification.	113
A.1	Histogram represent the distribution of proportional error model magnitude (CV%) with vertical red lines being 5th, median and 95th percentiles, respectively	131
C.1	Represent the average of residuals for scenario 1. Panel A represents the SUBSET model, and panel B represents the M3 method.	252
C.2	Represent the average sum of residuals for scenario 2. Panel A represents the SUBSET model, and panel B represents the M3 method.	253
C.3	Average deviation bias evaluation by individual; Scenario 1	253
C.4	Average deviation bias evaluation by individual; Scenario 2	254

D.1 structural Pharmacokinetic models; (a) First-order absorption; (b) Erlang distributive delay; and (c) shoulder models 261

Chapter 1

Introduction

A discussion on the examination of pharmacostatistical model components in a nonlinear mixed-effect approach is presented in this thesis. Chapter 1 and 2 will introduce the reader to the population pharmacokinetic approach, some of the estimation methods used in population approach to obtain parameter estimates, and sources of variability encountered in population analysis. In Chapter 3, we investigate the extent to which pharmacokinetic (PK) and residual unexplained variability (RUV) model misspecification, errors in recording dosing and sampling times, and variability in drug content uniformity contribute to the estimated magnitude of RUV and PK parameter bias. In Chapter 4, we evaluate the impact of including a random quantity to the recorded time and quantitate the bias in estimated parameters in the presence of erroneous collected time data; and examining the magnitude difference between the actual and recorded time that lead to biased pharmacokinetic (PK) estimates. In Chapter 5, the potential bias in weighted residual plots when M3 is applied to handle concentration data reported to be below the limit of quantification (BLQ) is examined, and a simulation study was conducted to evaluate this bias. In Chapter 6, we propose a perspective that individualized absorption models should be considered when multiple absorption profiles are evident in a population analysis.

In Chapter 7, the aim is to demonstrate that a deep neural network (DNN) can be used to prescreen data and assign an individualized absorption model consistent with either a first-order, Erlang, or split-peak process. Finally, Chapter 8 will include closing remarks and takeaway messages from this thesis, in addition to a discussion regarding the potential direction this work can take to understand the implication of variability on PK/PD analyses.

1.1 Overview

A nonlinear mixed-effect population pharmacokinetic (PPK) approach is a pharmacostatistical concept used to study pharmacokinetic (PK) and/or pharmacodynamic (PD) outcomes and variability on population level. More specifically, PPK quantifies the typical PK and/or PD population parameters values (central tendency measures) and the magnitude of variability among individuals (measures of dispersion). One of the common uses of this approach is to describe some of the variability in individual kinetic parameters using patient-specific information, e.g., the relationship between drug clearance and renal function that can be used to facilitate therapeutic benefits i.e., dose optimization. PPK is a well-established quantitative method for drug-development in the FDA (Food and Drug Administration - population pharmacokinetic guidance, 2022) and it is used frequently to guide PK/PD study designs, tailored studies, therapeutic dose optimization, and therapeutic individualization.

Types of data used in PPK are collected from either a well-controlled clinical trial or routine care (observational studies). In terms of samples collected, this method can handle dense and limited (sparse) data given a sufficient number of subjects, and assuming the recorded samples were withdrawn at times to allow PK/PD parameter estimation (see Chapter 3 and 4). PPK has a wide use in clinical and drug develop-

ment settings. It has been applied to study drug dose optimization (Rodríguez-Gascón et al. [2021]), dose selection (Lee et al. [2011]), therapeutic drug monitoring (Wicha et al. [2021]), and facilitate study design (Holford et al. [2010]). It is also important tool in designing pediatric studies and in dose extrapolation from adults to pediatrics (Vinks et al. [2015], Bi et al. [2019]). The latter is important due to challenges of pediatric drug development and the concern regarding safety and efficacy. Moreover, PPK models can be used as predictive tool for clinical trial simulations (Holford et al. [2010]), predicting clinical outcomes using pre-clinical information and as a precursor to collect information that facilitates target identification using quantitative systems pharmacology models.

PPK models can be empirical; describing the observation using a simple structure such as a one- or two-compartment models; or mechanistic models that describe the PK and PD data based on a physiological basis. The selection of such models depends on the purpose. For example, if one is interested in calculating drug clearance for dose optimization and a simple model describes the data adequately then this should be sufficient, however, if one is interested in a surrogate biomarker after given dose, this can necessitate the use of mechanistic PK/PD models.

Different approaches have been used to conduct a population pharmacokinetic analysis; (i) Standard two-stage approach, (ii) Naive pooling, and (iii) nonlinear mixed-effect approach. (i) and (ii) were acceptable approaches to study the PK/PD on population level using noncompartmental analyses or nonlinear regression. Later on, Sheiner conceptualized the use of nonlinear mixed-effects in the late 1970s (Sheiner et al. [1977]) to study population pharmacokinetic typical parameters that relates to biology or alteration in disease status, and the magnitude of variability in individual pharmacokinetic parameters and measurement error. In addition to that, the authors

discussed the advantages and disadvantages of population approach that some will be discussed in depth in this thesis.

Standard two-stage approach

The Standard two-stage (STS) method is conducted using two stages: Individual PK parameter estimation followed by variability assessment. Briefly, PK parameters are estimated for each individual separately in the population followed by summarizing all individual estimates to calculate central tendency measures (e.g. mean, median) and associated variability among individuals (coefficient of variation, standard deviation). Furthermore, the individual parameter estimates can be explored for relationships with some covariate of interest, say, creatinine clearance as a measure of renal function, or a phenotype or genotype as a measure of enzymatic efficiency. However, this method requires dense samples per subject to produce reliable individual parameter estimates and subsequent population parameter estimates. In addition, it was reported (Sheiner [1984]) that STS approach will produce upwardly biased estimate of variability magnitude since each subject's parameter estimates will have error from all sources that will propagate to PK estimates, which will then inflate the variance at the population level.

Naive pooling

Naive pooling (NP) is a straightforward method that requires pooling data from all subjects and estimating parameters as if being withdrawn from the same subject. This method can handle different study designs i.e. dense and sparse with different sampling times. However, while this simplistic method will produce typical PK/PD parameters values, it will ignore the difference in PK parameters among individuals and can produce severely biased estimates (Sheiner 1984).

Nonlinear mixed-effect approach

The nonlinear mixed-effect modeling (NLMEM) approach is currently the gold-standard method to analyze PPK data. NLMEM combines the advantages of both methods mentioned above. It estimates the population typical value and the magnitude of variability, simultaneously. While it is true all data from all individuals are pooled into one dataset, the pharmacostatistical model appropriately distinguishes data from different individuals.

In brief, NLMEM consists of two components: fixed-effects and random-effects. Fixed-effects are the pharmacostatistical component that represents point estimates such as a population-level typical value for a model parameter such as clearance, or a typical relationship between patient-specific information and a PK parameter (covariate effect), for example, the contributing information of creatinine clearance to drug clearance. In addition to fixed effects, there are two levels of random-effects in NLMEM: between-subject variability (BSV) and residual unexplained variability (RUV). The former describes the magnitude of variability in individual PK/PD parameters after accounting for patient specific information (covariates), e.g., body size, age, genotypes, or assessments of renal function.

The normality assumption can help us construct the individual's parameter set for the i^{th} subject, Φ_i , as a function of a fixed-effect parameter θ_{pop} and a random-effect parameter, η_i :

$$\Phi_i = \theta_{pop} + \eta_i \text{ where } \eta_i \sim N(0, \omega^2) \quad (1.1)$$

where η_i represents a random quantity with a mean value of 0 and variance equal to ω^2 . Thus, we define the magnitude of population-level variability for BSV as ω .

Different models are used to describe different assumptions regarding the distribution of individual parameters. The most commonly used are (i) exponential, (ii) proportional or (iii) additive:

$$\Phi_i = \theta_{pop} \cdot \exp(\eta_i) \tag{i}$$

$$\Phi_i = \theta_{pop} + \theta_{pop}\eta_i \tag{ii}$$

$$\Phi_i = \theta_{pop} + \eta_i \tag{iii}$$

Both (i) and (ii) in general assumes proportionality increases and a constant coefficient of variation; (iii) assumes a constant standard deviation. However, based on these models' distributions (iii) will allow the individual parameter estimates to drop below 0 when the modeler conducts simulation studies, which is biologically implausible. Other semiparametric models to describe variation in PK/PD parameters in the presence of outliers and more relaxed assumptions have been discussed in (Pettersson et al. [2009]).

The other level of variability, RUV, quantifies the left-over variability after we take into account structural PK, BSV, and covariate models. The easiest explanation of RUV magnitude is assay variability but other sources might contribute to RUV magnitude such as pharmacostatistical model misspecification, inaccuracies in recorded sample withdrawal, given dose, and dosing times.

The simplest way to present RUV in a model is by adding a random quantity presenting residual error. Letting $f(\Phi_i, x_i, t_{i,j})$ describes a PPK model with x_i dose for the i^{th} subject. Then we can describe the observed data $y_{i,j}$ for the j^{th} point and i^{th} subject as:

$$y_{i,j} = f(\Phi_i, x_i, t_{i,j}) + \epsilon_{i,j} , \epsilon_{i,j} \sim N(0, \sigma^2) \tag{1.2}$$

The term $\epsilon_{i,j}$ has similar distribution properties as $\epsilon_{i,j}$, which we assume a symmetrical distribution with mean of 0 and variance of σ^2 and σ represents the magnitude of RUV. We can describe the observation by using similar models discussed for BSV models, either additive, proportional, or exponential models. Based on 351 published models between 2019 and 2021, the proportional error model was the most common (89%), followed by combined error model (10%) and additive error model (1%). This analysis is reported in more detail in Chapter 3. The reason behind the lack of additive error models in PK modeling is due to the assumption of homoscedasticity of variance.

1.2 Estimation methods

PPK analyses are data-driven and we need data to obtain parameter estimates. The estimation process optimizes the parameters of the model to fit the data, usually using maximum likelihood estimation (MLE). MLE is a statistical method used to obtain parameters value that maximizes the likelihood function given an observed quantity.

Let Φ_i represent a collection of individual PK parameters in a hyperparameter space as described above, and let the Ω and Σ represent the full variance matrices of random effects BSV and RUV, respectively. These parameters (thetas, omegas, and sigmas) are being estimated by maximizing the likelihood function, $p(y; \theta_{pop}, \Omega, \Sigma)$ ¹. If we assume that the observed data y is independent vector $y = [y_1, y_2, \dots, y_i]$ for each subject i [$1 \leq i \leq M$], then the likelihood L can be presented as:

$$L(\Phi) = p(y; \theta_{pop}, \Omega, \Sigma) \tag{1.3}$$

¹This reads as the marginal probability of the data that is dependent on the parameters after the semicolon

The marginal distribution $p(y; \theta_{pop}, \Omega, \Sigma)$ can be obtained by integrating the joint distribution between the observed data and individual PK parameters:

$$L(\Phi) = p(y; \theta_{pop}, \Omega, \Sigma) \quad (1.4)$$

$$= \int_{-\infty}^{\infty} p(y, \Phi) d\Phi \quad (1.5)$$

$$= \int_{-\infty}^{\infty} p(y|\Phi)p(\Phi)d\Phi \quad (1.6)$$

$$= \int_{-\infty}^{\infty} \prod_{i=1}^M p(y|\Phi)p(\Phi)d\Phi \quad (1.7)$$

Then we further expand to include all observed time points j [$1 \leq j \leq N$] per individual i :

$$L(\Phi) = \prod_{j=1}^N \int_{-\infty}^{\infty} \prod_{i=1}^M p(y|\Phi)p(\Phi)d\Phi \quad (1.8)$$

Therefore, we integrate over all possible values for Φ . $p(\Phi)$ represents the weights based on prior individual distributions (assumed BSV model) and the right-hand side integrates the weighted average across all possible values of Φ . With that, we aim to maximize the likelihood:

$$\arg \max L(\Phi)$$

Or in a similar aspect, minimize the negative logarithm of the likelihood that will serve as our objective function:

$$\arg \min \{-2 \cdot \ln(L(\Phi))\} = \min \left\{ N + \ln(2\pi) + 2 \sum_{i=1}^M \ln(\sigma^2) + \sum_{i=1}^M \frac{(y_i - f(\Phi_i, x_i, t_i))^2}{\sigma^2} \right\} \quad (1.9)$$

More particularly we try to minimize extended least square (ELS) by dropping the

constant terms in the loglikelihood:

$$\arg \min\{-2 \cdot \ln(L(\Phi))\} = \arg \min\left\{2 \sum_{i=1}^M \ln(\sigma^2) + \sum_{i=1}^M \frac{(y_i - f(\Phi_i, x_i, t_i))^2}{\sigma^2}\right\} \quad (1.10)$$

However, with complex PK/PD models the integral cannot be calculated in a closed-form solution, thus, different algorithms were suggested and implemented in specific programs such as NONMEM, Monolix, nlmixr, and others to numerically perform MLE. Historically, a first-order approximation was used by taking the first-order Taylor series to obtain estimates. Let Γ represent the gradient column vector (partial derivative of objective function with respect to model parameters) then:

$$\Phi_{i0} + \log |\Omega| + \log \left| \Omega^{-1} + \frac{\mathbb{E}(\Gamma_i(\eta)\Gamma_i(\eta)^T) \Big|_{\eta=0}}{4} \right| - \left(\frac{\Gamma_{i0}}{2} \right)^T \left(\Omega^{-1} + \frac{\mathbb{E}(\Gamma_i(\eta)\Gamma_i(\eta)^T) \Big|_{\eta=0}}{4} \right)^{-1} \left(\frac{\Gamma_{i0}}{2} \right) \quad (1.11)$$

This algorithm was further improved to obtain the estimates conditional on the mode of .

$$\hat{\Phi}_i + \log |\Omega| + \hat{\eta}'_i \Omega^{-1} \hat{\eta}_i + \log \left| \Omega^{-1} + \frac{\mathbb{E}(\Gamma_i(\eta)\Gamma_i(\eta)^T)}{4} \right| \quad (1.12)$$

A more flexible method to handle complex PK/PD systems is expectation-maximization (EM) algorithms. EM algorithms are common for maximum likelihood estimation, and it has been shown that using EM the solution will converge to MLE estimate (Allasonnière and Kuhn [2010], Delyon et al. [1999], Kuhn and Lavielle [2004]). These algorithms are used generally used to handle incomplete or missing data in statistics literature and this can be related to PK/PD analysis since the individual parameters Φ_i are not observed. These approaches are beyond the scope of this thesis and readers interested in different sub-algorithms related to EM are advised to visit these references <add EM citations>.

In the current work, attention will be paid to a stochastic version of EM, the

so-called stochastic approximation EM (SAEM). SAEM shares with other EM algorithms the expectation or the exploratory phase (E-step) and maximization or sampling phase (M-step). E-step consists of simulation and integration steps. In the simulation step, we draw K samples from the conditional distribution $p(\Phi|y)$ followed by evaluating the quantity, Q for the k^{th} iteration:

$$Q_k(\theta_{pop}, \Omega, \Sigma) = \mathbb{E}(\log p(y, \Phi)|y; \theta_{pop,k-1}, \Omega_{k-1}, \Sigma_{k-1}) \quad (1.13)$$

Where \mathbb{E} represent the expectation.

Then by stochastic approximation, the quantity $Q_{k-1}(\theta_{pop}, \Omega, \Sigma)$ is updated according to:

$$Q_k = Q_{k-1} + \gamma_k (\log p(y, \Phi^k; \theta_{pop}, \Omega, \Sigma) - Q_{k-1}) \quad (1.14)$$

Where γ_k is a sequence of positive numbers $[1, \dots, \infty)$ ² decreasing by $(1/k)$. The final step, is M-step that we update θ_k based on:

$$\theta_k = \arg \max Q_k(\theta_{pop}, \Omega, \Sigma) \quad (1.15)$$

Where θ_k is a vector of estimated parameters. For more information regarding SAEM convergence criteria see (Delyon et al. [1999]). Comparison among different algorithms has been discussed in the literature. Sukarnjanaset et al. (Sukarnjanaset et al. [2018]) compared the performance of FOCE and SAEM using one- and two-compartment model with different sample collection designs, and they did not conclude a significant difference in the overall accuracy and precision, but they noted a significant difference in FOCE being faster than SAEM. Johansson et. al. (Johansson et al. [2014]) evaluated the performance among different algorithms and reported that FOCE and SAEM had closely related values of bias and imprecision, but FOCE had a

²convergence requires that $\sum_{k=1}^{\infty} \gamma_k = \infty$ and $\sum_{k=1}^{\infty} \gamma_k^2 < \infty$. See more in Delyon et al. [1999]

shorter run time. In a different study by Bach et. al (Bach 2021), they compared the performance of FOCE versus SAEM with simple and complex PK/PD models and concluded a superior performance for SAEM compared to FOCE in terms of precision and convergence. However, with simple models, FOCE had the advantage of faster run times.

1.3 Thesis Remarks

Given the decades of published methods and improvements in pharmacometrics methodology, one might think that all details are well worked out, but its not the case yet and we should embrace the discussions in this thesis. An important discussion is the assumption made when we enter PK data into a model that most measurements are absolute or with ignorable certainty. That is rarely the case even in a well-controlled clinical trial. Probably the easiest variability to understand is that due to the imprecision of our analytical techniques. Other sources include errors in recording dosing and sampling times, dose manufacturing variability, and pharmacostatistical model misspecification. Estimates of RUV are reported in relevant scientific publications and provided to the FDA when submitting results from model-informed drug development analyses. These estimates of unexplained variability in observations vary widely and range from 5% up to 80%. Few analyses addressing the typical sources of noise have been conducted (Alihodzic et al. [2020], Choi et al. [2013], Karlsson et al. [1998]), and few thoughts have been expressed regarding their implications in the design of clinical pharmacology studies (Sun et al. [1996]). Importantly, RUV is critical to the goal of individualized dosing and can simply be thought of as the deviation from perfect prediction. The basic principle is that the greater the variability we cannot explain, the further we are from the reality of precisely dosing each individual. In chapter 3 we explore the relative impact of these

sources of variability on RUV, how they propagate through the models used in drug development into the RUV, and how this variability adversely impacts the model parameters being estimated. For example, if it is found that the magnitude of analytical measurement variability has little impact on the RUV or model parameter estimates, then there would be little motivation to spend resources on developing more accurate measurement methods. Alternatively, if it is found that errors in recording sampling times greatly increase RUV, one might want to spend more time working with clinical research staff in the importance of recording exact times of blood draws, even when they might deviate only slightly from the nominal protocol-specified times. This work will provide valuable information that can be used to understand the reasons precision medicine has not become a reality. It may lead to recommendations from the pharmacometrics community that favor results from studies with lower RUV and minimize the “believability” of studies with large RUV.

Moving this work further, we wish to evaluate the ways to handle unrecorded time deviations in clinical data. Although times of dosing and blood sampling will be specified in the clinical protocol, some study personnel will record the true time when there is a deviation while others might record the nominal time. This variability, if not taken into account, can propagate and introduce bias and imprecise parameter estimates under an NLMEM approach (Sun, Ette, and Ludden 1996). We usually assume the errors arise from the response variable in NLMEM e.g., observed concentration, and we introduce residual error terms to estimate the magnitude of RUV. In 1950, Joseph Berkson (Berkson 1950) in his seminal paper “Are there two regressions?” argued that errors cannot only be seen in response (dependent variable) only, but one might expect errors to arise from independent variables as well. Since independent variables are a measured quantity, we would expect an error to some degree, and if not taken into account, this can lead to biased regression estimates

(Berkson 1950). To date, there is no consensus on the way to handle the potential for inaccurately recorded times, nor a recommendation regarding the maximum time deviation that will not cause biased PK estimates, nor which estimation method one should use when handling data with erroneous time data. Therefore, we were motivated in chapter 4 to conduct a simulation study to evaluate the impact of time deviations and suggest remedies to dilute the bias in model estimates.

Weighted residuals, both traditional weighted residuals (WRES) and conditional weighted residuals (CWRES), are common metrics to graphically evaluate model acceptability in population analyses (Nguyen et al. [2017]). They represent the difference between the observed concentration and the prediction under the model, which are then weighted to standardize and decorrelate the residuals. WRES and CWRES are commonly plotted against TIME and population predictions and are expected to be randomly scattered around zero with the bulk of the data points within two standard deviation units. Limited by the lower limit of quantification (LLOQ) of analytical techniques, it is not uncommon to have concentrations reported as below the LLOQ (BLQ) in PK studies. Although various approaches have been proposed to accommodate BLQ data as shown in (Bergstrand and Karlsson [2009]), Beal’s M3 method currently appears to be most common. It integrates the likelihood function over the interval $[-\infty; \text{LLOQ}]$ and maximizes the likelihood of the concentration being BLQ with respect to model parameters. The likelihood for censored observation at time t is:

$$L(t) = PHI \left(\frac{(\text{LLOQ} - f(\Phi_i, x_i, t))}{\sqrt{g(\Phi_i, x_i, t)}} \right) \quad (1.16)$$

Where PHI is the cumulative distribution function. This likelihood can be defined as the probability that the observation is BLQ. However, by default, the M3 method suppresses the computation of the entire set of weighted residuals for any subject with

at least one BLQ observation. In a 2010 NONMEM Users Network Archive thread, (NMUSERS Archive 2010) it was suggested that this was a bug in the NONMEM software (ICON plc Development Solutions). Tom Ludden provided an historical perspective that Stuart Beal intentionally excluded the calculation of weighted residuals for each subject with BLQ data due to a concern that all weighted residuals for that subject might be biased. A particularly lucid explanation was contributed by Matt Hutmacher, acknowledging that “residuals do not provide great diagnostic value unfortunately for data sets with censored data. BQL observations influence the fit through the censored likelihood, but these observations are not represented in the residual diagnostic plots.”. Therefore, this had motivated us to conduct a simulation study to investigate the extent to which weighted residual calculations in subjects having some BLQ data might be biased when using the M3 method. This analysis is presented in chapter 5

Another component of a pharmacostatistical model is the structural pharmacokinetic model, which is the first component we build to describe the variability in data. Structural PK models with extravascular inputs consist of absorption and disposition components, where the latter describes the distribution and elimination of drug in the body and is important to quantify. Absorption models in pharmacokinetic studies are typically empirical. There are multiple steps for a drug product to be absorbed into the body and the granularity of the absorption process that can be determined is a function of the sampling frequency. When sampling is relatively limited, simpler absorption models are preferred because inadequate data are available to support a more complicated model. Upon ingesting a tablet, it disaggregates, disperses, and the drug must go into solution before being absorbed, usually in the duodenum. Even ignoring complicating issues with poor aqueous solubility, the highest rates of absorption are not likely to occur for some time after administration. Nonetheless, the

first-order absorption model does dictate that the maximal transfer of drug into the central compartment occurs immediately upon dosing. This model misspecification is largely accepted as ignorable as there are usually little data to suggest a more complicated absorption process is needed. Given the physical reality of the pre-absorption steps that occur, our models are generally a highly simplified convenience. Looked at this way, the absorption process becomes little more than a nuisance model, at least from a pharmacokinetic perspective. However, one cannot always ignore early exposures and there are examples when the absorption process is associated with clinical outcomes (Swanson 1999, Gomeni 2017, US FDA 2018). In practice, we typically assume there is a single absorption process whether the model is simple or complex. However, it may not be the case that all subjects exhibit the same absorption profile. Some subjects may seem to have a first-order process, whereas other profiles may be better described using an Erlang process. In an Erlang model, for example, the post hoc absorption transit rate constant for someone with an apparent first-order absorption could be quite large, although it would be estimated to be smaller for another individual with a more distributed delay absorption process. We justify a single absorption process by assuming the random effect will accommodate individual differences, leading to the overall result of a decidedly large population variability. We have recent experience in a population PK analysis in which the absorption process demonstrated concentration-time profiles that, while not apparent on standard mean or spaghetti plots, appeared on closer examination to have individuals that conform to either a first-order, Erlang, or a split-peak process, depending on the individual. Our initial approach was to fit an Erlang-distribution absorption model to the data. Given that the specifics of the absorption process weren't of primary importance, the input process was considered a trivial component of the analysis. Subsequently we explored visually prescreening the individual profiles to make an assignment of the absorption model prior to modeling the data (see Chapter 6). It was an interesting

exercise, but we found this procedure to be less than satisfactory as visually assessing the profiles took considerable time and demonstrated inter-rater variability. The exercise motivated us to seek an alternative approach in assigning the absorption model. The goal of this study, chapter 7, was to build a deep neural network algorithm to recognize these absorption profiles as a prescreening tool and apply it to our data as a means to evaluate the performance of the method in assigning the absorption model structure for each individual.

Chapter 2

Sources of Variability

2.1 Overview

Drug concentrations from similar doses can vary among individuals with even similar characteristics e.g., body size, and renal function. Individuals can be similar, but they are not identical. This variability in pharmacokinetics and pharmacodynamics can be expressed in two terms; explainable variability and unexplainable variability. The former is predictable when incorporating patient-specific information in PK/PD models to describe the variation in PK/PD parameters, e.g., drug clearance using body-size or renal function. This type of variability is important in clinical practice and in the drug development pipeline as appropriate doses are being explored.

The other type of variability, the unexplainable, is divided into BSV, and RUV. BSV accounts for the variation in PK/PD parameters among individuals. In the population approach, one might try to explain the variability in PK/PD parameters using disease and demographic information, but unexplained variability is still present. Physiological and biological processes can vary considerably across individuals and BSV values less than 10-15% are rarely achieved even after incorporating

those fixed effects that are expected to describe large amounts of the variability.

After one takes into account structural PK, covariate, and BSV models, the remaining variability is termed unexplained residual variability, or RUV. We generally assume when we enter PK data into a model that the variables are absolute with no uncertainty. That is rarely the case even in a well-controlled clinical trial. Probably the easiest variability to understand is that due to the imprecision of our analytical techniques. Other sources include errors in recording dosing and sampling times, dose manufacturing variability, and pharmacostatistical model misspecification.

We usually assume the errors arise from the ordinate axis in nonlinear mixed-effect modeling, and we introduce residual error terms, usually symmetrical gaussian distribution, to estimate the magnitude of RUV. In 1950, Joseph Berkson (Berkson [1950]) asked the question in his paper “Are there two regressions?” and he argued that errors cannot only be seen in response only, but one might expect errors to arise from independent variables on the abscissa. Since independent variables are a measured quantity, we would expect an error to some degree, and if not taken into account, this can lead to biased regression estimates. If bias is present in PK parameters, this can affect our informed decision (see Chapter 4 for further analysis regarding Berkson approach).

2.2 Assay Variability

Concentrations are quantified using assay techniques such as high-performance liquid chromatography (HPLC), mass spectrometry (MS), and others Grebe and Singh [2011]. These methods undergo calibration and validation to quantitate concentrations with high precision. Two concepts are considered when it comes to assay cali-

bration: linearity and variability of an assay. A test for linearity is done to evaluate the linear dynamic range between the concentrations and the response of the analytical system. The variability in an assay is important and reflects confidence in assay results, and usually it is quantified as coefficient of variation based on a collection of concentrations that are used in the standard curve. The FDA guidance suggests the coefficient of variation of assay variability to be less than 20% for lower limit of quantification and 15% for other calibrators (U.S. Food and Drug Administration, [2015]).

On the impact of assay variability in a NLMEM approach, Graves et. al. (Graves et al. [1989]) studied the effect of assay variability on parameter estimates in a NLMEM approach and argued that increasing the magnitude of assay error can result in a PK model misspecification where one subject data would be described using a one-compartment model, while others can be described using a two-compartment model. In another study (Bonate [2013]) evaluated the effect of assay error on the estimation of slope and intercept in QTc prolongation studies and found a magnitude of >40% leading to a biased estimation in a linear mixed-effect approach.

2.3 Manufacturing

Variability in and within dosage batch manufacturing exists but usually ignored due to its small amount (US Food and Drug administration Generic manual 2018). However, it was recently shown that batch manufacturing can result in within-batch variability in some products that substantially affect PK metrics (maximum observed concentration, time of maximum observed concentration) resulting in bioequivalence studies among different batches (Burmeister Getz et al. [2017, 2021]). The United States pharmacopeia guidelines suggest a batch variability in oral dosage form to be

less than 15% (Pharmacopeia [2011]). That means the entire manufactured batch has a variability of 15% or less.

In population analyses, this variability can be translated to variable drug bioavailability from an oral depot. In the absence of intravenous input data, we usually make the assumption that PK parameters such as drug clearance (CL) and volume of distribution (V) are apparent and normalized to drug bioavailability (F). Therefore, it is expected that this batch variability is present will propagate to PK modeling (see Chapter 3).

2.4 Dosing times

In a single dose study with a protocol dosing time 0, one might expect the dose is given at time 0. This is not always the case, and it is not uncommon to deviate from the protocol time, e.g. given earlier or at later times from time 0. These deviations might not be well documented and can result in an inaccurate documentation of dosing times. Different route of administration can be impacted, for example, with an intravenous infusion, it is challenging to measure the exact time (in minutes) for an infusion unless an infusion pump is supplied to calculate the exact duration. Thus, uncertainty in dosing time is not well-documented in practice, which leads to an increase in the magnitude of variability in the system. Alihozidic et. al. (Alihozidic et al. [2020]) investigated the inaccurate documentation of infusion times on population pharmacokinetic study and concluded bias estimates on both the population and individual levels.

2.5 Sampling times

Obtaining accurate and precise PK parameters is important in trial design and dose optimization. Efficient designs to obtain these parameters is not the only factor for accuracy. Attention should be paid for the sample collection times and the variability between the actual and recorded times. In clinical trials, it is quite likely that some sampling times deviate from the protocol time. While the recorded time may be the actual time that sample was withdrawn from the patient, it is possible that the recorded time may be the protocol time, or some other time entirely. Study personnel should always be encouraged to record the exact times in a PK study, and data analysts should be aware that time discrepancies of even ten minutes may lead to biased PK structural model parameter estimates as well as inflated random effects (see Chapter 4).

sampling times unrecorded deviation variability, if not taken into account, can propagate and introduce bias in parameter estimates under the NLMEM approach (Sun et al. [1996]). Examination of sampling time error in NLMEM approach has appeared in previous work (Wang and Davidian [1996], Karlsson et al. [1998], Choi et al. [2013]). The consensus is sampling time would be affected by two elements: the curvature of pharmacokinetic (PK) profile (rate of change at the time of the deviation) and the magnitude of sampling error.

As a clinical consequence of inaccurate documentation of sampling times, Santalo et al. (Santalo et al. [2016]) studied the deviation in sampling time with vancomycin trough concentrations and reported sub-therapeutic dosing as a consequence of early measurement. Similarly, Wang et al. (Wang et al. [2020]) reported a biased tacrolimus trough concentration with inaccurate documentation that might lead to inappropriate

dosing.

2.6 Model misspecification

In NLMEM approach we assume a structural, BSV, covariate (if applicable), and residual models to describe the observed data. Structural model can be either empirical or mechanistic. The selection of which model used depends on the purpose of the analysis. In both cases, we assume a nonlinear function in respect to the model parameters, that do usually have a physiological meaning. While empirical or mechanistic models tend to adequately describe the data or answer modeling question, they do not reflect the reality. With more data we feed to the model, model misspecification is evident. Model misspecification is present in all analysis and we tend to minimize this by choosing appropriate models. For example, if a drug concentration versus time profile follows a biexponential decay, it would be appropriate to choose a two-compartment model as structural model and not using a one-compartment to avoid model misspecification that will lead to inaccuracies in PK estimates, which in turn might impact informed decisions. Kim et al (Kim 2019) assessed the calculation of probability target attainment (PTA) using one-compartment and two-compartment models to evaluate model misspecification and conclude that a significant difference in PTA was noted. In selecting appropriate residual error models to describe the observation, Silber et al. (Silber et al. [2009]) found misspecification in the residual error model can inflate Type I error and induce bias in covariate inclusion. Merle et. al. (Merlé et al. [2004]) evaluated the impact of model misspecification in population analysis and concluded that the magnitude of impact differs depending on the step when it occurs (optimization/design or estimation).

Chapter 3

Investigating The Contribution of Residual Unexplained Variability Components in a Nonlinear-Mixed Effect Approach

This work has been submitted to the Journal of Pharmacokinetics and Pharmacodynamics and has been accepted pending revision

Mutaz M. Jaber and Richard C. Brundage. Investigating the contribution of residual unexplained variability components in a nonlinear-mixed effect approach. In *Journal of Pharmacokinetics and Pharmacodynamics*, 2022

3.1 Overview

In a nonlinear mixed-effects modeling (NLMEM) approach of pharmacokinetic (PK) and pharmacodynamic (PD) data, two levels of random effects are generally modeled: between-subject variability (BSV) and residual unexplained variability (RUV). The goal of this simulation-estimation study was to investigate the extent to which PK and RUV model misspecification, errors in recording dosing and sampling times, and variability in drug content uniformity contribute to the estimated magnitude of RUV and PK parameter bias. A two-compartment model with first-order absorption and linear elimination was simulated as a true model. PK parameters were clearance 5.0 L/hr; central volume of distribution 35 L; inter-compartmental clearance 50 L/hr; peripheral volume of distribution 50 L. All parameters were assumed to have a 30% coefficient of variation (CV). One hundred in-silico subjects were administered a labeled dose of 120 mg under 4 sample collection designs. PK and RUV model misspecifications were associated with relatively larger increases in the magnitude of RUV compared to other sources for all levels of sampling design. The contribution of dose and dosing time misspecifications have negligible effects on RUV but result in higher bias in PK parameter estimates. Inaccurate documentation of sampling time results in biased RUV and increases with the magnitude of perturbations. Combined perturbation scenarios in the studied sources will propagate the variability and accumulate in RUV magnitude and bias in PK parameter estimates. This work provides insight into the potential contributions of many factors that comprise RUV and bias in PK parameters.

3.2 Introduction

In nonlinear mixed-effect modeling (NLMEM) of pharmacokinetic (PK) and pharmacodynamic (PD) data, we generally refer to two levels of random effects: between subject variability (BSV), and residual unexplained variability (RUV). The former quantifies the variability of PK/PD parameters within the population. The latter, RUV quantifies the residual variability in the model after accounting for the variability due to the PK structural model, the covariate model, the between-subject variability model, and when applicable, the between-occasion variability model.

We generally assume when we enter PK data into a model that most measurements are absolute with no variability, or at least an ignorable amount. That is rarely the case even in a well-controlled clinical trial. Probably the easiest variability to understand is variability due to the imprecision of our analytical techniques and is considered a given in the remainder of this paper. Other potential errors can occur, and we categorize those errors into three types: (i) Manufacturing, (ii) clinical trial execution, and (iii) technical execution errors.

Manufacturing error includes content uniformity variability that, in general, the US Pharmacopeia recommends to be less than 15% (Pharmacopeia [2011]). Clinical trial execution errors can occur in recording the time the dose is given as well as in recording the time of sampling blood (Wang et al. [2020], Santalo et al. [2016]). Technical errors include misspecification of the pharmacostatistical model components include PK structural model and RUV statistical model. Other technical errors include misspecification of covariate models or BSV models, but they are not addressed in this analysis.

To date, the degree to which these sources of variability contribute to the estimated value of RUV is not well characterized. The goal of this study is to quantify the extent to which pharmacostatistical model (PK and RUV) misspecification, errors in recording dose time, errors in recording blood sampling time, and drug content uniformity contribute to the value of RUV and bias of PK parameter estimates using a sensitivity analysis. We further evaluate the impact of sample collection density on the results.

3.3 Methods

To evaluate the contribution of different components on RUV magnitude, we divided the method section into several parts; *literature review* to collect RUV magnitude in recently published models ; *pharmacostatistical model* design including model inputs; *study design* simulations; and *perturbations* to the pharmacostatistical model. Fractional deviations from true parameters were calculated, and relative bias (rBias), and relative root mean squared error (rRMSE) were obtained to assess the accuracy and imprecision of estimates.

3.3.1 Literature review

To get a sense of RUV magnitude in recently published models, we evaluated studies published from 2019 to 2021. Keywords included: “Population pharmacokinetics”, “NONMEM”, and “First-order conditional estimation with interaction”. Our inclusion criteria were a pharmacokinetic structural model, first-order conditional estimation, and the usage of NONMEM software. For simplicity, we captured the magnitude of RUV from proportional error models and the proportional term from combined error models. Papers reported the RUV as a coefficient of variation (CV) calculated as the square root of the variance or using a more exact equation[4]. When

RUV was reported as a variance, values were converted to a CV using the square root of the variance estimate. An analytical methods section was sometimes included and the CV of the assay was recorded when available.

3.3.2 Pharmacostatistical model

A single 120 mg dose study with a two-compartment model, first-order absorption, and first-order elimination was assumed as the true simulated model. This provided a rapid distributive (alpha) half-life of 0.28 hours and a slower terminal elimination (beta) half-life of 12.2 hours. Individual PK parameters were assumed to have log-normal distributions with population typical values and CVs as reported in Table 1. A 5% CV for proportional RUV magnitude served as a somewhat optimistic baseline for analytical variability.

3.3.3 Sample collection design

We conducted our simulations with 4 levels of sample collection designs; (i) SD9: 9 samples per subject with nominal sampling times of 0.5, 1, 2, 4, 6, 8, 12, 24 and 48 hours; (ii) SD7: 7 samples per subject with nominal sampling times of 2, 4, 6, 8, 12, 24, and 48 hours; (iii) SD5: 5 samples per subject with nominal sampling times of 2, 8, 12, 24, and 48 hours; and (iv) SD4: 4 samples per subject with nominal sampling times of 2, 12, 24, and 48 hours. Sample collections were selected based on a typical concentration-time profile and optimal design was not evaluated in this study.

3.3.4 Perturbations to the Model

Starting with the reference pharmacostatistical model, various perturbations from the nominal values were made to the simulation dataset (*vide infra*). In addition, several levels of perturbations were included. For each perturbed dataset, 500 replicates

of 100 in-silico subjects were simulated. These datasets included the perturbed item of interest and simulated concentrations based on those perturbations. These datasets were then altered to include the original nominal value while maintaining the perturbed concentrations for estimation. Table 1S details the simulation and estimation models used in this study.

Manufacturing perturbation (MP)

Let assume that the protocol labeled dose (P_D) is 120 mg, thus, the true individual dose (I_D) for the j^{th} subject is:

$$I_{D,j} = P_D + \kappa_j \quad (3.1)$$

where κ_j is a random variable with mean of 0 and standard deviation of K . K was chosen to present to levels of variability, $CV = 10\%$ and 20% of P_D . Therefore, the model was independently simulated using $I_{D,j}$ under the two scenarios.

Clinical trial execution perturbations (CTEP)

Given the protocol dosing time (P_{DT}), the individual true dosing time (I_{DT}) for the j^{th} subject was simulated as:

$$I_{DT,j} = P_{DT} + \gamma_j \quad (3.2)$$

where γ_j is a random variable with mean of 0 and standard deviation of G . G was chosen to have two levels of variability associated with a standard deviation of $SD = 5$ minutes, and 10 minutes. Similarly, given the protocol sample collection times for the i^{th} point and j^{th} subject ($P_{ST,i,j}$), the true sample collection times at the i^{th} point and j^{th} subject ($I_{ST,i,j}$) is:

$$I_{ST,i,j} = P_{ST,i,j} + \rho_{i,j} \quad (3.3)$$

where $\rho_{i,j}$ is a random variable with mean of 0 and standard deviation of R . Four levels of variability were selected for R associated with standard deviations of SD=5, 10, 15, and 30 minutes.

Technical execution perturbations (TEP)

For PK model misspecification, we chose to fit the data using a one-compartment model with first-order absorption and first-order elimination instead of the true two-compartment model mentioned above.

An additive component was added to the 5% proportional component and simulated with 3 different magnitudes representing a percentage of approximately the lower 10th percentile of concentrations (0.1 mg/L). Specific perturbations were 10% ($\sigma_{add} = 0.01$ mg/L), 20% ($\sigma_{add} = 0.02$ mg/L) and 40% ($\sigma_{add} = 0.04$ mg/L). In these scenarios, data were fit using a proportional error model instead of combined error model.

Combined perturbations

Additional simulations were done using the true two-compartment model with the combined perturbations $I_{D,10\%}$, $I_{DT,5}$, $I_{ST,5min}$, and $\sigma_{add} = 0.04$ while fitting the data using a one-compartment model.

3.3.5 Software and Evaluation

The R package `mrgsolve` version 1.04 Baron [2022] was used to generate the simulated data. All generated datasets were carried over to the estimation process using `NONMEM` version 7.5 (ICON plc Development Inc.). Parameter estimation was obtained using first-order conditional estimation with interaction (FOCE-I). AD-

VAN4/TRANS4 was used for two-compartment model fitting and ADVAN2/TRANS2 was used to fit one-compartment model. Python (Python Software Foundation. Python Language version 3.9) was used to automate the assigning, creating control streams and executing NONMEM for estimation. All programs/scripts used in this project can be found in MMJ GitHub repository (<https://github.com/Mutaz94/residual>) under open-source creative commons attribution 4.0 license with a detailed documentation for research reproducibility.

Deviations of parameter estimates ($\hat{\theta}$) from the true parameter value (θ_T) were computed as fractional deviations (Ψ):

$$\Psi = \frac{\hat{\theta}}{\theta_T} \quad (3.4)$$

Relative bias (rBias), and relative root mean squared error (rRMSE) were calculated to assess the accuracy and imprecision of estimation, respectively.

$$\text{rBias}[\%] = \frac{1}{n} \sum_{i=1}^n (\Psi_i - 1) \cdot 100\% \quad (3.5)$$

$$\text{rRMSE}[\%] = \sqrt{\frac{1}{n} \sum_{i=1}^n (\Psi_i - 1)^2 \cdot 100\%} \quad (3.6)$$

For combined perturbations, the median RUV for the k^{th} sample collection design ($mCV_{RUV,k}$) is calculated as:

$$mCV_{RUV,k} = CV_{RUV,true} \cdot \text{median}(\Psi_{RUV,k}) \quad (3.7)$$

and a corresponding interquartile range (25th and 75th percentiles).

3.4 Results

The results from literature review is presented with corresponding median coefficient of variation and interquartile range. Contribution to RUV magnitude is divided into the subcategories; Manufacturing perturbations (MP); Clinical trial execution perturbations (CTEP); Technical execution perturbations (TEP); and combined perturbations.

3.4.1 Literature Review

In this study, 330 published studies from the literature were evaluated. In 239 of the 330 studies, authors used a proportional error model and 89 used a combined error model. Two used an additive error model which was not included in the analysis. The median and interquartile range [25th – 75th] of proportional RUV CV was 25% [17.6% – 37.1%]. The median reported analytical assay ($n = 72$) CV was 8.9% [5% – 11%]. Additional information is found in the supplementary material (Figure 1S).

3.4.2 MP

MP based on 4 different study designs is demonstrated in Figure 1. Dosage content uniformity that reflects on relative bioavailability of the drug had negligible effect on RUV magnitude and it contributes more to the value of rBias in random effects (BSV) on drug clearance (CL) and central volume of distribution (V). BSV on V had the larger effect by dosage content perturbations with bias up to 140% compared to CL that had bias up to 20%. A sparse study design had more rBias than an intense design on V.

3.4.3 CTEP

With CTEP, Figures 2 and 3 demonstrate the contribution of sampling and dose times on RUV magnitude and bias and imprecision on PK parameter estimates, respectively. We saw a small effect on inaccurate documentation of dosing times with the 5-minute perturbation on RUV magnitude which monotonically increases with higher perturbations. However, bias is noticeable with some estimated parameters. For instance, the typical value for V and corresponding BSV are sensitive to 5-minute perturbation and even larger with 10-minute perturbation. On the other hand, perturbations did not have much of effect on CL and intercompartmental clearance (Q). While dosing time perturbations have a small effect on RUV, inaccurate documentation of sampling times has a more noticeable rBias. The magnitude of RUV will increase with increasing the magnitude of inaccurate documentation. This pattern is more pronounced with intense designs compared to sparse design.

3.4.4 TEP

Figure 4 and 5 present the TEP deviation from the baseline RUV magnitude for both RUV model misspecifications. Residual error misspecification contributed the largest inflation in RUV magnitude compared to other sources we studied. Structural PK misspecification did not have a noticeable effect on CL and BSV associated with CL.

3.4.5 Combined perturbations

Combined perturbations are presented in Figure 6. Absorption rate constant, K_a , has high bias and imprecision with combined perturbation for sample collection designs SD7, SD5, and SD4 thus, the figure was truncated to a reasonably high value

(500%). The median RUV under the combined perturbations for different sample collection designs is shown in Table 2.

3.5 Discussion

Residual unexplained variability is an outcome of the NLMEM analysis. It is most often reported without much regard as to what constitutes it. Assay variability is the obvious component and we found the median to be 8.9% over a three-year review of published articles. This is considerably less than the CV of 25% reported for RUV in those same papers. Clearly, there are other components that contribute to RUV.

The selection of 10%-20% variability in dose content was based on the criteria for US pharmacopeia on batch variability with a guideline of uniformity should be less than 15% variability on average (Pharmacopeia [2011]). Thus, it is reasonable that the produced batch has a variability in the content corresponding to a 10% CV. We also examined 20% to better understand the behavior of more extreme variability in the content uniformity. The PK parameter V was more affected by dosage content perturbations with bias in BSV up to 140% compared to CL that had bias up to 20% with extreme 20% CV. The large bias can be explained due to the high imprecision in relative bioavailability; thus, the random effect could not be precisely estimated. A sparse study design had more bias than an intense design on V . The reason is likely due to the greater number of samples in the early distributive phase compared to the former. The low density sample design has more bias than intense design with Q and V_p BSV parameters which is expected due to practical identifiability related to study design (Lavielle and Aarons [2016]). The estimation of these parameters requires intense sampling and they are sensitive to the timing of samples.

Data quality in a clinical trial is an important factor to obtain a reliable PK/PD model estimates (Irby et al. [2021]). In regard to CTEP, we saw a small effect of inaccurate documentation of dosing times on RUV magnitude, and it was noted to

monotonically increase with higher perturbations. In an agreement with our results, Alihodzic et. al. (Alihodzic et al. [2020]) studied the effect on inaccurate documentation of infusion time on meropenem and caspofungin and they conclude even 5 minutes inaccuracy can lead to biased and imprecise estimation of typical population value of V and corresponding BSV. While dosing time perturbations had a small effect on RUV, inaccurate documentation of sampling times have a more noticeable effect. The resulting bias is more evident with intense designs compared to sparse design. The reason for this observation likely relates to the curvature of the structural PK profile. When the rate of change (dC/dt) is higher, the perturbations in time will cause greater deviations in concentrations compared to the later time points when dC/dt is usually smaller. Our results agreed with Karlsson et al, Choi et. al and Ludden et. al (Sun et al. [1996], Karlsson et al. [1998], Choi et al. [2013]) and supports the consensus that the sensitivity of parameter estimates to the deviation of recorded time would be affected by the curvature of PK profile and the magnitude of perturbed recorded time. As a clinical consequences of inaccurate documentation of sampling times, Santalo et al (Santalo et al. [2016]) studied the deviation in sampling time with vancomycin trough concentrations and report sub-therapeutic dosing as a consequence of early measurement. Similarly, Wang et al. (Wang et al. [2020]) reported a biased tacrolimus trough concentration with inaccurate documentation that might lead inappropriate dosing. Technical execution perturbations resulted in higher bias and imprecision in RUV magnitude compared to other sources. The magnitude of RUV increases with the misspecified structural PK model. Structural model misspecification did not have a noticeable effect on CL or BSV associated with CL, but that isn't the case with other parameters. Overall, misspecification that cannot be identified by residual plots can have a consequence on secondary PK parameters such as half-life due to a biased V . Study design also played a role here; with more data, model inadequacy is more readily apparent. With that said, times of sample

collection are important in the estimation of some parameter values more than others. For example, with limited absorption data points, K_a estimates would have high imprecision and it is common to see this value fixed to a reasonable value.

Residual error misspecification contributed the largest inflation in RUV magnitude compared to other sources we studied. Choosing the wrong error model can mask the additivity from analytical assay and lead to biased estimates in the studied situations, including CL. The ignored error from the additive component will propagate to the parameters leading to the inaccuracy in parameter estimates. Silber et al. (Silber et al. [2009]) found misspecification in the residual error model can inflate Type I error and induce bias in covariate inclusion.

Combined perturbations propagate to the magnitude of RUV and bias in PK parameter estimates. Recently, Al-Sallami et al (Al-Sallami et al. [2022]) published a commentary discussing the relationship of BSV from dose to response and the authors argued that variability in the system propagates linearly or nonlinearly based on the assumption of independency. This can be also observed in the current work. The propagation of all perturbations is not additive (the sum of variances squared is not equal to the RUV magnitude). For example, under the combined perturbations, the square root sum of variances is 17% (Table 2S) without taking into consideration the study sample collection design, which is larger than the median RUV shown in Table 2. The most likely explanation is due to the spread of variability between BSV and RUV.

It is noteworthy that median RUV value under the combined perturbations for all designs had smaller values compared to the median values captured in the published population pharmacokinetic analyses. Therefore, it might be that combined errors

in this simulation study was underestimated compared to the literature. Despite the predominant source of variability in the combined sources might be model misspecification (residual and PK structural models) one should embrace this and carefully review model evaluation step and follow good modeling practices.

In most of the studied scenarios, population typical values for primary PK parameters were robust for small perturbations in manufacturing, clinical trial execution, and technical errors, and resulted in relatively unbiased estimations. Random effects were more sensitive than fixed effects in the presence of perturbations, and that's due to the way the first-order approximation handles fixed-effect parameters (nonlinear approximation) and random-effect parameters (linear approximation) (Sun et al. [1996], Ette et al. [1993]). Even in the absence of error in data, the first-order approximation might lead to bias in random-effects with sparse designs. Al-Banna et al. (Al-Banna et al. [1990]) evaluated the impact of sample collection design on parameter estimation using a one-compartment model. It was concluded that one early and one late time point would be sufficient to estimate primary fixed-effect parameters such as CL and V but resulted in imprecise random-effects estimation.

Limitations of this study include that we did not study the inadequacy of covariate models nor the inaccurate documentation of covariates. We also did not assess the unexplained variability in scenarios with multiple dosing, other PK/PD models, or misspecification in covariate, BSV or BOV models. Finally, our misspecifications were chosen under an assumption of a well-controlled clinical trial. Bias and imprecision findings are likely to be higher in studies that include outpatient dosing and multiple dosing studies that assume steady-state conditions.

In conclusion, we assessed the contribution of hypothetical sources of variability

in RUV that occur during NLME modeling and offer these takeaway points:

- Pharmacostatistical model misspecifications were associated with relatively large increases in the magnitude of RUV compared to other sources for all levels of study design.
- The contribution of dose misspecification, and dosing time misspecifications have negligible effects on RUV but result in biased PK parameter estimates.
- Inaccurate documentation of sampling time results in biased RUV magnitude which is sensitive to the magnitude of perturbations, and this effect was greater with more intense sampling designs.

Errors of the type studied here are real and do occur in PK studies. It is important to consider the question of what one wants to answer from the analysis. For example, if one is primarily interested in drug clearance, then some of these perturbations have less consequence. Nonetheless, as pharmacometricians, we don't have control over the perturbations and our challenge is to choose a pharmacostatistical model that adequately explains the data provided to us. This work provides information that can be used to understand and give insight for the interpretation of RUV magnitude. It may lead to recommendations from the pharmacometrics community that favor results from studies with lower RUV and minimize the "believability" of studies with large RUV.

3.6 Tables

Table 3.1: Pharmacokinetic parameter values with corresponding between-subject variability reported as coefficient of variation.

Parameter		Value	BSV
CL	(L/hr)	5	30%
V	(L)	35	30%
Q	(L/hr)	50	30%
Vp	(L)	50	30%
ka	(1/hr)	0.7	30%
σ_{prop}	(%)	5	-

Table 3.2: Median RUV magnitude for combined sources based on different sample collection designs.

Sample collection design	median RUV magnitude (CV)	Range, CV [25th – 75th]
SD9	14.1	(13.8 - 15.2)
SD7	16.7	(15.5 - 17.0)
SD5	18.4	(17.5 - 19.6)
SD4	21.6	(20.4 - 22.8)

3.7 Figures

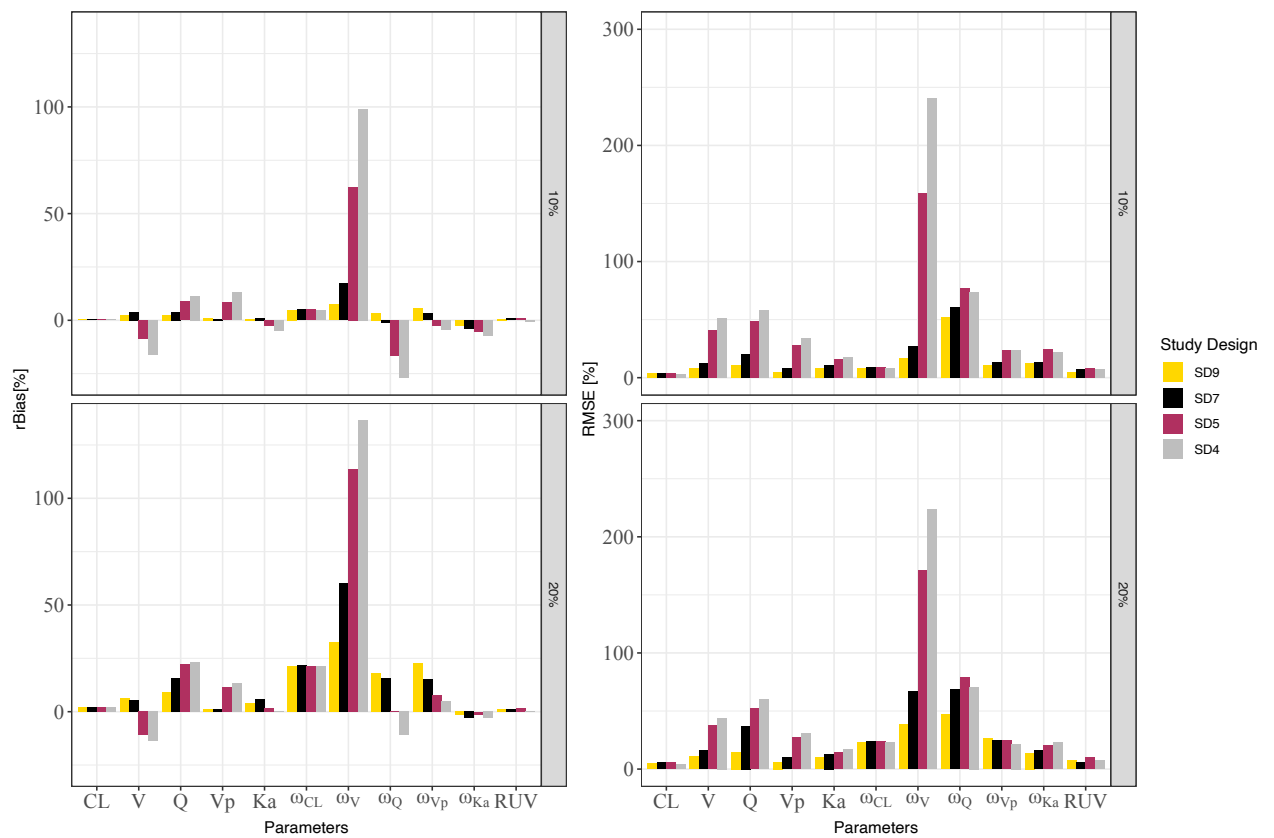


Figure 3.1: Contribution of Manufacturing perturbation on RUV and PK parameters; left-hand panel present relative bias; right-hand panel present the relative mean squared error. The Greek symbol Omega present between-subject variability magnitude

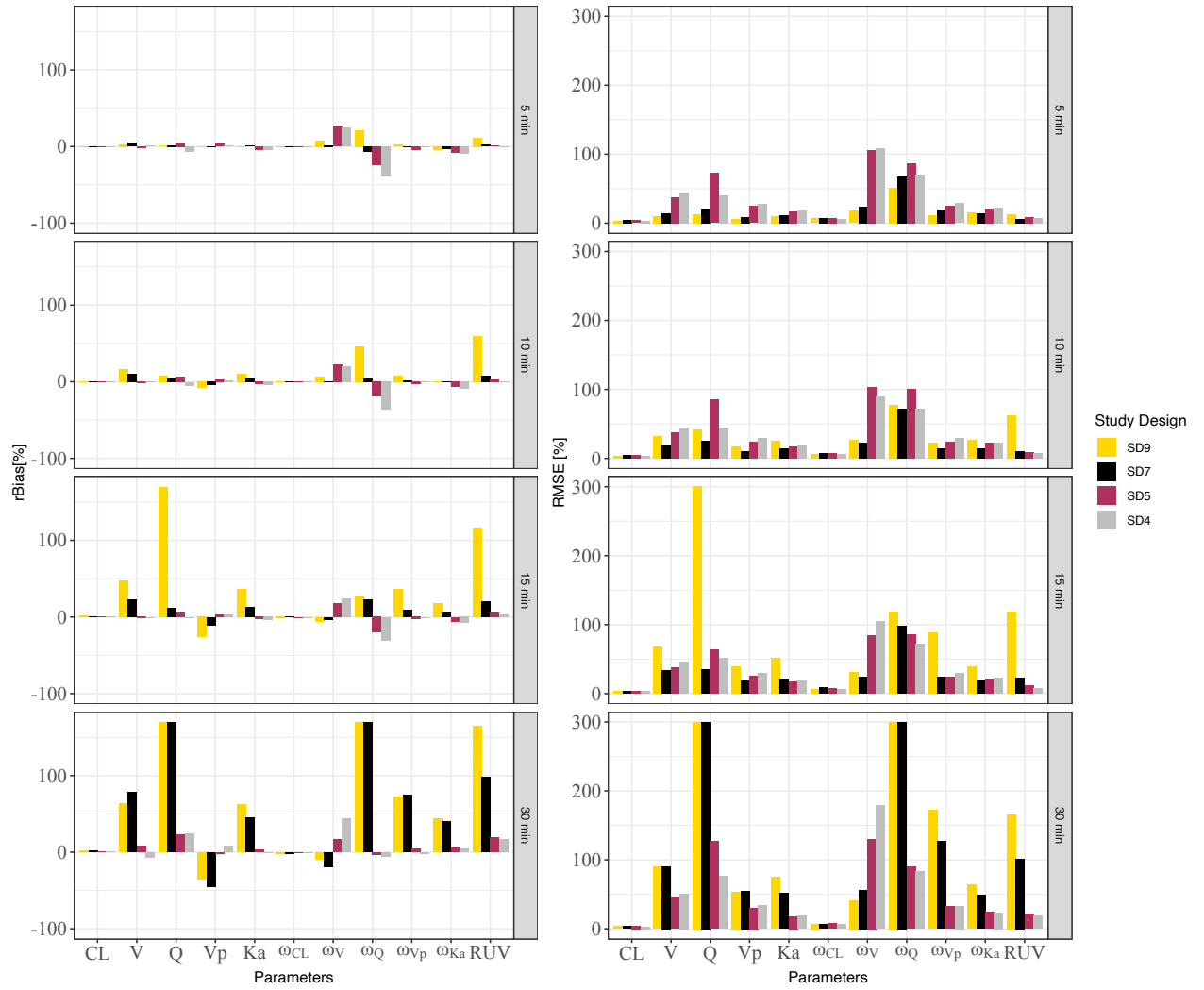


Figure 3.2: Contribution of inaccurate documentation of PK sampling time on RUV and PK parameters; left-hand panel present relative bias; right-hand panel present the relative mean squared error. The Greek symbol Omega present between-subject variability magnitude

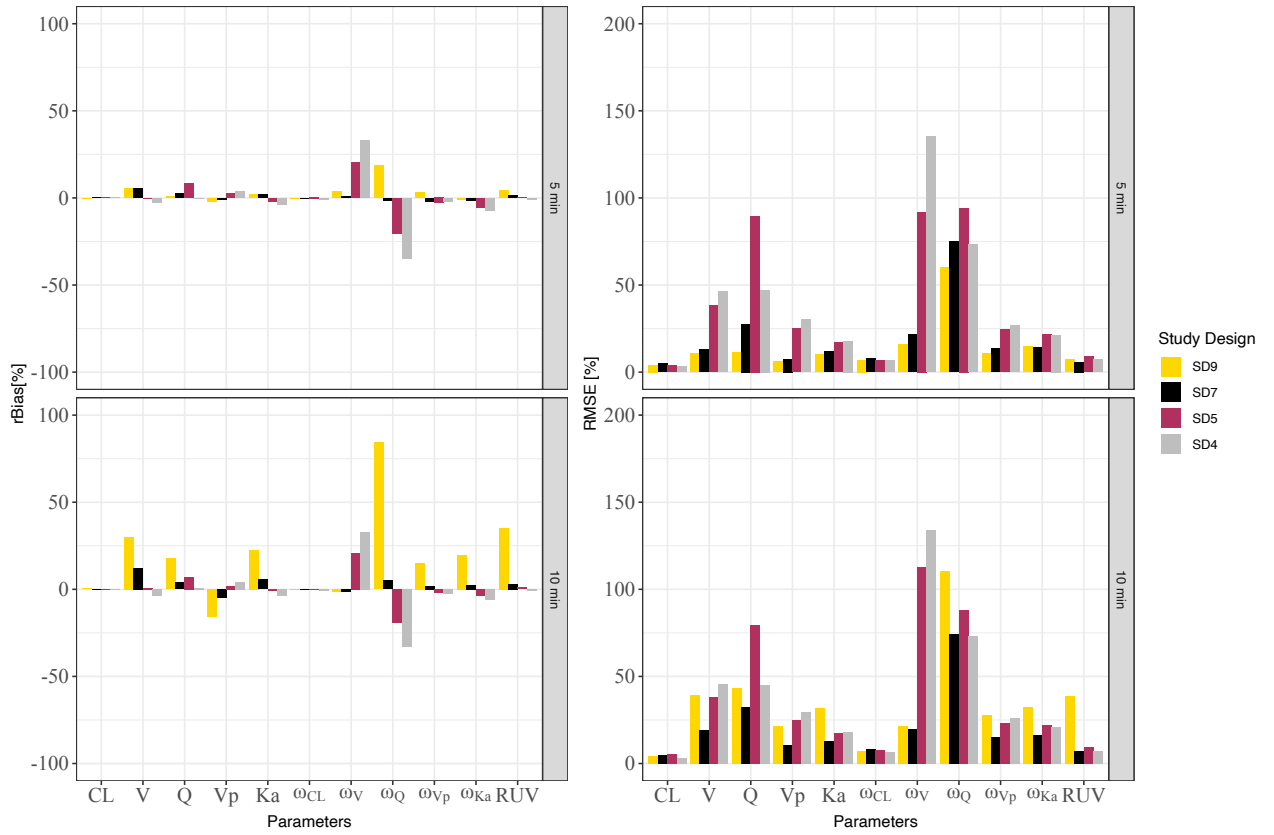


Figure 3.3: Contribution of inaccurate documentation of dosing time on RUV and PK parameters; left-hand panel present relative bias; right-hand panel present the relative mean squared error. The Greek symbol Omega present between-subject variability magnitude

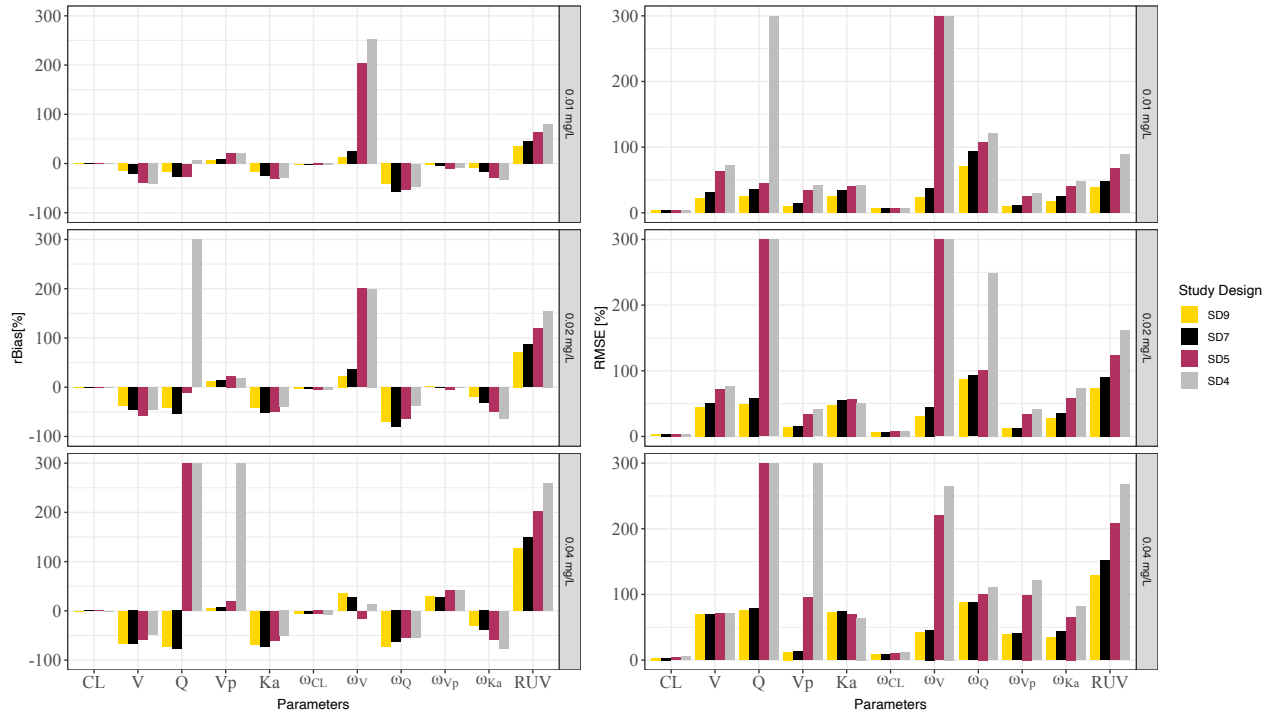


Figure 3.4: Contribution of residual model misspecification on RUV and PK parameters; left-hand panel present absolute bias; right-hand panel present the relative mean squared error. The Greek symbol Omega present between-subject variability magnitude

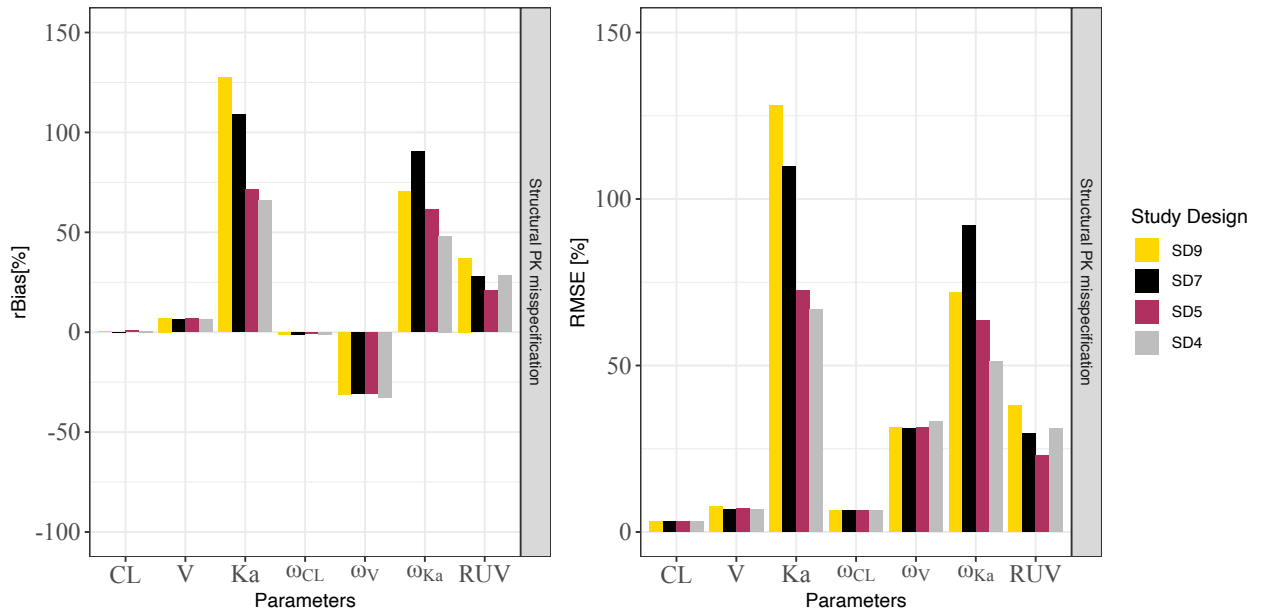


Figure 3.5: Contribution of structural PK model misspecification on RUV and PK parameters; left-hand panel present absolute bias; right-hand panel present the relative mean squared error. The Greek symbol Omega present between-subject variability magnitude



Figure 3.6: Contribution of combined perturbations on RUV and PK parameters; left-hand panel present relative bias; right-hand panel present the relative mean squared error. The Greek symbol Omega present between-subject variability magnitude

Chapter 4

The impact of unrecorded time deviation in nonlinear mixed-effect analyses

This work is under internal review and targeted to Journal of Pharmacokinetics and Pharmacodynamics

It was accepted and presented at the American Conference on Pharmacometrics 13 (ACoP13): Mutaz M. Jaber, Mahmoud Al-Kofahi, and Richard C. Brundage. Evaluation of recorded time deviations on parameter estimates in nonlinear mixed-effect analyses. In *American Conference on Pharmacometrics 13*, 2022

4.1 Overview

An assumption that recorded clinical data are recorded without any error is optimistically made. While some study personnel will record the actual times when there is a deviation others record the nominal time. In the current modeling and simulation work we investigate an approach that includes a correction error factor on recorded time and quantitate the bias in estimated parameters; examining the magnitude difference between the actual and recorded time that lead to biased pharmacokinetic (PK) estimates. These simulation study settings included a two-compartment structural PK model with first-order absorption and first-order elimination. A single 500mg dose administered to 500 in-silico subjects was simulated. PK parameter values were: clearance 5 L/hr, volume of distribution 20 L, intercompartmental clearance 5 L/hr, peripheral volume 30 L/hr, and absorption constant 0.7 (1/hr). Three sample collection designs were simulated: intense, sparse, and imbalanced designs. Errors in sample withdrawal are assumed to be independent and not expected to influence all samples. Thus, we evaluated the effect of error occurring in 100%, 50%, and 20% of samples. Adding a correction factor to the recorded time will lead to reducing the bias and imprecision in PK estimates compared to assuming the recorded time is absolute. A magnitude difference greater than 5 minutes between the actual and recorded times can lead to more than 10% bias and imprecision PK estimates. In conclusion, despite the limited settings, we believe this work provides general insight on the ways to handle suspected data with unrecorded time deviations.

4.2 Introduction

In nonlinear mixed-effect modeling (NLME) we consider two levels of variability; between-subject variability (BSV) and residual unexplained variability (RUV). The former quantifies the deviation in individual time-averaged pharmacokinetic (PK) and pharmacodynamic (PD) parameters. RUV quantifies the “left-over” variability after we take into the account structural PK model, covariates (patient-specific) information, and the BSV model. We usually assume the errors arise from the ordinate axis in NLMEM, and we introduce residual error terms, usually symmetrical gaussian distributions, to estimate the magnitude of RUV. This unexplained variability can be due to different sources and the simplest to understand is assay imprecision. Other sources can include the manufacturing process that leads to dose variability; clinical trial execution such as timing of sample collection or dosing time; and technical execution which include model misspecification (see Chapter 3).

In 1950, Joseph Berkson (Berkson [1950]) asked the question in his paper “Are there two regressions?” and he argued that errors are not likely to occur in response measurements only, and one might expect errors to arise from independent variables on the abscissa. Since independent variables are a measured quantity, we would expect an error to some degree, and if not taken into account, will lead to biased regression estimates.

To date, there is no consensus on the way to handle the potential for inaccurately recorded times, nor a recommendation regarding the maximum time deviation that will not cause biased PK estimates. In addition, there is little discussion regarding which estimation method might be better when handling data with potentially erroneous time data. Therefore, our aim in this simulation study is to evaluate (part

I) adding another term of random variability to the independent variable time error to assess the impact on NLMEM parameter estimation; (part II) determine the sensitivity of the magnitude of deviation between actual and recorded times on parameter estimation bias; and (part III) compare the performances of the first-order conditional estimation (FOCE) and the stochastic approximation expectation maximization (SAEM) algorithms in handling data with simulated sample collection times errors.

4.3 Methods

Two subsections are presented; *Notation* where we introduce terms and abbreviations used in this work, in addition to the general structure of NLMEM. In *Simulation methods*, we introduce the general design for this simulation study with further dividing this into two parts: (Part I) Berkson (kappa) model and (Part II) Magnitude difference between recorded and actual time.

4.3.1 Notation

In the theoretical framework of this paper, we will assume that concentration is an element of a truncated continuous (\mathbb{R}^+) set with a minimum value of 0 with no inputs (absence of dose) and a maximum value that represents the upper limit of quantification of assay analytics. This assumption is served to be more realistic compared to a continuous approximation (concentration is continuous on the real number set). The letter i will represent a time point in the time collection N , and the letter j will present a subject in the experimental unit M (population).

Two sources of error were modeled in this work: a classical error model (Part I-III) and a combined classical and Berkson error model (Part I). The former is what

the pharmacometrician/clinical pharmacologist frequently implements in NLMEM to characterize the errors in observed concentrations. The general structure for the j^{th} subject and i^{th} time point as:

$$y_{i,j} = f(\Phi_j, x_j, t_{i,j}) + g(\Phi_j, x_j, t_{i,j})\epsilon_{i,j} \quad (4.1)$$

Where:

- $y_{i,j}$ The observed dependent variable at the i^{th} time in subject j^{th} , and in this case is the concentration of drug
- f Pharmacokinetic structural model
- Φ_j Individual pharmacokinetic parameter set for the j^{th} subject and is a function of population typical value and random gaussian noise to reflect between subject variability
- x_j Given dose and covariates for the j^{th} subject
- $t_{i,j}$ Post-dose times.
- g Residual unexplained variability model
- $\epsilon_{i,j}$ A random quantity presenting the residual error for the i^{th} time point and j^{th} subject, which we assume it is an independent and identically distributed with mean 0 and variance of σ^2

This model we call the null model, M_0 , with no Berkson error incorporated. The Berkson error (discussed below) can be applied to any independent variable but we choose to assess the applicability on post-dose time. Hereafter, the authors will use the term kappa error model to refer to Berkson error model.

4.3.2 Simulation methods

Software and random numbers

All simulations were carried out using Julia version 1.8 (Julia language) and SciML (Rackauckas and Nie [2017]). Random numbers for the simulation purposes were generated using Mersenne Twister algorithm (Matsumoto and Nishimura [1998]) with different seeds to assure reproducibility of results. NONMEM version 7.5 (ICON plc development) was used for estimation process. All programs and scripts used to generate this work can be found in MMJ GitHub public repository (LINK) with documented steps for work reproducibility.

General design

Each of multiple scenarios (vide infra) was simulated as a 500 mg single dose study with 500 in silico subjects under a two-compartment, first-order absorption, and linear elimination model, f . Individual pharmacokinetic parameters were sampled from a multivariate log-normal distribution with a mean of the logarithmic typical values vector and diagonal variance matrix Ω . A 15% coefficient of variation (CV) served as a baseline residual unexplained variability (RUV) using a proportional error model, g . Table 1 presents the true simulated PK parameters with corresponding BSV CV, and RUV magnitude.

[Table 1 somewhere here]

Three sample collection intensity designs were examined; (a) Intense design [I] with 8 samples: 0.5, 1, 2, 4, 8, 12, 24, 48 hours post dose, (b) sparse design [S] with 4 samples: 0.5, 2, 24, 48 hours post dose and (c) mixed design [M] with 33% of subjects having 8 samples as in I, 33% of subjects having 6 samples (0.5, 2, 4, 12, 24, 48), and 33% of subjects having 4 samples as in S. The term we will use for k^{th} design sample

time is $T_{D,i,j}^{(k)}$. The selection of samples was based on a typical profile to obtain PK parameters and optimal sample design was not used.

Part I: Berkson error (kappa) model

Let us introduce the simulated times for the L^{th} design $T_{S,i,j}^{(k)}$ for the i^{th} time point in the j^{th} subject as a function of design sample time $T_{D,i,j}^{(k)}$ and gaussian noise, κ , that is an independent and identically distributed random variable with mean 0 and standard deviation π , representing the deviation of simulated times from the design time (equation 4.2). Four levels of perturbations were performed in the simulation that reflect a standard deviation of π_p for the p^{th} magnitude corresponding to 5-, 10-, 15-, and 30-minutes using equation 4.2. Time errors are assumed to be independent and all samples in the experimental unit are not expected to be influenced. Therefore, three levels of perturbed error fractions (γ) were evaluated: (1) E1, error will affect all sample collection times ($\gamma = 1$) (2) E2, error will affect 50% of sample collection times ($\gamma = 0.5$); (3) E3, error will affect 20% of sample collection times ($\gamma = 0.2$).

$$T_{S,i,j}^{(k)} = \begin{cases} \gamma, & T_{D,i,j}^{(k)} + \kappa_{i,j} \text{ where } \kappa \sim N(0, \pi^2) \\ 1 - \gamma, & T_{D,i,j}^{(L)} \end{cases} \quad (4.2)$$

Each of these scenarios was replicated 100 times and these datasets included the simulated times and concentrations based on those perturbations in time. The time column of these datasets was then replaced with the original design sample time $T_{D,i,j}^{(L)}$ creating a mismatch between the concentrations (at perturbed times) and times at $T_{D,i,j}^{(L)}$.

Two models were created and used to fit the data and obtain parameter estimates: the null model M_0 with estimation implemented using PREDPP, ADVAN4

and TRANS4 in the NONMEM system for the L^{th} design:

$$yS_{i,j}^{(k)} = f(\Phi_j, x_j, T_{D,i,j}^{(k)}) + g(\Phi_j, x_j, T_{D,i,j}^{(k)})\epsilon_{i,j} \quad (4.3)$$

where $yS_{i,j}^{(k)}$ are the mismatched observed concentrations.

In the second model, M_κ , a new random variable, $\kappa_{i,j}$, was created and adjusts the value of the independent variable time recorded in the data set. It is the variance (π^2) of this kappa distribution that is being estimated. let us call it time kappa $T_{\kappa,i,j}^{(k)}$ that is a function of $T_{D,i,j}^{(k)}$ and a random error term, $\kappa_{i,j}$:

$$T_{\kappa,i,j}^{(L)} = T_{D,i,j}^{(L)} + \kappa_{i,j} \quad \text{where } \kappa \sim N(0, \pi^2) \quad (4.4)$$

Thus, the model used to describe the observed concentrations can be presented as:

$$yS_{i,j}^{(L)} = f(\Phi_j, x_j, T_{\kappa,i,j}^{(L)}) + g(\Phi_j, x_j, T_{\kappa,i,j}^{(L)})\epsilon_{i,j} \quad (4.5)$$

where $yS_{i,j}^{(k)}$ are the mismatched observed concentrations, but in this model the variance π^2 of the kappa distribution is an estimable parameter.

The NONMEM PRED routine was used to estimate kappa model parameters because unlike the PREDPP subroutine, time is not the predefined independent variable and the model could be written to include a random effect on time itself. Parameters were estimated using first-order conditional estimation (FOCE) with interaction.

Part II: Magnitude difference between recorded and actual time

In part II, the aim is to evaluate the sensitivity of bias and imprecision on selected time deviation thresholds that achieve values less than 10%. Simulations were

performed with a standard deviation of 10 minutes ($\pi = 10$ minutes) in time using equation 2 with E1 scenario (100% of sample; $\gamma = 1$), then followed by creating a new column in the dataset presenting the time used in the estimation process, $t_{i,j}^{*,(L)}$ where this a mathematical case:

$$t_{i,j}^{*,(L)} = \begin{cases} T_{S,i,j}^{(L)} , & |T_{S,i,j}^{(L)} - T_{D,i,j}^{(L)}| > \delta_p \\ T_{D,i,j}^{(L)} , & \text{Otherwise} \end{cases} \quad (4.6)$$

where δ_p is the magnitude of the absolute difference between the perturbed simulated sample times and $T_{D,i,j}^{(L)}$ times for the p^{th} cutoff. The difference, δ_p , was selected to be 5, 10, 15, or 30 minutes. These $t_{i,j}^{*,(L)}$ values will replace the times used in the analysis data sets.

$$ym_{i,j}^{(L)} = f(\Phi_j, x_j, t_{i,j}^{*,(L)}) + g(\Phi_j, x_j, t_{i,j}^{*,(L)})\epsilon_{i,j} \quad (4.7)$$

Where $ym_{i,j}^{(L)}$ are the observed concentrations that are now mismatched with time $t_{i,j}^{*,(L)}$.

Evaluation Metrics

For all parts of this study, evaluation metrics were calculated as the following:

Deviations of the typical parameter estimate ($\hat{\theta}$) from the true parameter value (θ_T) were computed as fractional deviations (Ψ):

$$\Psi = \frac{\hat{\theta}}{\theta_T} \quad (4.8)$$

Relative bias (Bias), and relative root mean squared error (RMSE) were calculated to

assess the accuracy and imprecision of estimation for each scenario, S_N , respectively.

$$\text{Bias}_{S_N}[\%] = \frac{1}{R} \sum_{i=1}^R (\Psi_i - 1) \cdot 100\% \quad (4.9)$$

$$\text{RMSE}_{S_N}[\%] = \sqrt{\frac{1}{R} \sum_{i=1}^R (\Psi_i - 1)^2 \cdot 100\%} \quad (4.10)$$

Where R represent the replication number for each scenario, S_N .

4.4 Results

In this section we present the results for the two parts, Berkson (kappa) model, and evaluate the sensitivity of bias and imprecision on selected time deviation thresholds that achieve values less than 10%

4.4.1 Part I: Berkson error (kappa) model

In this first part of this study, models with the kappa error approach demonstrated consistently lower bias and imprecision compared to classical error models in all scenarios. The more Intense the sample collection design, the more bias and imprecision were observed compared to sparse sample collection design on fixed-effect parameters. In contrast, the reverse was found with random-effect parameters.

In comparing the percentage of error occurrence, as expected, when all samples in the experimental unit are affected by time deviation, bias and imprecision is larger than when a percentage of time are affected by unrecorded time deviations, Figure 1 (E1 in panel A compared to E2 and E3 in panels B, and C, respectively).

The primary PK parameters, CL and V, bias can reach up to 8% and 35%,

respectively. Inflation in these PK parameters can result in biased derived metrics such as the area-under the curve or the maximum concentration.

[Figure 1 & 2 (a,b,c) somewhere here]

When only the null model is used, RUV is the most biased parameter. Figure 1, and 2 shows the effect of null model M_0 versus kappa model M_κ stratified on the study collection design. The magnitude of deviation between the actual and recorded time estimated using kappa model are shown in Figure 3 with corresponding δ value (percentage of error) stratified by color using study design.

[Table 2 somewhere here]

4.4.2 Part II: Magnitude difference between recorded and actual time

In Figure 4, it was shown that a larger increase in magnitude difference between the simulated and mismatched times (> 5 minutes window error) can result in biased RUV and PK estimates greater than 10%. Sparse collection design had more bias and imprecision on BSV compared to fixed effects. V had larger than 10% bias in all study designs across all different error magnitudes. CL was a robust parameter with no more than a 10% increase in bias and imprecision. A shown in Figure 4B, high relative precision was noticed in RUV estimates across all magnitudes of deviations even with extreme difference between the simulated and design times ($\delta= 30$ minutes).

[Figure 3 (a,b) somewhere here]

Numerical values for all results can be found in the supplementary material accompanying this work.

4.5 Discussion

Data quality in a clinical trial is an important factor to obtain reliable PK/PD model estimates (Irby et al. [2021]) The authors of this work previously demonstrated that bias is more evident with intense designs compared to sparse design when errors in sample collection design are present (see Chapter 3). The reason for this observation likely relates to the curvature of the structural PK profile. In linear PK, it is usually the case that the rate of change (dC/dt) is higher at early time points, thus, the perturbations in time will cause greater deviations in concentrations at early time points compared to the later time points when dC/dt is usually smaller. Our results agreed with Karlsson et al, Choi et. al and Sun et. al (Karlsson et al. [1998], Choi et al. [2013], Sun et al. [1996]) and supports the consensus that the sensitivity of parameter estimates to the deviation of recorded time from the actual time would be affected by the curvature of PK profile and the magnitude of perturbed recorded time.

As a clinical consequence of inaccurate documentation of sampling times, Santalo et. al. (Santalo et al. [2016]) studied the deviation in sampling time with vancomycin trough concentrations and reported sub-therapeutic dosing as a consequence of early measurement. Similarly, Wang et al. (Wang et al. [2020]) reported a biased tacrolimus trough concentration detection with inaccurate time documentation that might lead to inappropriate dosing.

We demonstrate in this work the successful application of the kappa error model on the independent variable, time. The bias and imprecision were significantly reduced across PK parameters and most noticeably on the random-effect parameters. The assumption we make with this implementation is to relax the rigid criteria where no

error happens at the abscissa. The estimated kappa magnitude (π^2) is defined as the variance deviation of recorded time from the actual time. The assumption we made is that random error in time is independent and identically distributed among the points N within each subject. Adding the random quantity to the recorded time (additive model) is a realistic approach and more sophisticated models e.g. proportional kappa model, to describe the deviation in sampling window is not needed to generalize the idea. We might expect the deviation would be larger when the time within samples increases but with a conservative limit in a well-controlled clinical trial. However, despite these findings, a limitation of this approach that we couldn't capture the true deviation magnitude in higher deviations (> 15 minutes) and with small values of error in data (Figure 3).

In clinical trials, it is quite likely that some sampling times deviate from the protocol time. While the recorded time may be the actual time that sample was withdrawn from the patient, it can be possible that the recorded time may be the protocol time, or some other time entirely. In the studied settings of this work, if the deviation between actual and recorded time was within 5 minutes, bias and imprecision in estimated PK parameters was negligible. Study personnel should always be encouraged to record the exact times in a PK study, and data analysts should be aware that time discrepancies of even ten minutes may lead to biased PK structural model parameter estimates as well as inflated random effects. This may have particular importance when a biased volume of distribution parameter leads to biased simulations of derived PK variables such as C_{max} if a maximum concentration is being targeted for either safety or efficacy.

However, if the deviation was larger than that, the study personnel should address the actual time to avoid obtaining inaccurate PK parameters that will lead to mod-

eling fallacies. A deviation of a 10 minute window can affect V parameter that might result in inaccurate estimation of drug half-life, and perhaps the maximum concentration, which is a parameter used for dose optimization <cite>. Of note, the BSV parameter had larger deviation from the true due to uncertainty and perturbation in time provided from the data.

The settings used for this work is limited to a 2-compartment PK model without including covariates. Moreover, different magnitudes of BSV on PK parameters might also have an impact on our results as shown with Sun et. al. (Sun et al. [1996]) The effect of erroneous data might have a larger effect, perhaps on disposition parameters when fitting nonlinear PK models. Another limitation is that we assessed the performance of only two estimation algorithms. Other approaches such as Bayesian estimation may produce different results.

A future direction of this work can be extended to understand and reduce the underestimation of kappa model with higher deviations and assess the performance of the kappa model to handle multiple covariates e.g., dose variability, dosing time, continuous patient specific information, etc. and it would be of interest to quantify a correlation among the errors. Moreover, this work can be expanded to evaluate kappa models in pharmacodynamic study and the implication on clinical outcomes.

In summary, adding a random variable to independent variable time reported in clinical trials would reduce the bias in parameter estimation. In terms of sampling, it is advised to withdraw the sample at the times specified in the protocol and if samples are obtained at some other time, it is advised to record the actual time. However, despite the limited settings, we believe this work will give general insight on the ways to handle data unrecorded time deviations and appreciate that a small deviation in

time can affect our model-based informed decisions.

4.6 Tables

Table 4.1: Pharmacokinetic parameter values with corresponding between-subject variability reported as coefficient of variation.

Parameter	Value	BSV
CL	3.5	30%
V	20	30%
Q	5	30%
Vp	30	30%
ka	0.7	30%

Table 4.2: True simulated deviation and estimated deviation using kappa model stratified on the affected percentage in the experimental unit.

Error	True deviation	Estimated deviation
E1 - 100%	5.0	5.1
	10.0	10.8
	15.0	14.7
	30.0	17.7
E2 - 50%	5.0	3.6
	10.0	8.0
	15.0	10.9
	30.0	12.8
E3 - 20%	5.0	2.5
	10.0	5.4
	15.0	7.5
	30.0	8.6

4.7 Figures

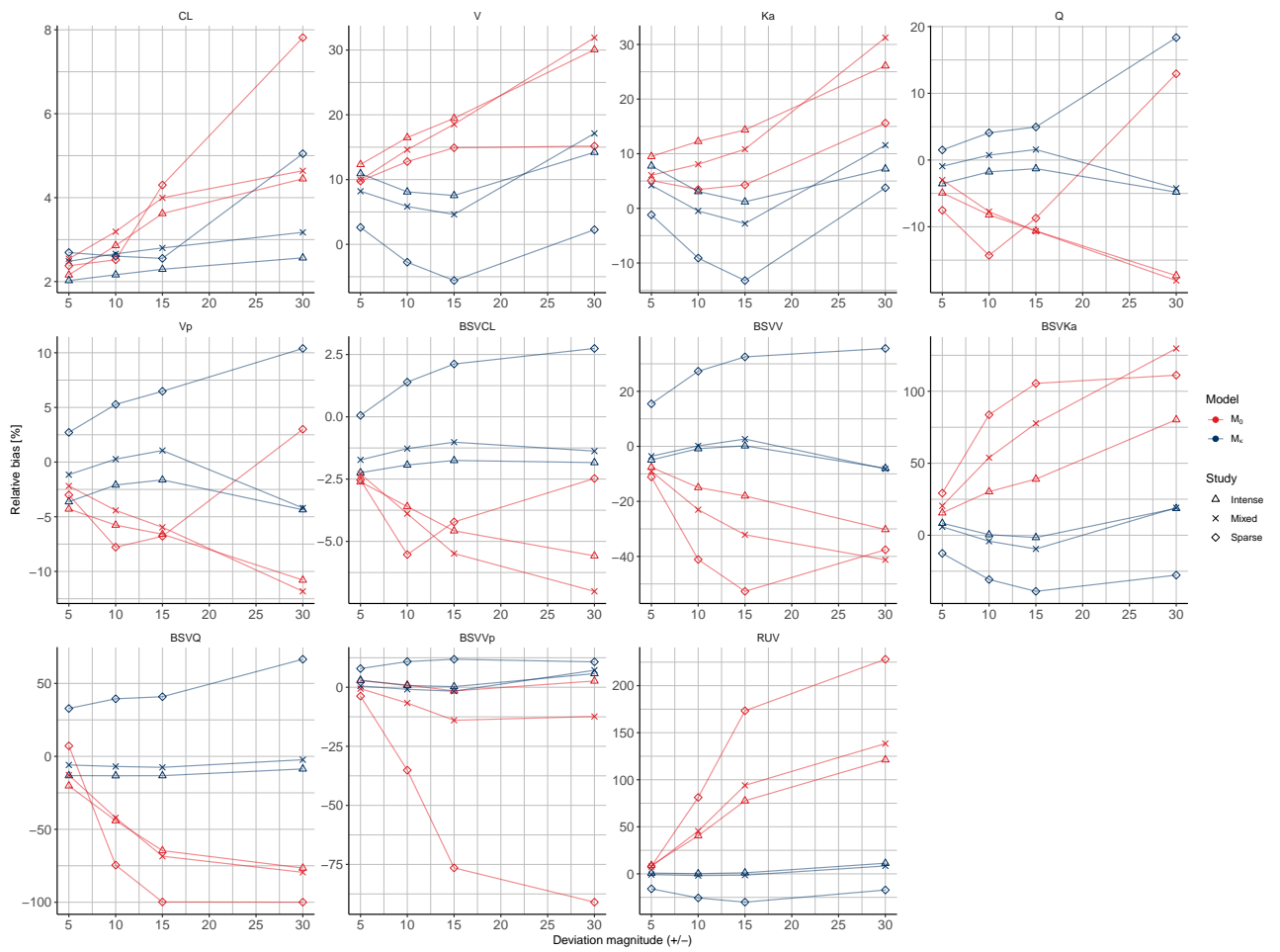


Figure 4.1: Comparison of the relative bias (yaxis) for the null model (red) and kappa model (blue) stratified on study design and percentage of error. Error magnitudes are shown on the x-axis. Panel A present 100% of samples are affected by error; Panel B present 50% of samples are affected by error; Panel C 20% of samples are affected by error.

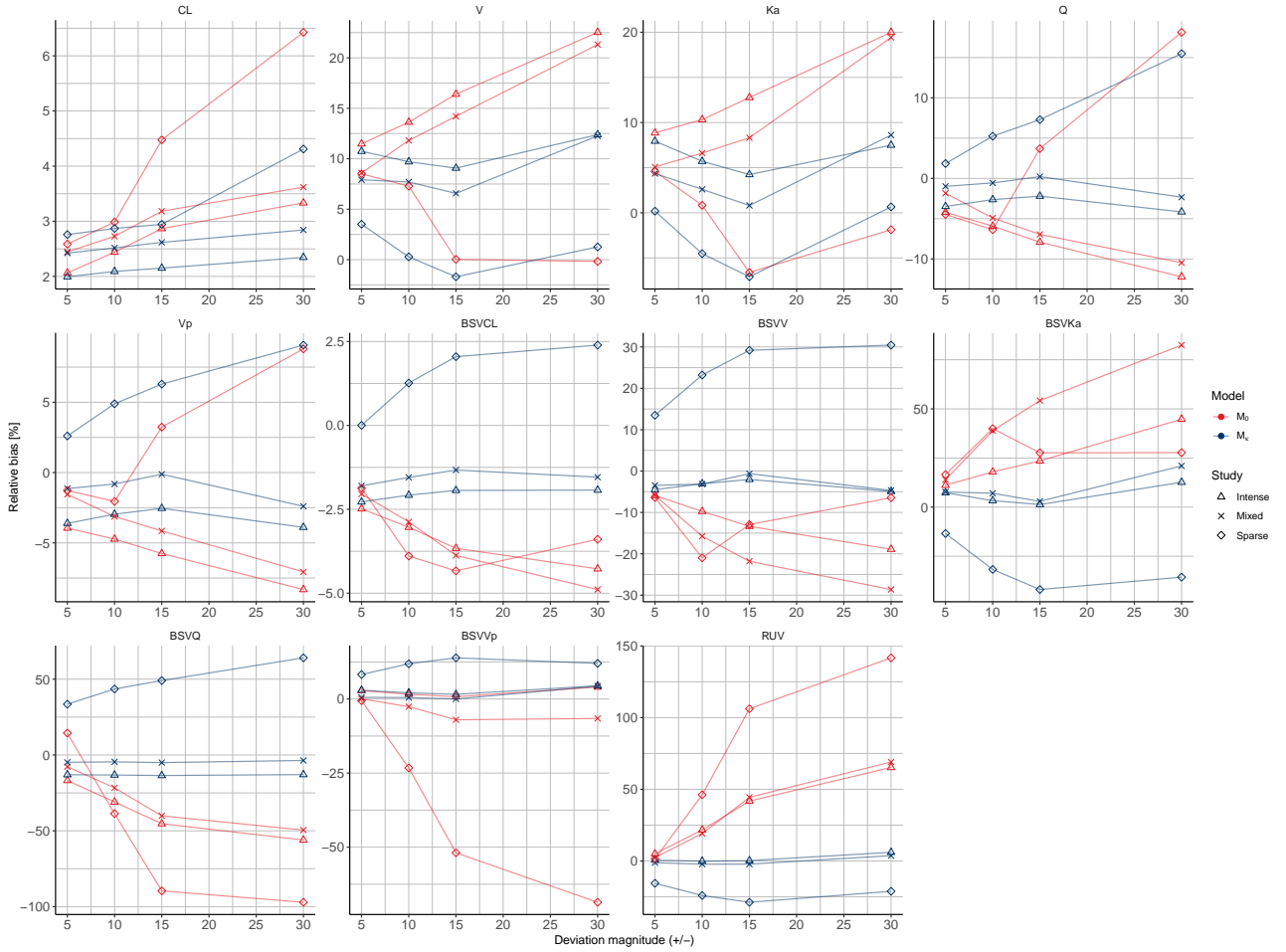


Figure 4.2: Comparison of the relative bias (yaxis) for the null model (red) and kappa model (blue) stratified on study design and percentage of error. Error magnitudes are shown on the x-axis. Panel A present 100% of samples are affected by error; Panel B present 50% of samples are affected by error; Panel C 20% of samples are affected by error.

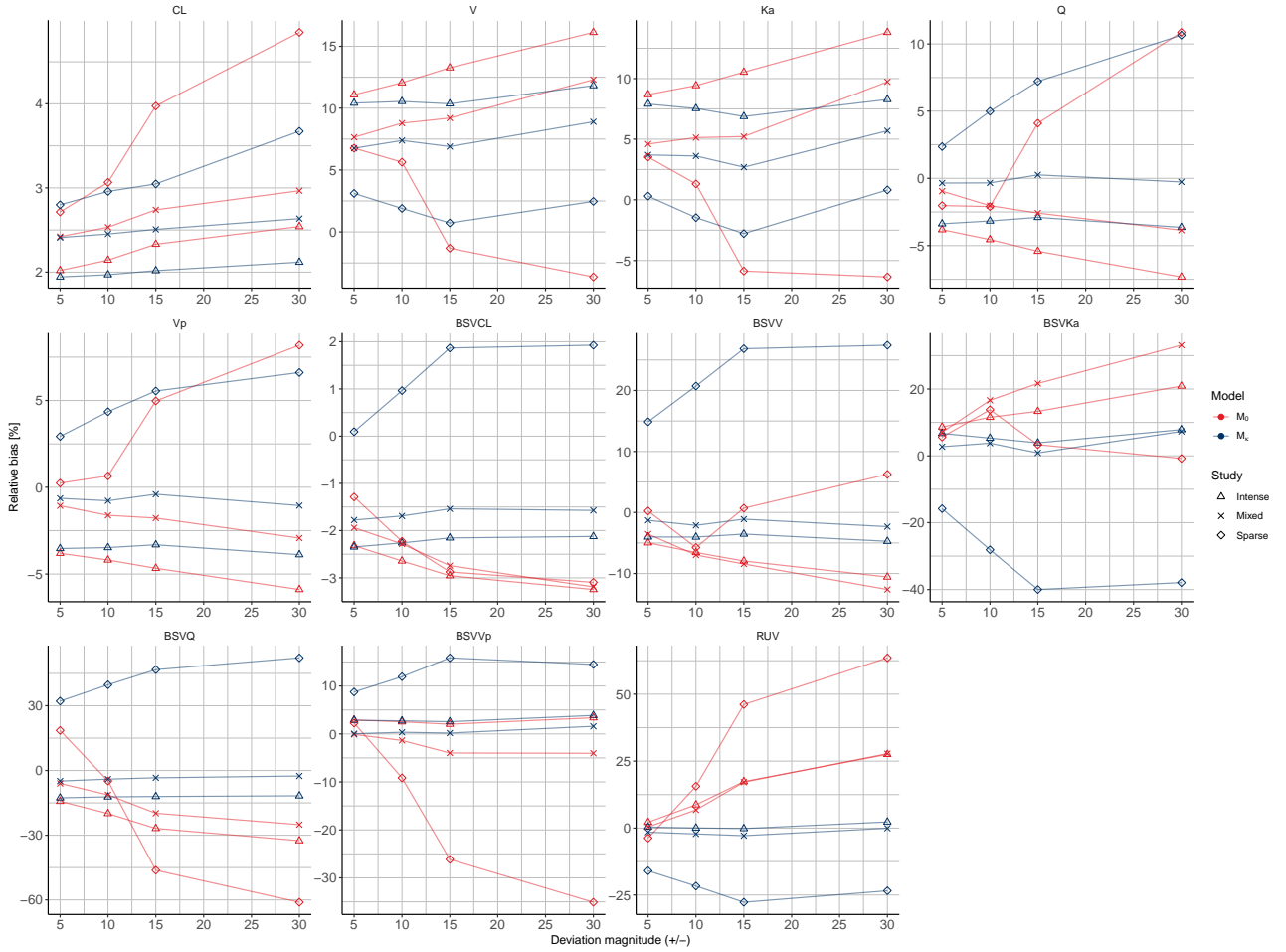


Figure 4.3: Comparison of the relative bias (yaxis) for the null model (red) and kappa model (blue) stratified on study design and percentage of error. Error magnitudes are shown on the x-axis. Panel A present 100% of samples are affected by error; Panel B present 50% of samples are affected by error; Panel C 20% of samples are affected by error.

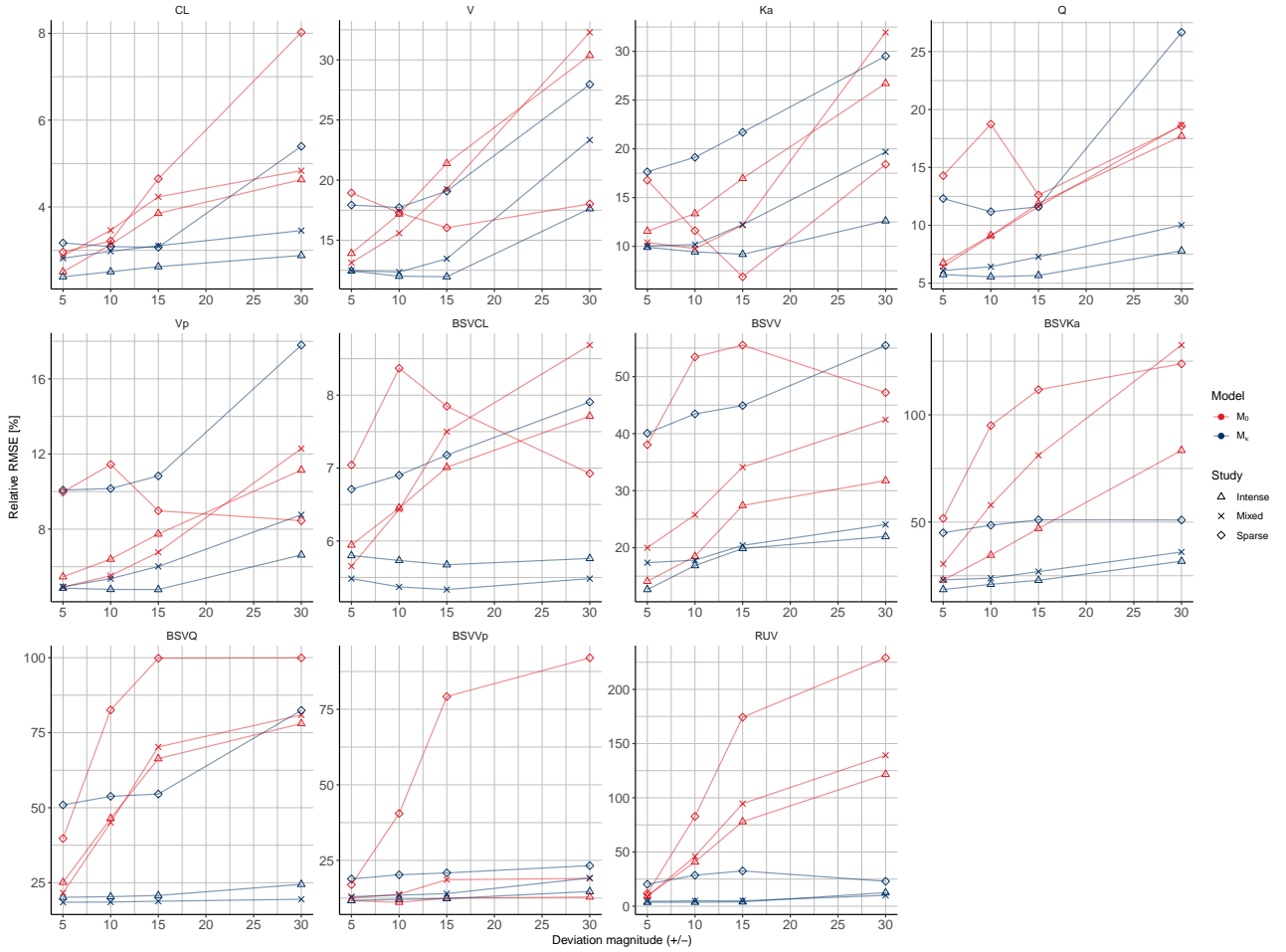


Figure 4.4: Comparison of the relative root mean squared error (yaxis) for the null model (red) and kappa model (blue) stratified on study design and percentage of error. Error magnitudes are shown on the x-axis. Panel A present 100% of samples are affected by error; Panel B present 50% of samples are affected by error; Panel C 20% of samples are affected by error.

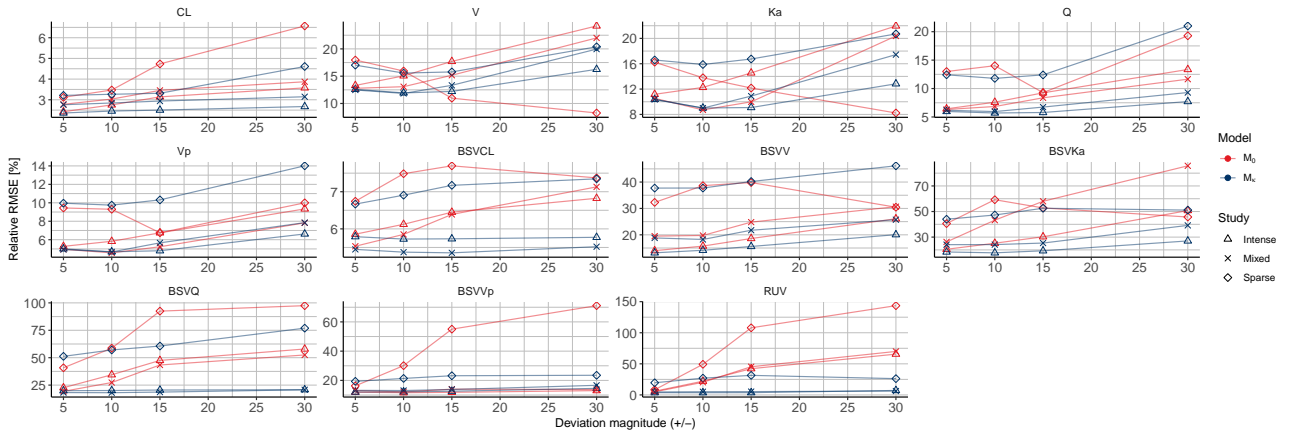


Figure 4.5: Comparison of the relative bias (yaxis) for the null model (red) and kappa model (blue) stratified on study design and percentage of error. Error magnitudes are shown on the x-axis. Panel A present 100% of samples are affected by error; Panel B present 50% of samples are affected by error; Panel C 20% of samples are affected by error.

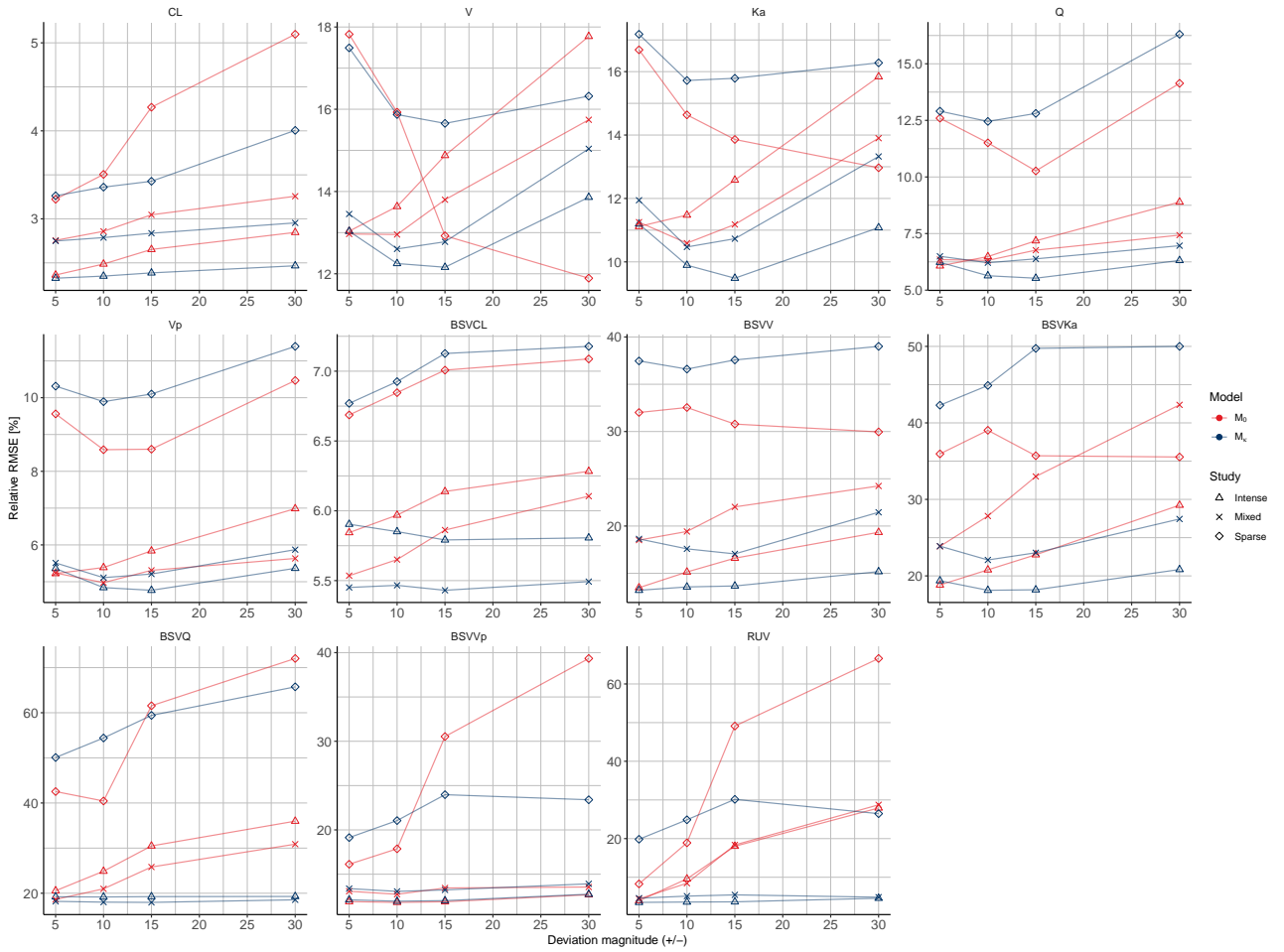


Figure 4.6: Comparison of the relative bias (yaxis) for the null model (red) and kappa model (blue) stratified on study design and percentage of error. Error magnitudes are shown on the x-axis. Panel A present 100% of samples are affected by error; Panel B present 50% of samples are affected by error; Panel C 20% of samples are affected by error.

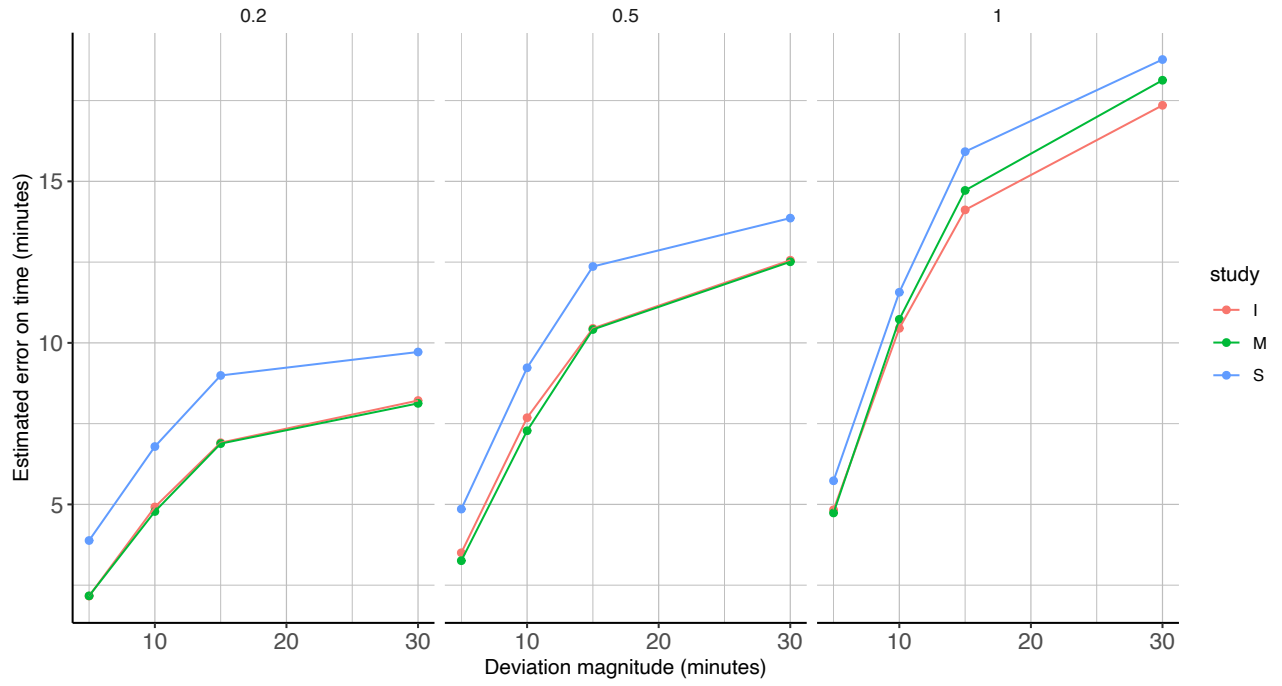


Figure 4.7: True simulated deviation (x axis) and estimated deviation using kappa model (y -axis) stratified on the affected percentage in the experimental unit and colored by study design.

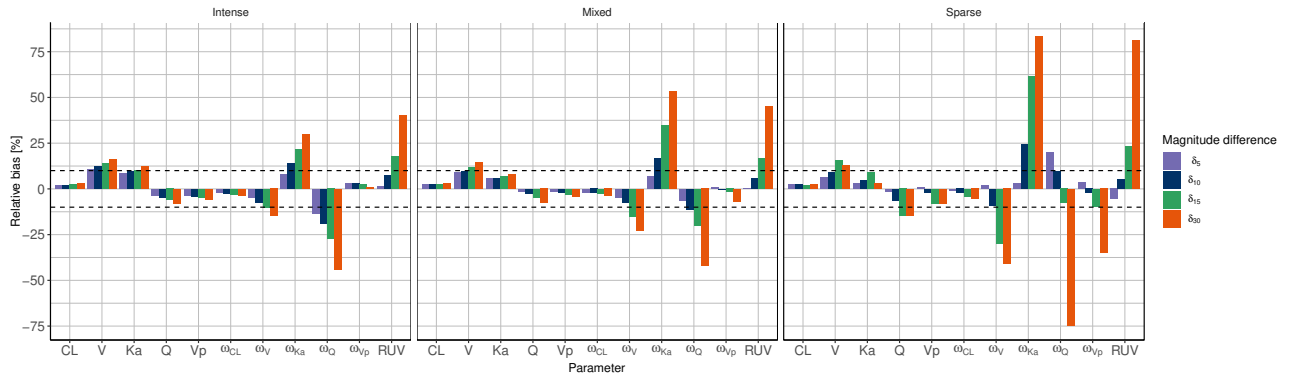


Figure 4.8: The magnitude difference (δ) between the actual time and recorded time. Panel (A) present the relative bias; Panel (B) present the root mean squared error.

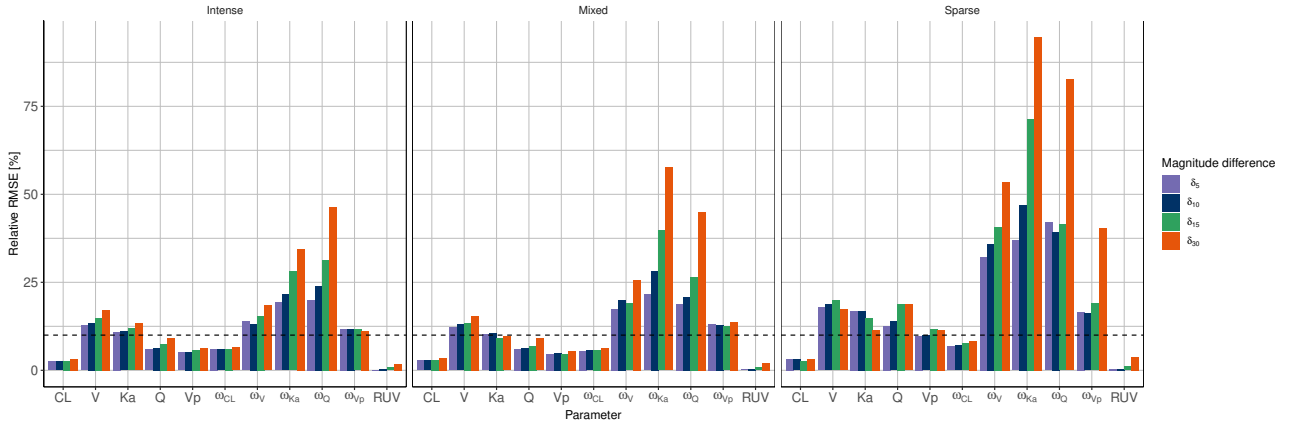


Figure 4.9: The magnitude difference (δ) between the actual time and recorded time. Panel (A) present the relative bias; Panel (B) present the root mean squared error.

Chapter 5

Evaluation of bias in weighted residual calculations when handling below the limit of quantification data

This work is published as a perspective in *Clinical Pharmacology and Therapeutics: Pharmacometrics and Systems Pharmacology*:

Mutaz M Jaber, Shen Cheng, and Richard C Brundage. Evaluation of bias in weighted residual calculations when handling below the limit of quantification data using beals m3 method. *CPT: pharmacometrics & systems pharmacology*, 10(4):275, 2021a

5.1 Overview

Concentration data below the limit of quantification (BLQ) are common in population pharmacokinetic (PK) analyses, and one method used to accommodate these during nonlinear mixed effects modeling is the M3 method. We aim in this study to examine the potential bias in weighted residual plots when M3 is applied, and a simulation study was conducted to evaluate this bias. Weighted-residual bias in subjects with BLQ data was found to be small and probably ignorable in both intense and sparse sampling designs.

5.2 Perspective

Weighted residuals, both traditional weighted residuals (WRES) and conditional weighted residuals (CWRES), are common metrics to graphically evaluate model acceptability in population analyses Nguyen et al. [2017]. They represent the difference between the observed concentration and the prediction under the model, which are then weighted to standardize and decorrelate the residuals. WRES and CWRES are commonly plotted against TIME and population predictions and are expected to be randomly scattered around zero with the bulk of the data points within two standard deviation units.

Limited by the lower limit of quantification (LLOQ) of analytical techniques, it is not uncommon to have concentrations reported as below the LLOQ (BLQ) in PK studies. Although various approaches have been proposed to accommodate BLQ data, Beal [2001], Ahn et al. [2008], Bergstrand and Karlsson [2009] Beal’s M3 method currently appears to be most common. It integrates the likelihood function over the interval $[-\infty; \text{LLOQ}]$ and maximizes the likelihood of the concentration being BLQ with respect to model parameters. However, by default, the M3 method suppresses the computation of the entire set of weighted residuals for any subject with at least one BLQ observation.

In a 2010 NONMEM Users Network Archive thread, NMU [2010] it was suggested that this was a bug in the NONMEM software (ICON plc Development Solutions). Tom Ludden provided an historical perspective that Stuart Beal intentionally excluded the calculation of weighted residuals for each subject with BLQ data due to a concern that all weighted residuals for that subject might be biased. A particularly lucid explanation was contributed by Matt Hutmacher, acknowledging that “residu-

als do not provide great diagnostic value unfortunately for data sets with censored data. BQL observations influence the fit through the censored likelihood, but these observations are not represented in the residual diagnostic plots.”

Although the concern for bias is real, recent NONMEM functionality, MDVRES (missing dependent variable for residual calculation), Bauer [2011] allows one to easily obtain previously suppressed weighted residuals for concentrations above the LLOQ in subjects that have at least one concentration reported as BLQ. While using the M3 method, assigning MDVRES = 1 to censored BLQ data excludes the residuals from being calculated for these observations while allowing residuals to be computed for observations above LLOQ. Our recent question raised in the forum NMU [2020] motivated us to conduct a simulation study to investigate the extent to which weighted residual calculations in subjects having some BLQ data might be biased when using the M3 method together with MDVRES. It was not our intent to evaluate bias in decisions made based on plots using weighted residuals.

Simulations were performed assuming a one-compartment PK model with a depot compartment using mrgsolve package version 0.10.1. Elmokadem et al. [2019]. Between-subject variability (BSV) was assumed to be log-normally distributed. Parameter values (and BSV) used for this simulation were the following: clearance (CL) 8.0 L/h/70 kg (20%), volume of distribution (V) 25.0 L/70 kg (25%), and absorption rate constant 1.5 h⁻¹ (30%). The residual error model (RUV) used in the simulation was a proportional error model with a coefficient of variation (CV) of 15%. Normally distributed body weights with a mean of 70 kg and a standard deviation of 10 kg were used for scaling CL (allometric exponent 3/4) and V (allometric exponent 1).

Each in silico subject received a dose of 100 mg. Sampling strategies were chosen to

assure that most simulated concentrations would be neither above nor below LLOQ. Two scenarios were considered. In the first scenario (scenario 1), single doses in a rich sampling scheme were assumed with concentrations simulated at 0.5, 1, 1.5, 2, 3, 4, 6, 9, and 12 h after dosing. In a second scenario (scenario 2), a sparse sampling scheme was assumed with dosing at steady state as might be seen in a clinical outpatient study. The administration of 100 mg doses every 12 h was simulated with 60% of subjects providing three samples and 40% of subjects providing four samples. Samples were randomly collected at approximately 0.5, 2, 6, and/or 12 h. A total of 1000 subjects were simulated for each scenario. From the simulated data set for each scenario, reduced data sets were created that included observations labeled as BLQ. An LLOQ was chosen as 0.1 mg/L to produce data sets in which approximately 50% of subjects had at least one BLQ observation. The reduced data set for scenario 1 included 48% of subjects with a BLQ observation at 12 h. In addition, 12% of those subjects also had BLQ data at 9 h, and 0.2% also demonstrated BLQ data at 6 h. For scenario 2, 40% of subjects demonstrated a BLQ observation at the 12-h trough collection.

Analysis was performed with the first-order conditional estimation with interaction algorithm using ADVAN2/TRANS2 subroutine in NONMEM 7.5 (ICON Development Solutions). The full data set containing no BLQ data in each scenario was analyzed to provide our least biased estimates of CWRES and WRES in the standard manner. The two data subsets that include BLQ observations were analyzed with the M3 method, and MDVRES functionality was used to allow the calculation of the weighted residuals for subjects with BLQ observations. The results from these scenario-paired analyses were nearly identical with the difference in all parameter values being <3%. WRES and CWRES from these four analyses were tabulated. From these four tables of weighted residuals, subsets were constructed that contained weighted

residuals from only subjects who had at least one BLQ observation as these are the residuals suspected of bias. The resulting weighted residual subsets, heretofore called SUBSET and M3, were compared to evaluate bias for both scenario 1 and scenario 2

Bias was evaluated at the population level, and because the original concern was that residuals for the entire individual could be biased, we also evaluated bias at the individual level. Bias was evaluated at the population level by plotting the paired CWRES (and WRES) for M3 versus SUBSET data. The averages and 95% confidence intervals (CIs) of the CWRES (WRES) without regard to individual identification numbers for the SUBSET and M3 data sets in both scenarios were also calculated. Finally, the pairwise deviations between the SUBSET CWRES (WRES) and the M3 CWRES (WRES) data were calculated. The mean and 95% CIs of the paired deviations were computed to determine the overlap in CIs.

To explore bias at the individual level, the set of weighted residuals for each individual was averaged and plotted as a histogram. Ideally, if there is no bias for an individual, the observations are expected to be randomly scattered about the predicted curve, providing an average weighted residual that is close to zero. If persistent bias existed in the predictions for an individual using the M3 method, the average of the weighted residuals could be large in either a positive or negative direction. For example, in scenario 1 with eight residuals calculated in most individuals, we considered a weighted residual sum that exceeds ± 8 standard deviation units, for an average exceeding ± 1 unit, as an indication that substantial bias might exist for that subject. The means and 95% CIs of these individual average weighted residuals were computed and compared between the SUBSET and M3 data. Finally, the pairwise deviations between the means of the individual average weighted residuals calculated with the SUBSET and the M3 data sets were plotted as a histogram for each scenario. The mean and 95% CIs of the pairwise deviations were also calculated.

For bias evaluation at the population level, the CWRES calculated with the M3 method align well with the SUBSET CWRES in both scenarios (Figure 1, upper panels). Although the WRES calculated with M3 method align well with the SUBSET WRES in scenario 1, the alignment in scenario 2 exhibits a distinct pattern (Figure 1, lower right panel). Although small, the very lowest WRES tend to be upwardly biased, whereas higher WRES tend to be downwardly biased. This pattern is largely absent in scenario 1, although the very highest WRES tend to be slightly downwardly biased (Figure 1, bottom left). The means of CWRES (WRES) in the SUBSET and M3 data sets are comparable and the 95% CIs overlap (Table 1, top).

For bias evaluation at the individual level, the 95% CIs of the means of individual average weighted residuals between the SUBSET and M3 data sets overlap in both scenarios, suggesting a difference that is not significant (Table 1, bottom). Histograms of the individual average weighted residuals also indicate that the distributions of individual average weighted residuals are comparable between SUBSET and M3 (Figures S1 and S2). In addition, histograms of individual average weighted residuals for both scenarios demonstrate that most of them are within the range of ± 1 standard deviation units with few individuals outside the range, although it is clear that the distribution of weighted residuals is wider for scenario 2 than scenario 1. The 95% CIs of the pairwise deviations do not include zero, and this deviation bias can readily be seen in the histograms (Figure S3). However, the mean deviations are quite small at less than 0.1 standard deviation units. These small deviations may simply be because of different amounts of data available for fitting between the two data sets. Also contributing to these deviations may be the nonnormality of these weighted residual distributions.

5.3 Conclusions

We conclude that bias in CWRES and WRES can be detected but is small and unlikely to impact decisions made based on weighted residual-based diagnostic plots when the M3 method with MDVRES is performed to accommodate BLQ observations in the scenarios we studied. However, the scope of the scenarios examined in this Perspective is limited and does not explore situations such as multicompartment models, alternative random effects models, the range of CVs in the RUV model, other sampling designs, or varying amounts of BLQ data. Hence, it is always good practice to evaluate goodness of fit using several approaches when looking for reasons to revise a particular model.

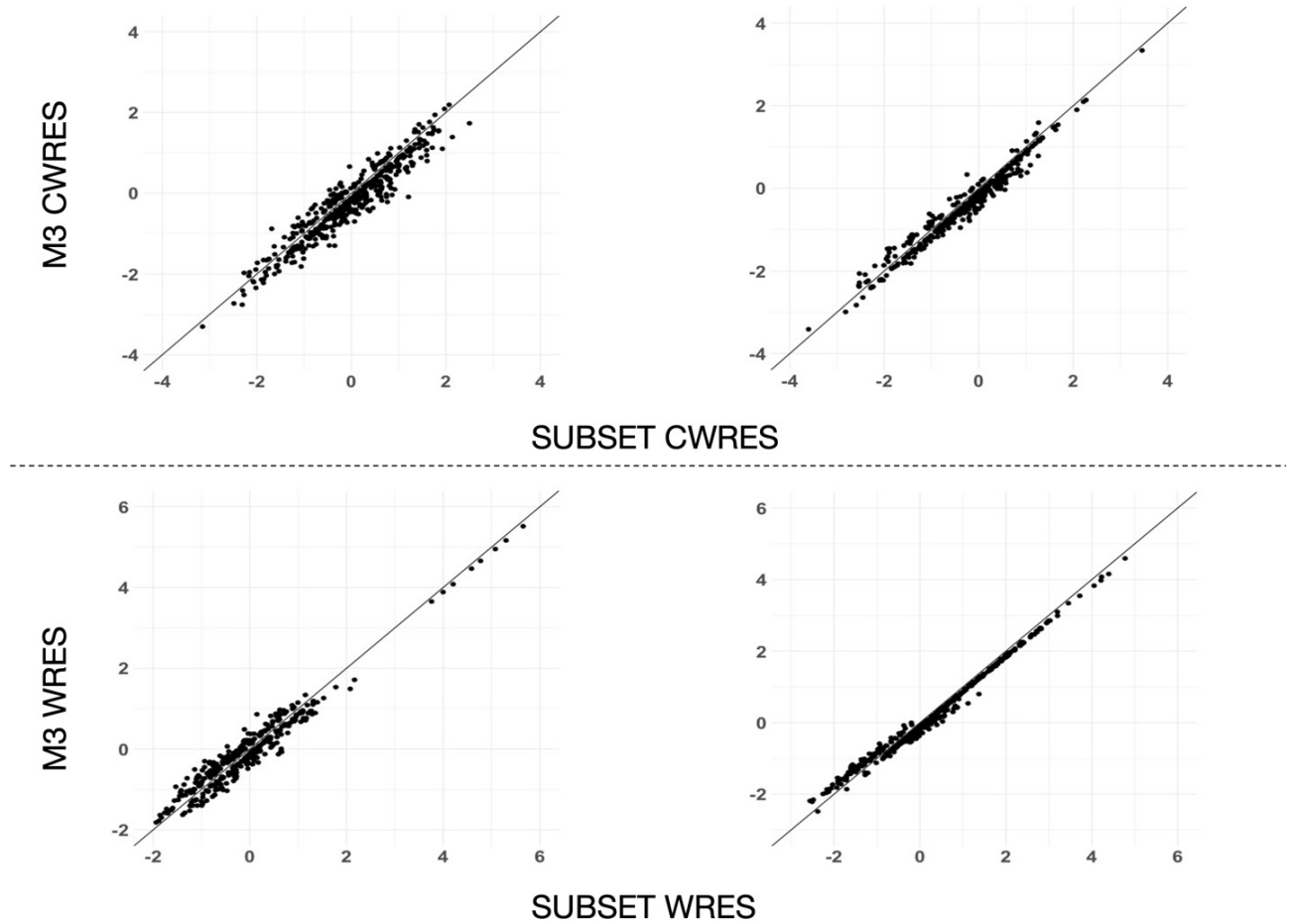
5.4 Tables

Table 5.1: Bias calculations on population and individual levels

POPULATION-LEVEL BIAS			
	SUBSET	M3	Pairwise Deviations Mean (95% CI)
	Mean (95% CI)	Mean (95% CI)	
Scenario 1: Intensive Sampling			
CWRES	-0.100 (-0.133, -0.067)	-0.138 (-0.170, -0.106)	-0.038 (-0.042, -0.034)
WRES	-0.036 (-0.069, -0.003)	-0.055 (-0.088, -0.023)	-0.019 (-0.022, -0.016)
Scenario 2: Sparse Sampling			
CWRES	-0.305 (-0.369, -0.242)	-0.390 (-0.451, -0.329)	-0.085 (-0.094, -0.076)
WRES	-0.188 (-0.255, -0.122)	-0.249 (-0.308, -0.187)	-0.059 (-0.068, -0.051)
INDIVIDUAL-LEVEL BIAS			
Scenario 1: Intensive Sampling			
CWRES	-0.106 (-0.139, -0.073)	-0.144 (-0.177, -0.111)	-0.038 (-0.041, -0.035)
WRES	-0.041 (-0.073, -0.009)	-0.059 (-0.092, -0.027)	-0.018 (-0.022, -0.016)
Scenario 2: Sparse Sampling			
CWRES	-0.352 (-0.415, -0.288)	-0.435 (-0.497, -0.374)	-0.084 (-0.091, -0.076)
WRES	-0.227 (-0.285, -0.169)	-0.286 (-0.341, -0.230)	-0.058 (-0.065, -0.051)

5.5 Figures

Figure 5.1: Weighted residuals for both the SUBSET and the M3 data in both scenarios. Upper panels present CWRES; Lower panels present WRES. Left panels present scenario 1; Right panels present scenario 2. The absolute values of the WRES and CWRES less than 0.1 units in all plots were censored to improve clarity.



Chapter 6

Individualized Absorption Models in Population Pharmacokinetic Analyses

This work has been published in *Clinical Pharmacology and Therapeutics: Pharmacometrics and Systems Pharmacology*:

Mutaz M. Jaber, Mahmoud Al-Kofahi, Kyriakie Sarafoglou, and Richard C. Brundage. Individualized absorption models in population pharmacokinetic analyses. *CPT: Pharmacometrics & Systems Pharmacology*, 9(6):307–309, 2020. doi: <https://doi.org/10.1002/psp4.12513>

This work serves as a precursor to Chapter 7

6.1 Overview

Absorption processes are complex but rarely have sufficient data to capture parameters of a mechanistic model. Typically, a single absorption model (e.g., first-order, mixed-order, lag, or distributive delay model), is assumed to apply to all individuals with the expectation that random effects will accommodate individual differences. However, distinct absorption profiles may coexist in a given dataset. We propose that individualized absorption models should be considered when multiple absorption profiles are evident in a population analysis.

6.2 Perspective

Absorption models in pharmacokinetic studies are typically empirical. There are multiple steps for a drug product to be absorbed into the body and the granularity of the absorption process that can be determined is a function of the sampling frequency. When sampling is relatively limited, simpler absorption models are preferred because inadequate data are available to support a more complicated model. Upon ingesting a tablet, it disaggregates, disperses, and the drug must go into solution before being absorbed, usually in the duodenum. Even ignoring complicating issues with poor aqueous solubility, the highest rates of absorption are not likely to occur for some time after administration. Nonetheless, the first-order absorption model does dictate that the maximal transfer of drug into the central compartment occurs immediately upon dosing. This model misspecification is largely accepted as ignorable as there are usually little data to suggest a more complicated absorption process is needed. Furthermore, confidence intervals around absorption parameters are usually quite large (often with relative standard errors $> 100\%$) and include zero. That does not mean we do not need an absorption parameter, but does speak to our contention that the absorption model is a mathematical necessity that allows the drug concentration to be zero (or low) at time zero and increase over time.

Given the physical reality of the pre-absorption steps that occur, our models are generally a highly simplified convenience. Looked at this way, the absorption process becomes little more than a nuisance model, at least from a pharmacokinetic perspective. However, one cannot always ignore early exposures and there are examples when the absorption process is associated with clinical outcomes (Swanson et al. [1999], Gomeni et al. [2017], U.S. Food and Drug Administration [2015]). In such cases, it is necessary to have an appropriate study design to collect samples when

they make a difference, have an absorption model that reasonably reflects those observations, and have an outcome model that links early exposure to outcome. This would be particularly important in simulation projects that are optimizing dosing to outcomes.

Absorption models become more complicated when we move into population pharmacokinetic analyses. One may examine absorption in a population via a concentration-time plot and make a decision to use, for example, a first-order absorption model. This practice, however, can mask a multitude of misspecifications. It might initially seem that a simple absorption model might be sufficient from inspection of the pooled data, but, on closer examination, a more complicated absorption profile may be observed in individual profiles. Some drugs demonstrate an observed delay in absorption or multiple irregular peaks and more complicated models have been described (Holford et al. [1992], Koch et al. [2014], Savic and Karlsson [2006]) to accommodate these observations. Indeed, mechanism-based absorption models have been described and successfully applied (Hénin et al. [2012]) as have mixture models (Woillard et al. [2011]). However, they become quite complicated and require considerable data to estimate the parameters.

Beyond our compelling fanaticism to predict all observations as closely as possible, perhaps the reason we invest time in considering the absorption process is that it may influence other estimated parameters in an adverse way. Many long-term survivors of nonlinear mixed-effects model building have examples of absorption misspecification impacting other parameters. Notably, the estimates of volume of distribution (V/F) or perhaps bioavailability may be biased, with upwardly biased estimates of the population variability, while total apparent clearance seems less likely to be sensitive to model misspecification in absorption.

In practice, we typically assume there is a single absorption process whether the model is simple or complex. However, it may not be the case that all subjects exhibit the same absorption profile. Some subjects may seem to have a first-order process, whereas other profiles may be better described using an Erlang process (Matis and Wehrly [1990]). In an Erlang model, for example, the post hoc absorption transit rate constant for someone with an apparent first-order absorption could be quite large, although it would be estimated to be smaller for another individual with a more distributed delay absorption process. We justify a single absorption process by assuming the random effect will accommodate individual differences, leading to the overall result of a decidedly large population variability.

The concept of using different absorption processes for different groups is not foreign. It is what we often do when we create a FAST/FED covariate in our data sets. That co- variate may be useful to identify differences in the rates (KA) or extents (F) of absorption between two groups, or allow parameters to change within an individual in crossover studies.

It may be the case that no covariate is available to explain a difference in absorption profiles. One may postulate two groups and create a mixture model that allows any individual to be in one group or the other. However, that level of sophistication is perhaps unnecessary, particularly if one considers absorption to be more of a nuisance process. Our contention is that it may be possible to examine data from an individual and make a reasonable assignment to an appropriate group. Although such an approach may be sufficiently arbitrary to make one uncomfortable, it need not. The difference in absorption between two subjects may be immediately obvious on visual inspection. There has been little discussion in the community regarding the selection of different absorption models at the individual level within a single

population analysis when absorption data are limited.

In this perspective, we wish to provide an example to illustrate differences seen when prespecifying the absorption model for each individual by visual inspection of the data from a cohort of children with congenital adrenal hyperplasia being treated with hydrocortisone. The study was approved by the University of Minnesota Institutional Review Board. Informed consents and assents were obtained. Concentration-time data consisting of 682 hydrocortisone observations from 53 patients were subject to a population analysis. Samples were obtained at 0, 0.25, 0.5, 0.75, 1, 1.25, 1.5, 2, 2.5, 3, 4, and 6 hours. Upon visual inspection of the data, it became obvious that three distinct absorption profiles existed (see Figure 1). It seemed that absorption data from many subjects would conform to a simple first-order absorption process ($n = 20$). Many others demonstrated a delayed absorption process, which would conform to an Erlang model with four transit compartments ($n = 21$) (Matis and Wehrly [1990]). Finally, some subjects demonstrated distinct shoulders on the peak indicating a double peak process ($n = 12$) (Lee et al. [2015]). The input process for such a model does become more complicated, but it is tractable. It requires two dosing depot compartments with the fraction of the total dose split between each compartment being estimated. One dose was put into the first transit compartment of the distributed-delay model (delayed fraction), whereas the remaining dose was placed in a depot compartment immediately prior to the central compartment (first-order). The schematic for each of these models is provided in Figure S1. We fit the data using NONMEM version 7.4 (ICON Development Solutions) with first-order conditional estimation method with interaction to each of three approaches that differed in terms of absorption assignment: (i) all subjects assigned to first-order absorption; (ii) all subjects assigned to Erlang absorption; and (iii) assignment via visual inspection to first-order, Erlang, or the shoulder model. For the visual assignment, two authors

(M.M.J. and R.C.B.) classified and agreed upon the patterns.

The differences among the three analyses are summarized in Table 1. As expected, prespecifying the absorption process based on visual inspection provided the lowest objective function value, with the longest computational times. Because this is not a formal simulation study, the degree of bias and imprecision that exists in the estimates cannot be commented on. Nonetheless, the total apparent clearance point estimate and variability changed little across the three analyses, whereas the estimates for V/F were more affected. Although the differences are relatively small, it is apparent that the choice of the absorption model does influence V/F . It was also noted that the residual unexplained variability was not highly sensitive to the absorption model, although more of a difference from the visual assignment approach was expected given that approximately half of our data were obtained during the absorption phase.

If one accepts that different individuals may need different absorption models, by extension, different doses for each individual may perhaps require different absorption models. Many intensively sampled population PK studies are single dose and this is a moot point. However, when intensively sampled multiple dose studies involving a drug with variable absorption patterns are being analyzed, it may become important to consider the visual inspection of absorption data to choose the more relevant absorption model for each individual at each dose. This can easily be envisioned with a subject that has a variable lag time for absorption on two different doses. A single realization of the random effect will split the difference and may not fit either profile well. This case might be accommodated by incorporating between-occasion variability into the model but this will not always be useful.

Limitations of visual inspection could arise from personal bias for a particular

model; the time commitment required to classify each individual when data sets are large; and the need for a procedure to resolve ambiguous absorption data.

6.3 Conclusion

Early exposures may be important in drug therapy and an accurate description of early concentrations is desirable that requires more intensive sampling after the dose. With more intensive sampling, the likelihood of observing different absorption profiles is increased. In conclusion, it may be conventional, but it is not necessary, that one choose a single absorption model to be applied to all individuals in a population analysis. We suggest that the visual inspection of absorption profiles can be used to assign different individuals to different absorption models. Our perspective is that we should embrace those differences and feel comfortable assigning different models on an individual-by-individual or even dose-by-dose basis.

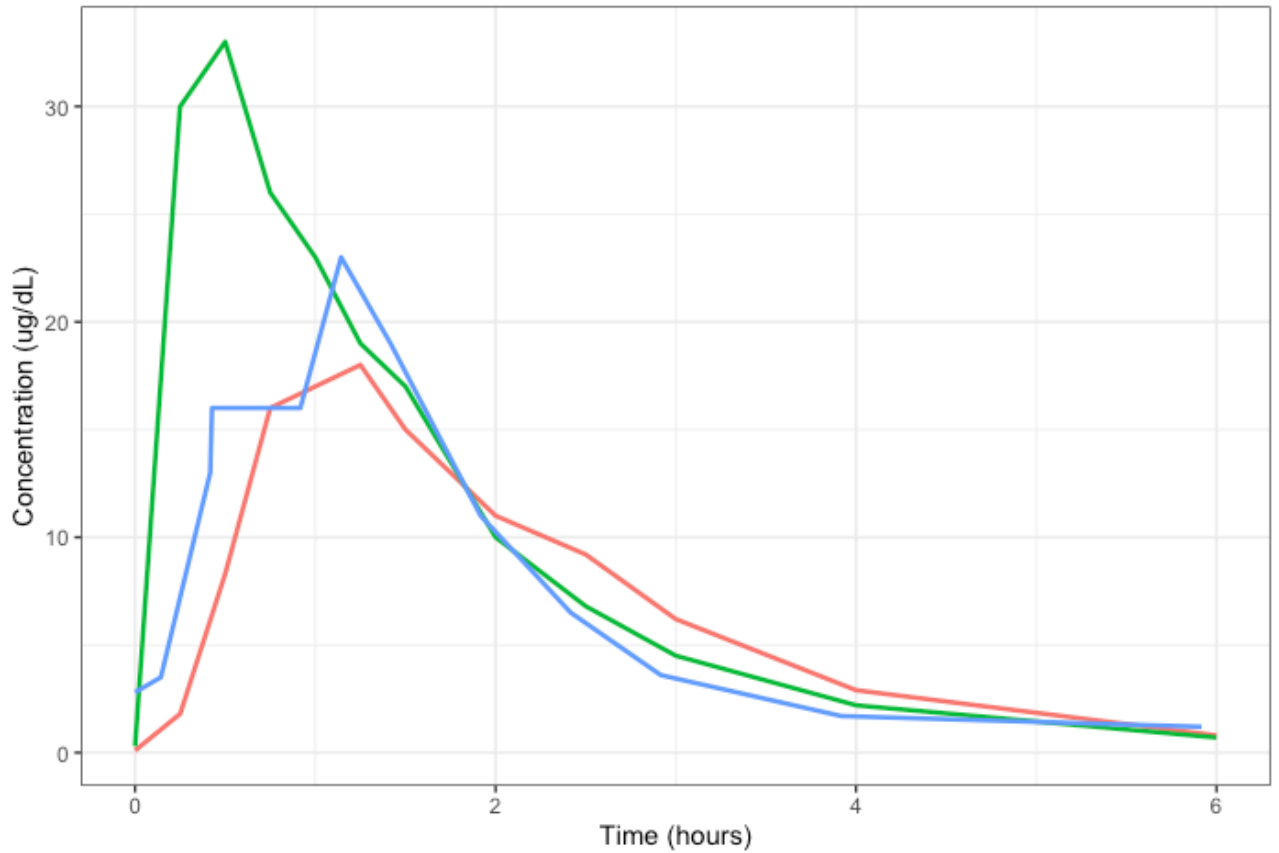
6.4 Tables

Table 6.1: Comparison of key analysis metrics

	First order	Erlang	Visual assignment
Objective function	1740.16	1559.57	1455.61
BIC	1817.5	1653.3	1571.6
CL/F (L/hr)	22.8 (29%)	22.6 (29%)	22.9 (29%)
V/F (L)	35.4 (16%)	41.2 (21%)	39.0 (23%)
KA (hr^{-1})	1.96 (49%)	-	3.29 (48%)
KTR (hr^{-1})	-	10.5 (40%)	7.7 (29%)
Residual variability (% CV)	23	18	17
Computational time (sec)	1136	2703	3212

6.5 Figures

Figure 6.1: Observed concentration-time profile for three representative subjects, each demonstrating a different absorption shape: first order process (green), an Erlang absorption process (red), and shoulder model for simultaneous distributed-delay and first-order processes (blue).



Chapter 7

Application of Deep Neural Networks in Pharmacokinetic Analysis

This work has been published in *pharmaceutics 2021*:

Mutaz M Jaber, Burhaneddin Yaman, Kyriakie Sarafoglou, and Richard C Brundage. Application of deep neural networks as a prescreening tool to assign individualized absorption models in pharmacokinetic analysis. *Pharmaceutics*, 13(6):797, 2021b

7.1 Overview

A specific model for drug absorption is necessarily assumed in pharmacokinetic (PK) analyses following extravascular dosing. Unfortunately, an inappropriate absorption model may force other model parameters to be poorly estimated. An added complexity arises in population PK analyses when different individuals appear to have different absorption patterns. The aim of this study is to demonstrate that a deep neural network (DNN) can be used to prescreen data and assign an individualized absorption model consistent with either a first-order, Erlang, or split-peak process. Ten thousand profiles were simulated for each of the three aforementioned shapes and used for training the DNN algorithm with a 30% hold-out validation set. During the training phase, a 99.7% accuracy was attained, with 99.4% accuracy during in the validation process. In testing the algorithm classification performance with external patient data, a 93.7% accuracy was reached. This algorithm was developed to prescreen individual data and assign a particular absorption model prior to a population PK analysis. We envision it being used as an efficient prescreening tool in other situations that involve a model component that appears to be variable across subjects. It has the potential to reduce the time needed to perform a manual visual assignment and eliminate inter-assessor variability and bias in assigning a sub-model.

7.2 Introduction

In population pharmacokinetic/pharmacodynamic (PK/PD) modeling, specific structural models are chosen to characterize the shape of the observed concentrations or effects vs. time. These structures are usually obvious and common to all subjects. However, sometimes additional consideration needs to be given to the absorption process from the depot compartment to the central compartment. Given the biological complexity that underlies absorption models and the inherent variability associated with the processes across individuals, it is not surprising that data from different individuals in a dataset may need different models to describe the data. In population analyses, two approaches are frequently used. We might completely ignore the model misspecification that exists in some individuals and allow the inflation of between-subject variability (BSV) and residual unexplained variability (RUV) to accommodate the misspecification; or we might assume a more highly complex model and borrow parameter information from those subjects who are able to support the complexity of the model while letting others shrink toward the typical values of the estimates. When observations taken during the period of drug absorption are sparse, the choice of absorption model or even their specific parameter values are likely trivial and have little impact on the remaining parameter estimates (Wade et al. [1993]). In addition, the relative sparse sampling during absorption generally results in absorption parameter estimates with high imprecision (large relative standard errors) and frequently large BSV. However, as the frequency of observations taken during absorption increases, the complexities of drug absorption become apparent and obvious misspecification can sometimes be seen in diagnostic plots. Although the absorption sub-model can be adapted to provide a better fit to the data, the increased complexity of the model will then require an increased frequency of sampling at critical times to capture those absorption parameters with acceptable precision. A further complicating consideration can occur in population PK analyses as the intensity of

sampling during absorption increases. Some subjects might clearly demonstrate one absorption pattern while others a different pattern. Nonetheless, a single absorption model is generally assumed. Examples of more involved techniques such as mechanistic models (Hénin et al. [2012]), or mixture modeling (Kaila et al. [2007]) have been applied in these situations.

Machine learning is gaining wider attention in clinical pharmacology as computational capacity increases. Methods for machine learning use statistical algorithms that are capable of doing automated learning from existing data to uncover patterns (Murphy [2012], Jones et al. [2017], Angermueller et al. [2016], McComb et al. [2021], Gong et al. [2018]). Deep learning is a branch of machine learning that involve artificial neural networks in their structure to facilitate developing algorithms capable of learning from data [5,6]. Neural networks are not new to clinical pharmacology and have been applied in response classification, dose selection, and quantitative system pharmacology model reduction (Huang et al. [2020], Saleh and Alzubiedi [2014], Derbalah et al. [2021]).

We have recent experience in a population PK analysis in which the absorption process demonstrated concentration-time profiles that, while not apparent on standard mean or spaghetti plots, appeared on closer examination to have individuals that conform to either a first-order, Erlang, or a split-peak process, depending on the individual. Our initial approach was to fit a Erlang-distribution absorption model to the data (Al-Kofahi et al. [2021]). Given that the specifics of the absorption process weren't of primary importance, the input process was considered a trivial component of the analysis. Subsequently we explored visually prescreening the individual profiles to make an assignment of the absorption model prior to modeling the data (Jaber et al. [2020]). It was an interesting exercise, but we found this procedure to

be less than satisfactory as visually assessing the profiles took considerable time and demonstrated inter-rater variability. The exercise motivated us to seek an alternative approach in assigning the absorption model. The goal of this study was to build a deep neural network (DNN) algorithm to recognize these absorption profiles and apply it to our data as a means to evaluate the performance of the method in assigning the absorption model structure for each individual.

7.3 Methods

In this section we introduce the reader to the methods used in this study. It is divided among five parts; real world data, PK parameter estimation; simulation of PK profile to create training dataset; development/training of deep neural network (DNN); and evaluation of DNN.

7.3.1 Observed Data and Visual Assignment

The data used for this study are previously described in a nonlinear mixed-effects analysis of cortisol (Al-Kofahi et al. [2021]). Briefly, after the study was approved by the University of Minnesota Institutional Review Board (Project 1209M21101 approved on 5 July 2017). Following each subject’s morning dose at 0800, 12 concentrations were obtained at times 0 (Predose), 0.25, 0.5, 0.75, 1, 1.25, 1.5, 2, 2.5, 3, 4, and 6 hours after the dose. Concentration-time data consisting of 682 cortisol observations from 53 patients were available. Post-publication, we visually assessed the concentration-time data and assigned each individual as having either a first-order absorption process ($n = 20$), absorption consistent with an Erlang distributed delay model ($n = 21$), or a split-peak absorption process (mixed first-order, and Erlang models; $n = 12$) Jaber et al. [2020] These absorption patterns are exemplified in Figure 1.

7.3.2 Estimation of Pharmacokinetic Model

With these individualized absorption models assigned, we performed an additional population PK re-analysis that estimated the parameters of the pre-specified absorption models in addition to clearance (CL) and the volume of distribution (V). NONMEM 7.5 (ICON plc development LLC) using first-order estimation with interaction (FOCE-I) was used. Figure 2 illustrates the pharmacokinetic structural models

of the three absorption profiles. Table 1 presents the final parameter estimates from the re-analysis. The NONMEM control stream, and individual profiles of observed and predicted concentrations as linear (Figure S1) and semi-log (Figure S2)

7.3.3 Simulation of Training Profiles

The parameters from the above analysis were used to generate simulated data sets for training the DNN. Between-subject and residual unexplained variability random effects were included in the simulation to assure a different profile for each simulated individual. For the purpose of training the DNN, simulations were based on a standard 20-kg subject with a 10-mg dose being administered. Concentrations were simulated at the same 12 time points as the external dataset. Ten thousand profiles were simulated for each of the three distinct absorption models (first-order, Erlang, and split-peak shapes) with CL and V shared among the three absorption models. The R package `mrgsolve` v0.10.7 used for the simulations Elmokadem et al. [2019].

These simulated concentration-time profiles were then standardized using the Feature scaling method Juszcak et al. [2002], in Equation (1) to standardize all concentrations between zero and one while maintaining the shape of the profile.

$$CS_{i,j} = \frac{C_{i,j} - C_{min,j}}{C_{max,j} - C_{min,j}} \quad (7.1)$$

where $CS_{i,j}$ is the i th standardized concentration for the j^{th} individual, $C_{i,j}$ is the i th simulated concentration for the j^{th} individual, $C_{min,j}$ is the minimum concentration for the j^{th} individual, and $C_{max,j}$ is the maximum concentration for the j^{th} individual. From this simulated dataset of 30,000 standardized profiles, 30% (10% from each absorption model) were randomly selected as hold-out validation data to evaluate the performance of the algorithm during the training.

7.3.4 Deep Learning Algorithm

The open-source R library packages TensorFlow version 2.2 and Keras version 2.0 were used to develop the DNN algorithm. A DNN consists of an input layer, hidden layers, and an output layer. Each hidden layer consists of a number of nodes that represents the computational unit. The output from each node in a layer will propagate as input to each node of the subsequent layer. More formally, the layers of a DNN and a diagram of one node is presented in Figure 3. Equation (2) presents the output of a given node.

$$y_{n,l} = f\left(b_l + \sum_{n=1}^N x_n w_{n,l-1}\right) \quad (7.2)$$

where $y_{n,l}$ is the output value of the n^{th} node in the l^{th} layer. b_l is the bias in the l^{th} layer, N represents the number of nodes in layer $l - 1$ (the previous layer), x_n is the value of n^{th} node that is being propagated forward from layer $l - 1$, and $w_{n,l-1}$ is the weight associated with the n^{th} input from the $l - 1$ layer to the n^{th} node in the l^{th} layer. $f(.)$ is the activation function defined in the algorithm (vide infra)

In our case, the input layer consisted of the 12 Feature-scaled simulated concentrations (CS_{i,j}) at the aforementioned sampling times for each of the simulated subjects. The number of hidden layers was sequentially tested from 1 to 6 and evaluated using the resulting accuracy and loss function value (vide infra). The final output from the DNN was simply the probability that the data set was represented by each of the three absorption profiles (first-order, Erlang, or split-peak).

ReLU was used as a linear activation function at the hidden layers for each node and the softmax activation was used in the last layer (output) for the purpose of classification Nwankpa et al. [2018]. Categorical cross-entropy was defined as the

loss function Zhang and Sabuncu [2018] with a batch size of 32 over 100 epochs.

7.3.5 Evaluation

The “true” absorption profile shape was taken to be the shape decided by visual inspection in the estimation process and used for the accuracy determinations. At the end of the training phase, the overall categorical cross-entropy loss function value for both the training data split (70%) and the validation data split (30%) was calculated and the accuracy of the algorithm was evaluated using the number of correct predictions over the total number of simulated profiles (training and validation) in the dataset Alaiz-Moreton et al. [2019]. The accuracy selection is based on the index of the highest probability in a vector of three indexes that represent the probabilities of the three absorption shapes. Hence, if the predicted and observed shape match, it will count as an accurate prediction.

Of the 53 external subject profiles, 5 profiles were not complete datasets and 48 profiles from the PK study were used as external data to evaluate the algorithm classification performance as a prescreening tool. The percentages of correct classifications were calculated using a confusion matrix that summarizes the performance of algorithm prediction in comparison to the “true” absorption profile. In addition, the accuracy rate was compared to the uninformative rate (correct classification due to chance) of the external data to determine the extent to which the algorithm chose the correct shape using a binomial test with $p < 0.05$ regarded as significant.

7.4 Results

No improvement was noted in the accuracy or in the loss function value when increasing the number of hidden layers beyond three and all results are shown for

three hidden layers. Table 2 summarizes the number of profiles used in training, validation and external datasets with corresponding overall accuracy and the values of loss function.

Classification results are presented in Table 3 as a confusion matrix and contains the percentages of predicting the correct shape on the diagonal and the percentage of choosing the incorrect model on the off diagonals. A difference between the accuracy rate of 93.7% and the uninformative rate of 45.8% was significant ($p < 0.001$).

Of the 45 correct decisions, all were above the probability of 0.75; 89% exceeded a probability of 0.9 ($N = 40$). For the three incorrect decisions, the probabilities were 0.53, 0.50, 0.56, while the true shape probabilities were 0.47, 0.48, and 0.42, respectively. Figure 5 displays a histogram of the probabilities of the classifications for all 48 subjects.

7.5 Discussion

The suggested DNN algorithm can be used in the pre-modeling setting but it must be recognized that the approach might be most appropriate when the precision of a sub-model is perhaps of little consequence as with absorption. The *raison d'être* of the method can be stated as an approach to minimize the potential of having misspecification in one sub-model adversely affect the estimation of parameters in another part of the model, say, clearance or volume of distribution. It is important to note that our visual labeling of a profile as the “true shape” does not make it truth. A “true shape” does not exist in real data. It is encouraging that when the DNN algorithm is not in agreement with the original visual classification, the certainty of that decision is low as evidenced by lower probabilities. Indeed, when the DNN

probabilities are relatively balanced across outcomes as we observed with incorrect classifications, the choice of pattern is likely inconsequential.

Mixture models are an alternative approach in addressing these issues. It assumes that a given parameter distribution can be composed of 2 or more subpopulations and the software will compute the probability of being in each subpopulation and classify each individual to the subpopulation that is most probable Kaila et al. [2007]. Although applying a mixture model to absorption may minimize misspecification of another part of the PK model, this approach will likely consume several degrees of freedom during the estimation step. Additionally, it is noteworthy that the computational time is increased. To our knowledge, while mixture models are frequently used to better understand multimodal parameter distributions, they have not yet been applied to classify subjects into having one of several competing absorption models.

Knowledge of the steps and processes involved with pharmacokinetics are becoming better understood and the complexities of absorption are captured by physiologically-based mechanistic models that have been adapted to explain differences in absorption profiles Bergstrand et al. [2012]. However, due to the intensive demand of these models for prior information, approximate mechanistic models have been developed. A gastro-intestinal transit time model (GITT) Hénin et al. [2012] was used to characterize the timing of tablet movement in the intestine using a step function based on prior information, and with the help of mixture modeling, different absorption rates in different GI regions were estimated. Ruiz-Garcia et al. Ruiz-Garcia et al. [2020] observed non-standard absorption profiles for dacomitinib with and without proton pump inhibitors. They evaluated a series of increasingly complex absorption models before assuming a global transit compartment model. As is the usual case, it does not appear that they attempted to allow more than one absorption model across the

subjects. A more complicated method to describe absorption process has been suggested by Csajka et al. [2005] where they described the absorption after the administration of hydromorphone and verapride by the sum of inverse Gaussian functions. Although empirical, this method was able to describe complicated absorption shapes such as the double peak phenomena with much more flexibility than simpler ones, was also able to characterize BSV. A more complicated empirical method using fractional-order kinetics have been suggested to describe anomalous absorption kinetics based upon drug dissolution processes Dokoumetzidis and MacHeras [2009].

With all the simplifications that are often imposed on the absorption process, it is not always trivial. The early exposure of drug is certainly affected by drug absorption characteristics and has been shown to be important since it is associated with the onset of response and clinical outcomes. This has led the US Food and Drug Administration to issue draft guidances for methylphenidate U.S. Food and Drug Administration [2015], hydromorphone U.S. Food and Drug Administration [2014], and amantadine U.S. Food and Drug Administration [2011]. This underscores the potential importance of the absorption process, particularly in the development of generic formulations.

A limitation of this report is that the current DNN algorithm has been developed and trained using parameters from a cortisol population-based PK analysis, and then using that same data as the external data set for qualification. A more fair assessment would of course be to use an independent data set, but one wasn't available. The purpose of this report is to demonstrate the potential utility of using DNN to classify model components. It has not been applied to another situation and it might be the case that the DNN will need to be trained uniquely with data relevant to each setting.

It is also recognized that while the training sets were balanced across the shapes, the external dataset were not. We acknowledge that the approach may perform differently with drugs having different PK characteristics. DNN algorithms are by nature data-driven and this approach can be used in conjunction with pharmacometrics analyses to improve model building and estimation process. In the future, it may be possible to build these approximation functions directly into the estimation process.

7.6 Conclusions

In summary, the developed DNN algorithm was capable of predicting different absorption profiles in a population with high accuracy in both simulated and external datasets. This DNN pre-specification algorithm may reduce the computational time of a mixture model analysis and avoid consuming unnecessary degrees of freedom during estimation and may obviate the need to obtain or generate compound-specific prior information for complex physiological absorption processes. Finally, this algorithm will reduce valid concerns of inter-assessor variability and bias when visually assigning the absorption shapes.

7.7 Tables

Table 7.1: Population-level pharmacokinetic estimates and the between-subject variability (% CV) from the re-analysis used in the simulation.

Parameter	First-order	Erlang	Split-peak
CL (L/h/70 kg)		22.6 (29%)	
V (L/70 kg)		38.9 (21%)	
K_{TR} (h^{-1})	-	8.2 (23%)	5.2 (23%)
K_A (h^{-1})	3.3 (48%)	-	7.6 (48%)
Fraction (%)	-	-	78 (80%)
RUV_{prop}		16.5%	

Table 7.2: Collection of data with associated overall accuracy and loss value

Data	N	Overall Accuracy	Overall Loss Value
Training	21,000	99.7%	<0.01
Validation	9000	99.4%	<0.01
External	48	93.7%	0.17

Table 7.3: Confusion matrix presents the classification of the external patient data

DNN Prediction	Visual assignment		
	First-order	Erlang	Split-peak
First-order	18	1	1
Erlang	0	21	1
Split-peak	0	0	6

7.8 Figures

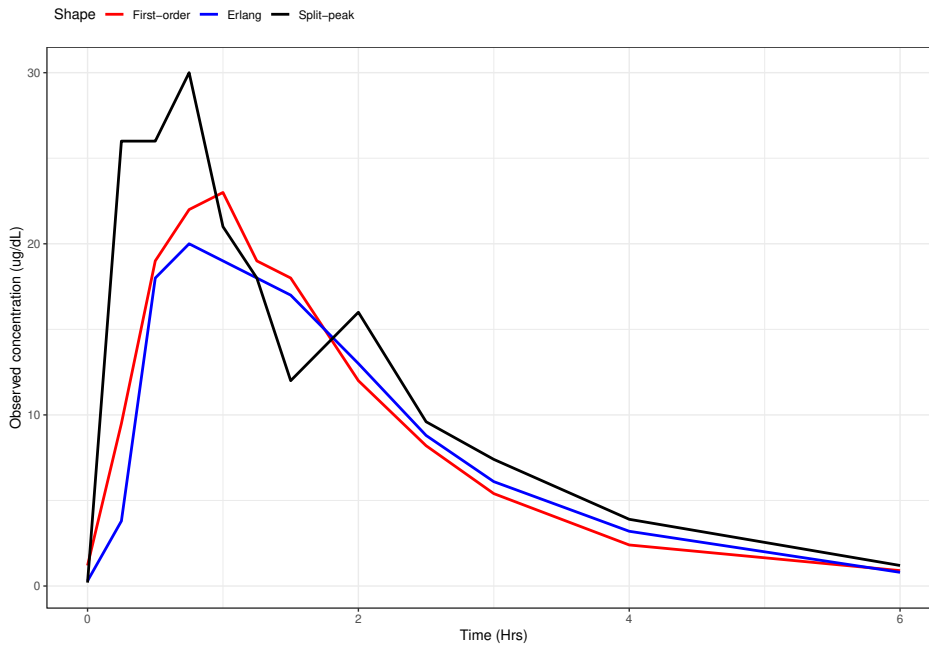
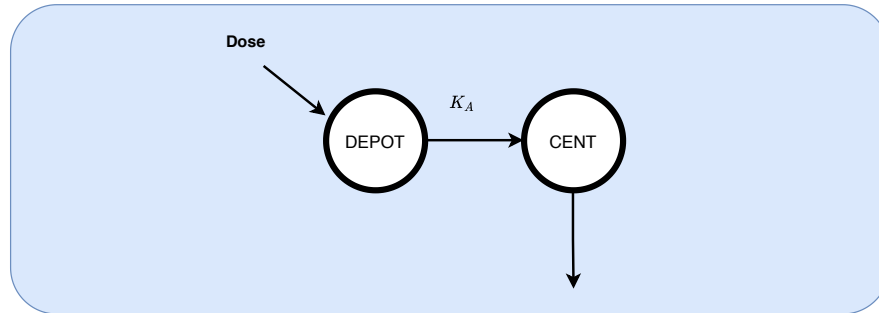


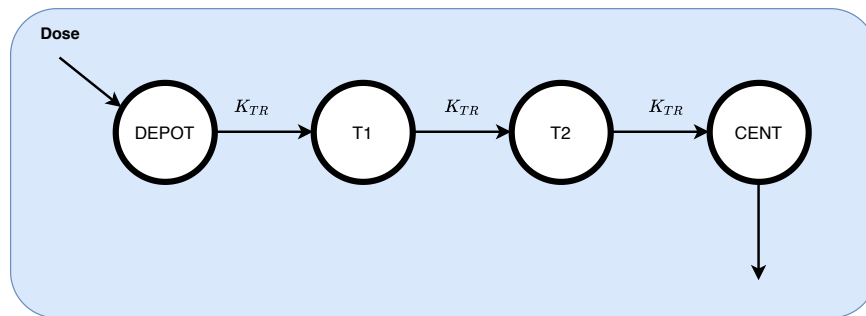
Figure 7.1: Observed concentration-time profiles for three representative shapes. (red) presents the first-order process; (blue) presents the Erlang process; (black) presents the mixed first-order and Erlang processes.

Figure 7.2: Pharmacokinetic structural models of the three absorption profiles. (A) First-order absorption; (B) Erlang absorption process; (C) Mixed first-order and Erlang absorption.

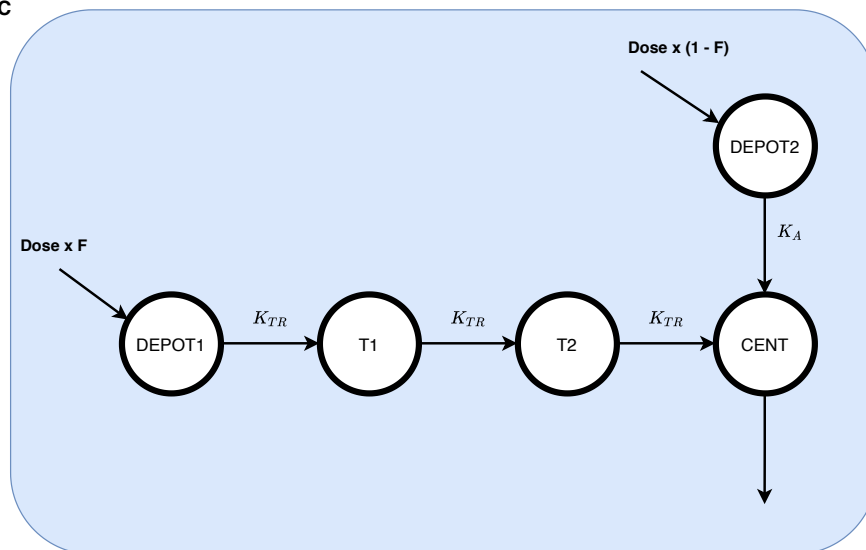
A



B



C



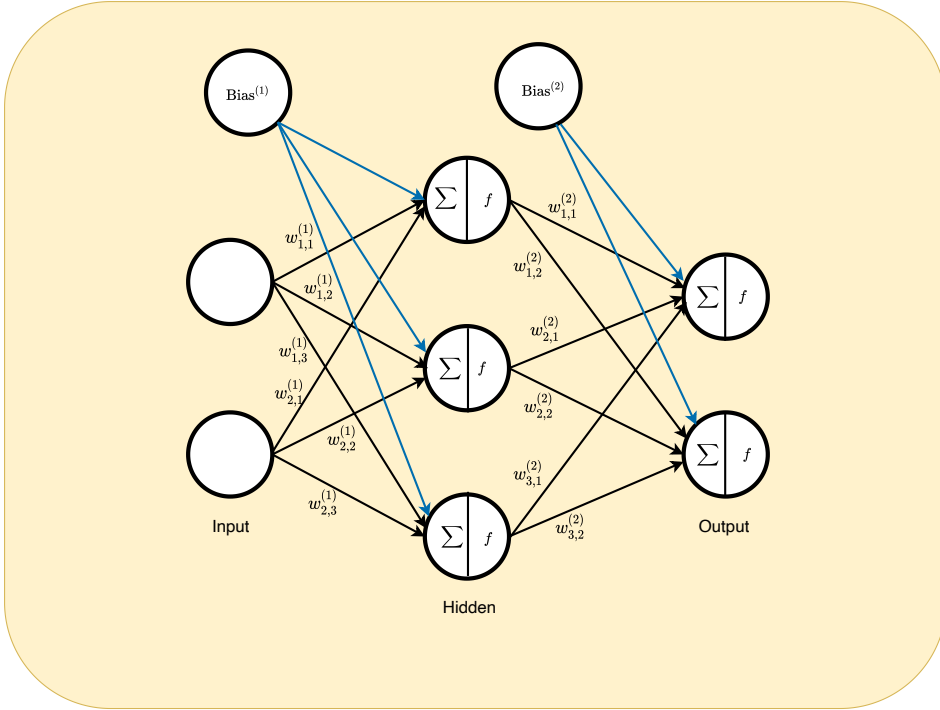


Figure 7.3: Overview of deep neural network algorithm structure.

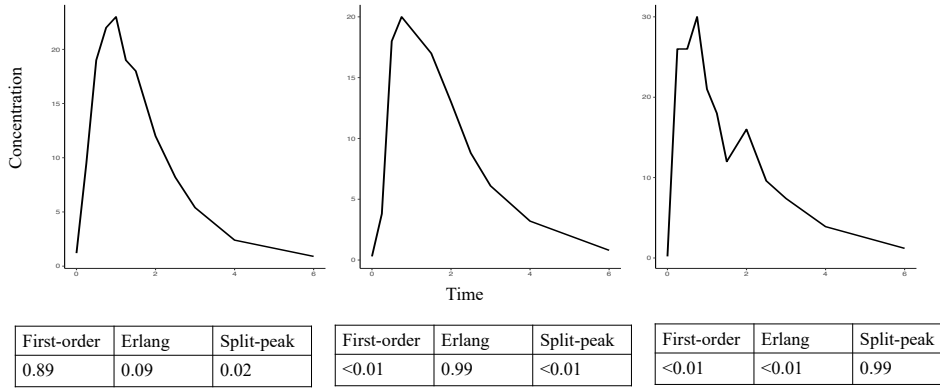


Figure 7.4: The output of the developed DNN with three examples from the external cortisol data.

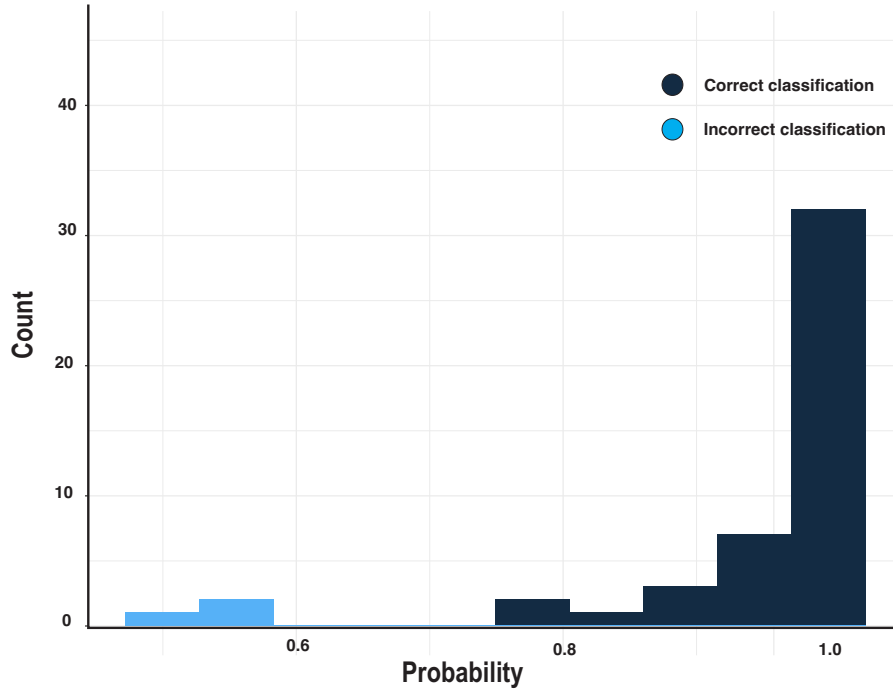


Figure 7.5: Probability counts for DNN model prediction. Dark blue presents the correct classification; Light blue presents the incorrect classification.

Chapter 8

Summary and final thoughts

The knowledge gained in this thesis will advance our abilities to individualize patient care and to further use pharmacometric methodologies to help patients. We anticipate that understanding sources of variability will help us give recommendations and insight to the clinical and pharmacometrics community that will guide clinical studies and better inform model-informed drug development.

In chapter 3, we assessed the contribution of hypothetical sources of variability in RUV that occur during NLMEM modeling and offer these takeaway points:

- I Pharmacostatistical model misspecifications were associated with relatively large increases in the magnitude of RUV compared to other sources for all levels of study design.
- II The contribution of dose misspecification, and dosing time misspecifications have negligible effects on RUV but result in biased PK parameter estimates.
- III Inaccurate documentation of sampling time results in biased RUV magnitude which is sensitive to the magnitude of perturbations, and this effect was greater with more intense sampling designs.

Errors of the type studied here are real and do occur in PK studies. It is important to consider the question of what one wants to answer from the analysis. For example, if one is primarily interested in drug clearance, then some of these perturbations have less consequence. Nonetheless, as pharmacometricians, we don't have control over the perturbations and our challenge is to choose a pharmacostatistical model that adequately explains the data provided to us. This work provides information that can be used to understand and give insight for the interpretation of RUV magnitude. It may lead to recommendations from the pharmacometrics community that favor results from studies with lower RUV and minimize the "believability" of studies with large RUV.

Limitations of this study include that we did not study the inadequacy of covariate models nor the inaccurate documentation of covariates. We also did not assess the unexplained variability in scenarios with multiple dosing, other PK/PD models, or misspecification in covariate, BSV or BOV models. Finally, our misspecifications were chosen under an assumption of a well-controlled clinical trial. Bias and imprecision findings are likely to be higher in studies that include outpatient dosing and multiple dosing studies that assume steady-state conditions.

In chapter 4, we found adding an additional random effect term to erroneous independent variables measured in clinical trials would reduce the bias in parameter estimation. The magnitude of error can result in more bias and necessitate intervention. In terms of PK sampling times, it is advised to withdraw the sample at the times specified in the protocol. The pharmacometric analyst however can take comfort in understanding that samples drawn within 5 minutes of the recorded time will cause little bias and imprecision. Despite the limited scenario settings, we believe this work will give general insight on the ways to handle suspected data recorded with time de-

viations and appreciate that deviations in time can affect our mode-based informed decisions.

A future direction of this work can be extended to assess the performance of an additional random effect on time to handle multiple independent variables and it would be of interest to quantify a correlation among the errors in independent variables. Moreover, this work can be expanded to evaluate correction error models in pharmacodynamic study and the implication on clinical outcomes.

In chapter 5, We conclude that bias in CWRES and WRES can be detected but is small and unlikely to impact decisions made based on weighted residual-based diagnostic plots when the M3 method with MDVRES is performed to accommodate BLQ observations in the scenarios we studied. However, the scope of scenarios examined in this Perspectives paper is limited and does not explore situations such as multi-compartment models, alternative random-effects models, the range of CVs in the RUV model, other sampling designs, or varying amounts of BLQ data. Hence, it is always good practice to evaluate goodness-of-fit using several approaches when looking for reasons to revise a particular model.

Finally, in chapter 6 & 7, we assess model individualization and suggested a tool for prespecifying absorption models using deep neural networks (DNN). The developed DNN algorithm was capable of predicting different absorption profiles in a population with high accuracy in both simulated and external datasets. This DNN pre-specification algorithm may reduce the computational time of a mixture model analysis and avoid consuming unnecessary degrees of freedom during estimation and may obviate the need to obtain or generate compound-specific prior information for complex physiological absorption processes. Finally, this algorithm will reduce valid

concerns of inter-assessor variability and bias when visually assigning the absorption shapes. A limitation of this report is that the current DNN algorithm has been developed and trained using parameters from a cortisol population-based PK analysis, and then using that same data for qualification. A fairer assessment would of course be to use an independent data set, but one wasn't available. The purpose of this report is to demonstrate the potential utility of using DNN to classify model components. It has not been applied to other situations and it might be the case that the DNN will need to be trained uniquely with data relevant to each setting. It is also recognized that while the training sets were balanced across the shapes, the external dataset was not. We acknowledge that the approach may perform differently with drugs having different PK characteristics. DNN algorithms are by nature data driven and this approach can be used in conjunction with pharmacometrics analyses to improve model building and estimation process. In the future, it may be possible to build these approximation functions directly into the estimation process.

References

Bibliography

Nmusers discussion group. res and wres output with beals m3 method. <https://www.cognigen.com/nmusers/2010-April/2444.html>, 2010.

Nmusers discussion group. m3 method wres, and cwres. <https://www.cognigen.com/nmusers/2020-September/7971.html>, 2020.

Jae Eun Ahn, Mats O Karlsson, Adrian Dunne, and Thomas M Ludden. Likelihood based approaches to handling data below the quantification limit using nonmem vi. *Journal of pharmacokinetics and pharmacodynamics*, 35(4):401–421, 2008.

Mahir K Al-Banna, Andrew W Kelman, and Brian Whiting. Experimental design and efficient parameter estimation in population pharmacokinetics. *Journal of pharmacokinetics and biopharmaceutics*, 18(4):347–360, 1990.

Mahmoud Al-Kofahi, Mariam A. Ahmed, Mutaz M. Jaber, Thang N. Tran, Brian A. Willis, Cheryl L. Zimmerman, Maria T. Gonzalez-Bolanos, Richard C. Brundage, and Kyriakie Sarafoglou. An integrated pk-pd model for cortisol and the 17-hydroxyprogesterone and androstenedione biomarkers in children with congenital adrenal hyperplasia. *British Journal of Clinical Pharmacology*, 87(3):1098–1110, 2021. doi: <https://doi.org/10.1111/bcp.14470>.

- Hesham S Al-Sallami, Daniel FB Wright, and Stephen B Duffull. The propagation of between-subject variability from dose to response. *British Journal of Clinical Pharmacology*, 88(4):1414–1417, 2022.
- Hector Alaiz-Moreton, Jose Aveleira-Mata, Jorge Ondicol-Garcia, Angel Luis Muñoz-Castañeda, Isaías García, and Carmen Benavides. Multiclass Classification Procedure for Detecting Attacks on MQTT-IoT Protocol. *Complexity*, 2019, 2019. ISSN 10990526. doi: 10.1155/2019/6516253.
- Dzenefa Alihodzic, Astrid Broecker, Michael Baehr, Stefan Kluge, Claudia Langebrake, and Sebastian Georg Wicha. Impact of inaccurate documentation of sampling and infusion time in model-informed precision dosing. *Frontiers in pharmacology*, 11, 2020.
- Stéphanie Allasonnière and Estelle Kuhn. Stochastic algorithm for bayesian mixture effect template estimation. *ESAIM: Probability and Statistics*, 14:382–408, 2010.
- Christof Angermueller, Tanel Pärnamaa, Leopold Parts, and Oliver Stegle. Deep learning for computational biology. *Molecular Systems Biology*, 12(7):878, 2016. doi: <https://doi.org/10.15252/msb.20156651>. URL <https://www.embopress.org/doi/abs/10.15252/msb.20156651>.
- Kyle T. Baron. *mrgsolve: Simulate from ODE-Based Models*. Metrum Research Group, 1.0.4 edition, 2022.
- Robert J Bauer. Nonmem users guide: introduction to nonmem 7.2. 0. *ICON Development Solutions Ellicott City, MD*, 2011.
- Stuart L Beal. Ways to fit a pk model with some data below the quantification limit. *Journal of pharmacokinetics and pharmacodynamics*, 28(5):481–504, 2001.

- Martin Bergstrand and Mats O Karlsson. Handling data below the limit of quantification in mixed effect models. *The AAPS journal*, 11(2):371–380, 2009.
- Martin Bergstrand, Erik Söderlind, Ulf G. Eriksson, Werner Weitschies, and Mats O. Karlsson. A semi-mechanistic modeling strategy for characterization of regional absorption properties and prospective prediction of plasma concentrations following administration of new modified release formulations. *Pharmaceutical Research*, 29(2):574–584, 2012. ISSN 07248741. doi: 10.1007/s11095-011-0595-2.
- Joseph Berkson. Are there two regressions? *Journal of the American Statistical Association*, 45(250):164–180, 1950.
- Youwei Bi, Jiang Liu, Lingjue Li, Jingyu Yu, Atul Bhattaram, Michael Bewernitz, Ruo-jing Li, Chao Liu, Justin Earp, Lian Ma, et al. Role of model-informed drug development in pediatric drug development, regulatory evaluation, and labeling. *The Journal of Clinical Pharmacology*, 59:S104–S111, 2019.
- Peter L Bonate. Effect of assay measurement error on parameter estimation in concentration–qtc interval modeling. *Pharmaceutical Statistics*, 12(3):156–164, 2013.
- E Burmeister Getz, KJ Carroll, J Mielke, LZ Benet, and B Jones. Between-batch pharmacokinetic variability inflates type i error rate in conventional bioequivalence trials: a randomized advair diskus clinical trial. *Clinical Pharmacology & Therapeutics*, 101(3):331–340, 2017.
- Elise Burmeister Getz, Kevin J Carroll, J David Christopher, Beth Morgan, Scott Haughie, Alessandro Cavecchi, Christopher Wiggernhorn, Hayden Beresford, Helen Strickland, and Svetlana Lyapustina. Performance of multiple-batch approaches to pharmacokinetic bioequivalence testing for orally inhaled drug products with batch-to-batch variability. *AAPS PharmSciTech*, 22(7):1–11, 2021.

- Leena Choi, Ciprian M. Crainiceanu, and Brian S. Caffo. Practical recommendations for population pk studies with sampling time errors. *European journal of clinical pharmacology*, 69(12):2055–2064, 2013.
- Chantal Csajka, David Drover, and Davide Verotta. The use of a sum of inverse gaussian functions to describe the absorption profile of drugs exhibiting complex absorption. *Pharmaceutical Research*, 22(8):1227–1235, 2005. ISSN 07248741. doi: 10.1007/s11095-005-5266-8.
- Bernard Delyon, Marc Lavielle, and Eric Moulines. Convergence of a stochastic approximation version of the em algorithm. *Annals of statistics*, pages 94–128, 1999.
- Abdallah Derbalah, Hesham S. Al-Sallami, and Stephen B. Duffull. Reduction of quantitative systems pharmacology models using artificial neural networks. *Journal of Pharmacokinetics and Pharmacodynamics*, Mar 2021. ISSN 1573-8744. doi: 10.1007/s10928-021-09742-3. URL <https://doi.org/10.1007/s10928-021-09742-3>.
- Aristides Dokoumetzidis and Panos MacHeras. Fractional kinetics in drug absorption and disposition processes. *Journal of Pharmacokinetics and Pharmacodynamics*, 36(2):165–178, 2009. ISSN 1567567X. doi: 10.1007/s10928-009-9116-x.
- Ahmed Elmokadem, Matthew M Riggs, and Kyle T Baron. Quantitative systems pharmacology and physiologically-based pharmacokinetic modeling with mrgsolve: a hands-on tutorial. *CPT: pharmacometrics & systems pharmacology*, 8(12): 883–893, 2019.
- Ene I Ette, Andrew W Kelman, Catherine A Howie, and Brian Whiting. Interpretation of simulation studies for efficient estimation of population pharmacokinetic parameters. 1993.

- R Gomeni, FMM Bressolle-Gomeni, TJ Spencer, SV Faraone, L Fang, and A Babiskin. Model-based approach for optimizing study design and clinical drug performances of extended-release formulations of methylphenidate for the treatment of adhd. *Clinical Pharmacology & Therapeutics*, 102(6):951–960, 2017.
- Xiajing Gong, Meng Hu, and Liang Zhao. Big Data Toolsets to Pharmacometrics: Application of Machine Learning for Time-to-Event Analysis. *Clinical and translational science*, 11(3):305–311, may 2018. ISSN 1752-8062 (Electronic). doi: 10.1111/cts.12541.
- David A Graves, Charles S Locke, Keith T Muir, and Richard P Miller. The influence of assay variability on pharmacokinetic parameter estimation. *Journal of pharmacokinetics and biopharmaceutics*, 17(5):571–592, 1989.
- Stefan KG Grebe and Ravinder J Singh. Lc-ms/ms in the clinical laboratory—where to from here? *The Clinical biochemist reviews*, 32(1):5, 2011.
- Emilie Hénin, Martin Bergstrand, Joseph F. Standing, and Mats O. Karlsson. A mechanism-based approach for absorption modeling: The gastro-intestinal transit time (GITTT) model. *AAPS Journal*, 14(2):155–163, 2012. ISSN 15507416. doi: 10.1208/s12248-012-9324-y.
- N Holford, SC Ma, and BA Ploeger. Clinical trial simulation: a review. *Clinical Pharmacology & Therapeutics*, 88(2):166–182, 2010.
- Nicholas HG Holford, Reinhard J Ambros, and Klaus Stoeckel. Models for describing absorption rate and estimating extent of bioavailability: application to cefetamet pivoxil. *Journal of pharmacokinetics and biopharmaceutics*, 20(5):421–442, 1992.
- Ruihao Huang, Qi Liu, Ge Feng, Yaning Wang, Chao Liu, Mathangi Gopalakrishnan, Xiangyu Liu, Yutao Gong, and Hao Zhu. A novel approach for personalized response model: deep learning with individual dropout feature ranking.

Journal of Pharmacokinetics and Pharmacodynamics, 0123456789, 2020. ISSN 15738744. doi: 10.1007/s10928-020-09724-x. URL <https://doi.org/10.1007/s10928-020-09724-x>.

Donald J Irby, Mustafa E Ibrahim, Anees M Dauki, Mohamed A Badawi, Sílvia M Illamola, Mingqing Chen, Yuhuan Wang, Xiaoxi Liu, Mitch A Phelps, and Diane R Mould. Approaches to handling missing or “problematic” pharmacology data: Pharmacokinetics. *CPT: pharmacometrics & systems pharmacology*, 10(4):291–308, 2021.

Mutaz M. Jaber and Richard C. Brundage. Investigating the contribution of residual unexplained variability components in a nonlinear-mixed effect approach. In *Journal of Pharmacokinetics and Pharmacodynamics*, 2022.

Mutaz M. Jaber, Mahmoud Al-Kofahi, Kyriakie Sarafoglou, and Richard C. Brundage. Individualized absorption models in population pharmacokinetic analyses. *CPT: Pharmacometrics & Systems Pharmacology*, 9(6):307–309, 2020. doi: <https://doi.org/10.1002/psp4.12513>.

Mutaz M Jaber, Shen Cheng, and Richard C Brundage. Evaluation of bias in weighted residual calculations when handling below the limit of quantification data using beals m3 method. *CPT: pharmacometrics & systems pharmacology*, 10(4):275, 2021a.

Mutaz M Jaber, Burhaneddin Yaman, Kyriakie Sarafoglou, and Richard C Brundage. Application of deep neural networks as a prescreening tool to assign individualized absorption models in pharmacokinetic analysis. *Pharmaceutics*, 13(6):797, 2021b.

Mutaz M. Jaber, Mahmoud Al-Kofahi, and Richard C. Brundage. Evaluation of recorded time deviations on parameter estimates in nonlinear mixed-effect analyses. In *American Conference on Pharmacometrics 13*, 2022.

- Åsa M Johansson, Sebastian Ueckert, Elodie L Plan, Andrew C Hooker, and Mats O Karlsson. Evaluation of bias, precision, robustness and runtime for estimation methods in nonmem 7. *Journal of pharmacokinetics and pharmacodynamics*, 41(3):223–238, 2014.
- William Jones, Kaur Alasoo, Dmytro Fishman, and Leopold Parts. Computational biology: deep learning. *Emerging topics in life sciences*, 1(3):257–274, Nov 2017. ISSN 2397-8554. doi: 10.1042/ETLS20160025. URL <https://doi.org/10.1042/ETLS20160025>. 76782[PII].
- P Juszczak, D M J Tax, and Robert P W Duin. Feature scaling in support vector data description. *Proc. ASCI*, pages 95–102, 2002.
- Nitin Kaila, Robert J. Straka, and Richard C. Brundage. Mixture models and sub-population classification: A pharmacokinetic simulation study and application to metoprolol CYP2D6 phenotype. *Journal of Pharmacokinetics and Pharmacodynamics*, 34(2):141–156, 2007. ISSN 1567567X. doi: 10.1007/s10928-006-9038-9.
- Mats O. Karlsson, E. Niclas Jonsson, Curtis G. Wiltse, and Janet R. Wade. Assumption testing in population pharmacokinetic models: Illustrated with an analysis of moxonidine data from congestive heart failure patients. *Journal of Pharmacokinetic and Biopharmaceutics*, 26(2):207–246, 1998.
- Gilbert Koch, Wojciech Krzyzanski, Juan Jose Pérez-Ruixo, and Johannes Schropp. Modeling of delays in pkpd: classical approaches and a tutorial for delay differential equations. *Journal of pharmacokinetics and pharmacodynamics*, 41(4):291–318, 2014.
- Estelle Kuhn and Marc Lavielle. Coupling a stochastic approximation version of em with an mcmc procedure. *ESAIM: Probability and Statistics*, 8:115–131, 2004.

- Marc Lavielle and Leon Aarons. What do we mean by identifiability in mixed effects models? *Journal of pharmacokinetics and pharmacodynamics*, 43(1):111–122, 2016.
- Joo Yeon Lee, Christine E Garnett, Jogarao VS Gobburu, Venkatesh A Bhattaram, Satjit Brar, Justin C Earp, Pravin R Jadhav, Kevin Krudys, Lawrence J Lesko, Fang Li, et al. Impact of pharmacometric analyses on new drug approval and labelling decisions. *Clinical pharmacokinetics*, 50(10):627–635, 2011.
- Joomi Lee, Mi-sun Lim, Sook Jin Seong, Sung-Min Park, Mi-Ri Gwon, Seunghoon Han, Sung Min Lee, Woomi Kim, Young-Ran Yoon, and Hee-Doo Yoo. Population pharmacokinetic analysis of the multiple peaks phenomenon in sumatriptan. *Translational and Clinical Pharmacology*, 23(2):66–74, 2015.
- James H Matis and Thomas E Wehrly. Generalized stochastic compartmental models with erlang transit times. *Journal of pharmacokinetics and biopharmaceutics*, 18(6):589–607, 1990.
- Makoto Matsumoto and Takuji Nishimura. Mersenne twister: a 623-dimensionally equidistributed uniform pseudo-random number generator. *ACM Transactions on Modeling and Computer Simulation (TOMACS)*, 8(1):3–30, 1998.
- Mason McComb, Robert Bies, and Murali Ramanathan. Machine learning in pharmacometrics: Opportunities and challenges. *British Journal of Clinical Pharmacology*, (February):1–18, 2021. ISSN 13652125. doi: 10.1111/bcp.14801.
- Yann Merlé, Azzedine Aouimer, and Michel Tod. Impact of model misspecification at design (and/or) estimation step in population pharmacokinetic studies. *Journal of Biopharmaceutical Statistics*, 14(1):213–227, 2004.
- Kevin P Murphy. *Machine Learning : A Probabilistic Perspective*. MIT Press, Cambridge, UNITED STATES, 2012. ISBN 9780262305242. URL <http://ebookcentral.proquest.com/lib/umn/detail.action?docID=3339490>.

- THT Nguyen, M-S Mouksassi, Nicholas Holford, N Al-Huniti, I Freedman, Andrew C Hooker, J John, Mats O Karlsson, DR Mould, JJ Pérez Ruixo, et al. Model evaluation of continuous data pharmacometric models: metrics and graphics. *CPT: pharmacometrics & systems pharmacology*, 6(2):87–109, 2017.
- Chigozie Nwankpa, Winifred Ijomah, Anthony Gachagan, and Stephen Marshall. Activation Functions: Comparison of trends in Practice and Research for Deep Learning. pages 1–20, 2018. URL <http://arxiv.org/abs/1811.03378>.
- Klas JF Petersson, Eva Hanze, Radojka M Savic, and Mats O Karlsson. Semiparametric distributions with estimated shape parameters. *Pharmaceutical research*, 26(9):2174–2185, 2009.
- US Pharmacopeia. <905> *Uniformity of dosage units*, stage 6 harmonization edition, December 2011.
- Christopher Rackauckas and Qing Nie. Differentialequations.jl—a performant and feature-rich ecosystem for solving differential equations in julia. *Journal of Open Research Software*, 5(1):15, 2017.
- Alicia Rodríguez-Gascón, María Ángeles Solinís, and Arantxa Isla. The role of pk/pd analysis in the development and evaluation of antimicrobials. *Pharmaceutics*, 13(6):833, 2021.
- Ana Ruiz-Garcia, Weiwei Tan, Jerry Li, May Haughey, Joanna Masters, Jennifer Hibma, and Swan Lin. Pharmacokinetic Models to Characterize the Absorption Phase and the Influence of a Proton Pump Inhibitor on the Overall Exposure of Dacomitinib. *Pharmaceutics*, 12(4)(4):330, 2020. ISSN 19994923. doi: 10.3390/pharmaceutics12040330.
- Mohammad I. Saleh and Sameh Alzubiedi. Dosage individualization of warfarin using

- artificial neural networks. *Molecular Diagnosis and Therapy*, 18(3):371–379, 2014. ISSN 11792000. doi: 10.1007/s40291-014-0090-7.
- Oscar Santalo, Umima Baig, Mara Poulakos, and Daniel Brown. Early vancomycin concentrations and the applications of a pharmacokinetic extrapolation method to recognize sub-therapeutic outcomes. *Pharmacy*, 4(4):37, 2016.
- Rada Savic and Mats O Karlsson. Overview of oral absorption models and modelling issues. *Population Approach Group Europe Population Approach Group Europe*, 2006.
- Lewis B Sheiner. The population approach to pharmacokinetic data analysis: rationale and standard data analysis methods. *Drug metabolism reviews*, 15(1-2): 153–171, 1984.
- Lewis B Sheiner, Barr Rosenberg, and Vinay V Marathe. Estimation of population characteristics of pharmacokinetic parameters from routine clinical data. *Journal of pharmacokinetics and biopharmaceutics*, 5(5):445–479, 1977.
- Hanna E Silber, Maria C Kjellsson, and Mats O Karlsson. The impact of misspecification of residual error or correlation structure on the type i error rate for covariate inclusion. *Journal of pharmacokinetics and pharmacodynamics*, 36(1):81–99, 2009.
- Waroonrat Sukarnjanaset, Thitima Wattanavijitkul, and Sutep Jarurattanasirikul. Evaluation of focei and saem estimation methods in population pharmacokinetic analysis using nonmem® across rich, medium, and sparse sampling data. *European journal of drug metabolism and pharmacokinetics*, 43(6):729–736, 2018.
- He Sun, Ene I Ette, and Thomas M Ludden. On the recording of sample times and parameter estimation from repeated measures pharmacokinetic data. *Journal of Pharmacokinetic and Biopharmaceutics*, 24(6):637–650, 1996.

- James Swanson, Suneel Gupta, Diane Guinta, Daniel Flynn, Dave Agler, Marc Lerner, Lillie Williams, Ira Shoulson, and Sharon Wigal. Acute tolerance to methylphenidate in the treatment of attention deficit hyperactivity disorder in children. *Clinical Pharmacology & Therapeutics*, 66(3):295–305, 1999.
- U.S. Food and Drug Administration. Draft Guidance on Amantadine Hydrochloride. https://www.accessdata.fda.gov/drugsatfda_docs/psg/Amantadine_HCl_tab_76186_RC11-10.pdf, 2011.
- U.S. Food and Drug Administration. Draft Guidance on Hydromorphone Hydrochloride. https://www.accessdata.fda.gov/drugsatfda_docs/psg/Hydromorphone_ER_Tablets_021217_RC07-14.pdf, 2014.
- U.S. Food and Drug Administration. Draft Guidance on Methylphenidate Hydrochloride. https://www.accessdata.fda.gov/drugsatfda_docs/psg/MethylphenidateHydrochloride_draft_OraltabER_RLD21121_RC07-18.pdf, 2015.
- AA Vinks, C Emoto, and T Fukuda. Modeling and simulation in pediatric drug therapy: application of pharmacometrics to define the right dose for children. *Clinical Pharmacology & Therapeutics*, 98(3):298–308, 2015.
- Janet R. Wade, Andrew W. Kelman, Catherine A. Howie, and Brian Whiting. Effect of misspecification of the absorption process on subsequent parameter estimation in population analysis. *Journal of Pharmacokinetics and Biopharmaceutics*, 21(2):209–222, 1993. ISSN 0090466X. doi: 10.1007/BF01059771.
- Junyan Wang, Peng Gao, Huifen Zhang, Yan Hu, Yinghua Ni, Zhengyi Zhu, Liwen Zhang, Huijuan Wang, Jufei Yang, Cai Ji, et al. Evaluation of concentration errors and inappropriate dose tailoring of tacrolimus caused by sampling-time deviations

- in pediatric patients with primary nephrotic syndrome. *Therapeutic Drug Monitoring*, 42(3):392–399, 2020.
- Naisyin Wang and Marie Davidian. A note on covariate measurement error in non-linear mixed effects models. *Biometrika*, 83(4):801–812, 1996.
- Sebastian G Wicha, Anne-Grete Mårtson, Elisabet I Nielsen, Birgit CP Koch, Lena E Friberg, Jan-Willem Alffenaar, Iris K Minichmayr, and Infectious Diseases (EPASG) International Society of Anti-Infective Pharmacology (ISAP), the PK/PD study group of the European Society of Clinical Microbiology. From therapeutic drug monitoring to model-informed precision dosing for antibiotics. *Clinical Pharmacology & Therapeutics*, 109(4):928–941, 2021.
- Jean-Baptiste Woillard, Brenda CM de Winter, Nassim Kamar, Pierre Marquet, Lionel Rostaing, and Annick Rousseau. Population pharmacokinetic model and bayesian estimator for two tacrolimus formulations—twice daily prograf® and once daily advagraf®. *British journal of clinical pharmacology*, 71(3):391–402, 2011.
- Zhilu Zhang and Mert R. Sabuncu. Generalized cross entropy loss for training deep neural networks with noisy labels. *Advances in Neural Information Processing Systems*, 2018-Decem(NeurIPS):8778–8788, 2018. ISSN 10495258.

Appendix A

Investigating The Contribution of Residual Unexplained Variability Components in a Nonlinear-Mixed Effect Approach

A.1 Literature review

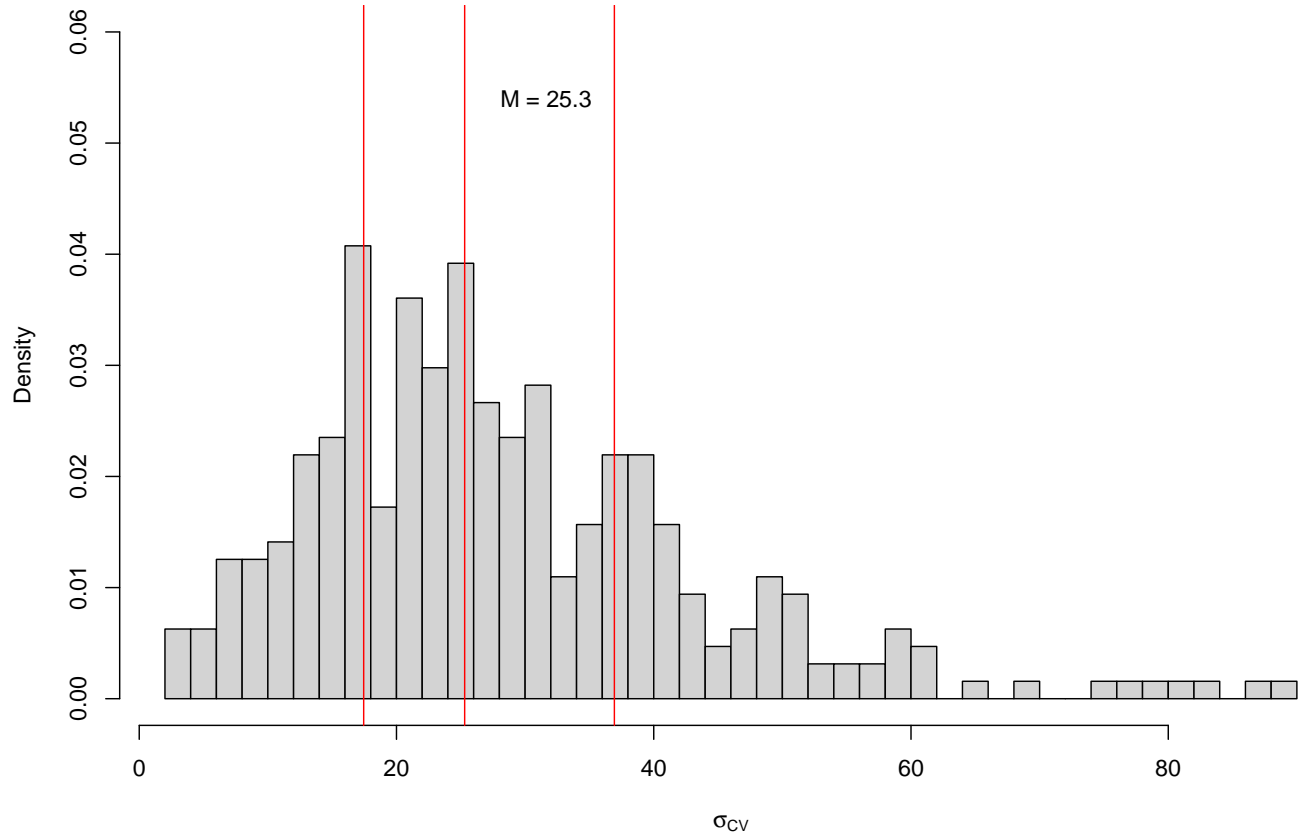


Figure A.1: Histogram represent the distribution of proportional error model magnitude (CV%) with vertical red lines being 5th, median and 95th percentiles, respectively

Dose variability - Manufacturing

Study design	Parameter	Median	rBias	rRMSE
SD9	CL	1.01	0.4	3.96
SD9	V	1.02	2.57	8.23
SD9	Q	1.01	2.59	11.06
SD9	Vp	1.01	0.96	4.92
SD9	Ka	1.01	0.6	8.18
SD9	BCL	1.05	4.88	8.55
SD9	BV	1.08	7.46	16.57
SD9	BQ	0.94	3.34	52.32
SD9	BVp	1.06	5.77	11.13
SD9	BKa	0.97	-2.67	12.34
SD9	RUV	1.01	0.7	4.79
SD9	CL	1.02	2	5.09
SD9	V	1.05	6.21	10.83
SD9	Q	1.08	9.23	14.75
SD9	Vp	1.01	0.95	6.09
SD9	Ka	1.03	3.94	10.01
SD9	BCL	1.21	21.39	23.02
SD9	BV	1.32	32.34	38.18

continued on next page

Study design	Parameter	Median	rBias	rRMSE
SD9	BQ	1.12	17.82	47.07
SD9	BVp	1.24	22.89	26.6
SD9	BKa	0.98	-1.65	13.79
SD9	RUV	1.01	1.21	7.37
SD7	CL	1.01	0.46	4.26
SD7	V	1.03	3.78	12.83
SD7	Q	1.01	3.77	20.31
SD7	Vp	1.01	0.7	7.99
SD7	Ka	1.01	1.17	10.74
SD7	BCL	1.05	5.08	9.36
SD7	BV	1.16	17.21	27.46
SD7	BQ	0.91	-1.4	61.04
SD7	BVp	1.02	3.12	13.54
SD7	BKa	0.96	-3.76	13.63
SD7	RUV	1.01	0.76	7
SD7	CL	1.02	2.01	5.64
SD7	V	1.04	5.59	16.28
SD7	Q	1.1	15.47	37.09
SD7	Vp	1.02	1.33	10.09

continued on next page

Study design	Parameter	Median	rBias	rRMSE
SD7	Ka	1.05	5.85	13.05
SD7	BCL	1.21	21.84	23.79
SD7	BV	1.61	60.06	66.47
SD7	BQ	1.07	15.79	68.59
SD7	BVp	1.14	15.02	24.88
SD7	BKa	0.96	-2.83	15.72
SD7	RUV	1.01	0.98	5.98
SD5	CL	1.01	0.36	4.07
SD5	V	0.96	-8.74	40.95
SD5	Q	0.98	8.81	48.5
SD5	Vp	1.05	8.41	27.74
SD5	Ka	0.95	-2.6	15.75
SD5	BCL	1.04	4.97	9.14
SD5	BV	1.36	62.47	159.18
SD5	BQ	0.8	-16.78	77.2
SD5	BVp	0.94	-2.54	23.74
SD5	BKa	0.93	-5.62	24.58
SD5	RUV	1.01	0.84	7.92
SD5	CL	1.02	2.02	5.93

continued on next page

Study design	Parameter	Median	rBias	rRMSE
SD5	V	0.96	-10.84	37.53
SD5	Q	1.1	22.08	52.18
SD5	V _p	1.07	11.68	26.9
SD5	K _a	0.99	1.59	14.55
SD5	BCL	1.21	21.32	23.58
SD5	BV	1.91	113.47	171.33
SD5	BQ	1.01	0.44	78.51
SD5	BV _p	1.04	7.56	24.55
SD5	BK _a	0.98	-1.25	20.16
SD5	RUV	1.01	1.75	10.24
SD4	CL	1	0.43	3.13
SD4	V	0.86	-15.99	50.98
SD4	Q	0.94	11.41	57.89
SD4	V _p	1.1	12.94	34.08
SD4	K _a	0.95	-4.75	17.84
SD4	BCL	1.05	4.56	8.25
SD4	BV	1.42	98.98	240.89
SD4	BQ	0.66	-26.9	74
SD4	BV _p	0.89	-4.39	23.98

continued on next page

Study design	Parameter	Median	rBias	rRMSE
SD4	BKa	0.92	-7.46	22.37
SD4	RUV	1.01	-0.64	7.31
SD4	CL	1.02	2.02	4
SD4	V	0.88	-13.61	44.03
SD4	Q	1.08	23.42	59.85
SD4	Vp	1.12	13.43	30.87
SD4	Ka	0.99	0.43	16.97
SD4	BCL	1.21	21.25	22.73
SD4	BV	2.00	136.38	223.43
SD4	BQ	0.98	-10.9	70.65
SD4	BVp	1.02	5.12	21.61
SD4	BKa	0.96	-3.08	22.66
SD4	RUV	1.01	-0.29	7.45

Dosing time variability - Clinical trial execution

Study design	Level	Parameter	Median	rBias	rRMSE
SD9	5	CL	1	-0.19	4.15
SD9	5	V	1.05	5.43	10.8
SD9	5	Q	0.99	0.81	11.34
SD9	5	Vp	0.98	-1.88	6.08
SD9	5	Ka	1.01	2.07	10.21
SD9	5	BCL	0.99	-0.55	7.03
SD9	5	BV	1.04	3.86	15.82
SD9	5	BQ	1.09	18.74	60.26
SD9	5	BVp	1.03	3.36	10.68
SD9	5	BKa	0.99	-0.93	14.86
SD9	5	RUV	1.04	4.55	7.24
SD9	10	CL	1	0.53	4.39
SD9	10	V	1.28	29.88	39.04
SD9	10	Q	1.09	17.6	43.26
SD9	10	Vp	0.86	-15.78	21.64
SD9	10	Ka	1.22	22.58	31.64
SD9	10	BCL	1	-0.39	7.24
SD9	10	BV	0.97	-1.59	21.75

continued on next page

Study design	Level	Parameter	Median	rBias	rRMSE
SD9	10	BQ	1.78	84.3	110.47
SD9	10	BVp	1.13	15.15	27.88
SD9	10	BKa	1.22	19.73	32.22
SD9	10	RUV	1.34	35.31	38.62
SD7	5	CL	1	0.18	4.8
SD7	5	V	1.04	5.52	13.19
SD7	5	Q	0.98	2.48	27.61
SD7	5	Vp	1	-0.93	7.57
SD7	5	Ka	1.01	1.81	11.97
SD7	5	BCL	0.99	-0.52	7.8
SD7	5	BV	1.02	1.06	21.53
SD7	5	BQ	0.87	-1.39	75.12
SD7	5	BVp	0.99	-1.81	13.38
SD7	5	BKa	0.98	-1.39	14.02
SD7	5	RUV	1.01	1.24	5.86
SD7	10	CL	1	0.22	5.05
SD7	10	V	1.11	12.25	19.01
SD7	10	Q	0.99	3.91	32.62
SD7	10	Vp	0.96	-5.03	10.69

continued on next page

Study design	Level	Parameter	Median	rBias	rRMSE
SD7	10	Ka	1.04	5.59	13.06
SD7	10	BCL	0.99	-0.11	8.55
SD7	10	BV	0.99	-1.41	19.93
SD7	10	BQ	0.95	5.01	74.08
SD7	10	BVp	1.01	1.89	15.38
SD7	10	BKa	1.02	2.48	16.33
SD7	10	RUV	1.03	3	7.42
SD5	5	CL	1	0.08	3.85
SD5	5	V	1.02	-0.28	38.26
SD5	5	Q	0.91	8.4	89.59
SD5	5	Vp	1.01	2.45	25.18
SD5	5	Ka	0.96	-1.88	17.01
SD5	5	BCL	0.99	-0.63	6.81
SD5	5	BV	1.08	20.59	91.98
SD5	5	BQ	0.7	-20.25	94.2
SD5	5	BVp	0.94	-2.94	24.4
SD5	5	BKa	0.94	-5.39	21.68
SD5	5	RUV	1	0.57	9.13
SD5	10	CL	1	0.1	5.54

continued on next page

Study design	Level	Parameter	Median	rBias	rRMSE
SD5	10	V	1.03	0.76	38.23
SD5	10	Q	0.92	7.14	79.79
SD5	10	V _p	1	1.83	25.08
SD5	10	K _a	0.97	-1.14	17.32
SD5	10	BCL	1	-0.14	7.77
SD5	10	BV	1.07	20.69	112.78
SD5	10	BQ	0.71	-19.15	88.04
SD5	10	BV _p	0.94	-2.2	22.98
SD5	10	BK _a	0.95	-3.99	21.88
SD5	10	RUV	1	1.02	9.45
SD4	5	CL	1	0.19	3.41
SD4	5	V	0.97	-2.85	46.09
SD4	5	Q	0.87	-0.5	47.2
SD4	5	V _p	1.04	3.74	30.09
SD4	5	K _a	0.96	-3.77	17.9
SD4	5	BCL	0.99	-0.71	6.61
SD4	5	BV	1.11	33.19	135.38
SD4	5	BQ	0.54	-34.53	73.27
SD4	5	BV _p	0.93	-2.03	26.68

continued on next page

Study design	Level	Parameter	Median	rBias	rRMSE
SD4	5	BKa	0.93	-7.26	21.34
SD4	5	RUV	0.99	-0.76	7.24
SD4	10	CL	1	0.17	3.2
SD4	10	V	0.97	-3.56	45.48
SD4	10	Q	0.89	0.94	45.32
SD4	10	Vp	1.03	4.33	29.74
SD4	10	Ka	0.96	-3.53	17.8
SD4	10	BCL	0.99	-0.73	6.6
SD4	10	BV	1.13	32.72	134.31
SD4	10	BQ	0.54	-32.87	73
SD4	10	BVp	0.92	-2.34	26.24
SD4	10	BKa	0.94	-5.86	21.02
SD4	10	RUV	0.99	-0.78	7.21

Pharmacokinetic sampling time variability - Clinical trial execution

Study design	Level	Parameter	Median	rBias	rRMSE
SD9	5	CL	1	0.09	3.6
SD9	5	V	1.02	2.64	10.45
SD9	5	Q	1	0.88	12.46
SD9	5	V _p	1	-0.11	5.9
SD9	5	K _a	0.99	0.21	9.74
SD9	5	BCL	0.99	-0.87	6.72
SD9	5	BV	1.08	7.55	17.67
SD9	5	BQ	1.14	21.43	51.54
SD9	5	BV _p	1.02	1.95	11.08
SD9	5	BK _a	0.96	-4.29	15.82
SD9	5	RUV	1.11	11.56	13.02
SD9	10	CL	1.01	0.59	3.27
SD9	10	V	1.11	16.52	32.15
SD9	10	Q	1.01	7.98	41.78
SD9	10	V _p	0.96	-8.08	17.77
SD9	10	K _a	1.07	10.5	25.74

continued on next page

Study design	Level	Parameter	Median	rBias	rRMSE
SD9	10	BCL	0.99	-1.16	6.79
SD9	10	BV	1.05	6.7	26.38
SD9	10	BQ	1.36	46.75	77.72
SD9	10	BVp	1.06	8.32	22.2
SD9	10	BKa	1.03	0.49	27.2
SD9	10	RUV	1.6	59.79	61.85
SD9	15	CL	1.01	1.29	3.37
SD9	15	V	1.42	47.9	67.99
SD9	15	Q	1.02	3525.27	78229.8
SD9	15	Vp	0.79	-26.15	39.6
SD9	15	Ka	1.37	36.61	50.9
SD9	15	BCL	0.98	-1.83	6.81
SD9	15	BV	0.88	-5.67	30.26
SD9	15	BQ	1.09	25.94	117.89
SD9	15	BVp	1.12	35.75	88.52
SD9	15	BKa	1.24	18.02	38.95
SD9	15	RUV	2.17	116.78	118.69
SD9	30	CL	1.02	1.93	3.69
SD9	30	V	1.62	63.8	90.02

continued on next page

Study design	Level	Parameter	Median	rBias	rRMSE
SD9	30	Q	1.52	246415793.14	4216875490.89
SD9	30	Vp	0.69	-34.66	53.58
SD9	30	Ka	1.67	61.98	75.06
SD9	30	BCL	0.98	-2.37	6.99
SD9	30	BV	0.79	-8.75	41.39
SD9	30	BQ	1.64	410.19	3007.64
SD9	30	BVp	1.08	72.5	172.1
SD9	30	BKa	1.52	43.8	64.15
SD9	30	RUV	2.63	164.04	165.68
SD7	5	CL	1	0.09	4.88
SD7	5	V	1.04	4.55	14.45
SD7	5	Q	0.97	1.64	20.75
SD7	5	Vp	1	-0.38	8.61
SD7	5	Ka	1	1.17	11.52
SD7	5	BCL	0.99	-0.53	7.5
SD7	5	BV	1.02	1.79	23.66
SD7	5	BQ	0.85	-6.63	68.2
SD7	5	BVp	0.99	-0.12	19.74
SD7	5	BKa	0.97	-2.54	14.04

continued on next page

Study design	Level	Parameter	Median	rBias	rRMSE
SD7	5	RUV	1.02	2.22	5.61
SD7	10	CL	1	0.06	4.35
SD7	10	V	1.1	10.35	18.85
SD7	10	Q	0.99	4.54	24.99
SD7	10	V _p	0.97	-3.8	10.33
SD7	10	Ka	1.04	4.82	13.84
SD7	10	BCL	0.99	-0.42	7.84
SD7	10	BV	1.01	0.8	22.13
SD7	10	BQ	0.93	4.53	72.18
SD7	10	BV _p	1.01	1.57	14.57
SD7	10	BKa	1	-0.36	15.04
SD7	10	RUV	1.07	7.8	10.52
SD7	15	CL	1	0.47	4.09
SD7	15	V	1.18	22.24	32.89
SD7	15	Q	1.02	11.28	34.71
SD7	15	V _p	0.91	-10.87	18.58
SD7	15	Ka	1.13	12.9	20.87
SD7	15	BCL	0.99	-0.43	9.33
SD7	15	BV	0.97	-3.17	24.12

continued on next page

Study design	Level	Parameter	Median	rBias	rRMSE
SD7	15	BQ	1.11	22.8	97.33
SD7	15	BVp	1.06	8.77	24.32
SD7	15	BKa	1.05	5.84	19.6
SD7	15	RUV	1.18	20.2	22.53
SD7	30	CL	1.01	1.34	3.43
SD7	30	V	1.83	77.85	90.75
SD7	30	Q	0.88	11694317.24	190101482.81
SD7	30	Vp	0.52	-45.3	54.77
SD7	30	Ka	1.47	45.5	51.26
SD7	30	BCL	0.99	-1.44	6.75
SD7	30	BV	0.74	-19.57	56.33
SD7	30	BQ	0.4	205.81	2163.02
SD7	30	BVp	1.54	74.32	126.67
SD7	30	BKa	1.41	39.79	48.6
SD7	30	RUV	1.97	98.37	101.67
SD5	5	CL	1	-0.03	4.01
SD5	5	V	0.99	-2.32	37.57
SD5	5	Q	0.89	4.01	72.42
SD5	5	Vp	1.02	3.52	24.58

continued on next page

Study design	Level	Parameter	Median	rBias	rRMSE
SD5	5	Ka	0.94	-3.75	16.62
SD5	5	BCL	0.99	-0.52	7.32
SD5	5	BV	1.15	26.63	106.39
SD5	5	BQ	0.65	-23.94	86.27
SD5	5	BVp	0.92	-3.97	24.83
SD5	5	BKa	0.92	-7.65	21.5
SD5	5	RUV	1.01	1.16	8.47
SD5	10	CL	1	0.32	4.49
SD5	10	V	1	-1.98	37.58
SD5	10	Q	0.91	6.4	85.18
SD5	10	Vp	1.03	3.69	24.52
SD5	10	Ka	0.95	-3.06	17.51
SD5	10	BCL	0.99	-0.43	7.83
SD5	10	BV	1.11	23.32	103.8
SD5	10	BQ	0.68	-18.78	100.51
SD5	10	BVp	0.92	-3.6	23.62
SD5	10	BKa	0.93	-6.67	22.04
SD5	10	RUV	1.02	2.53	8.54
SD5	15	CL	1	0.19	4.1

continued on next page

Study design	Level	Parameter	Median	rBias	rRMSE
SD5	15	V	1	-1.54	38.06
SD5	15	Q	0.91	5.31	64.04
SD5	15	V _p	1.03	3.45	25.04
SD5	15	K _a	0.95	-2.96	16.69
SD5	15	BCL	0.99	-0.72	7.33
SD5	15	BV	1.08	17.89	83.76
SD5	15	BQ	0.71	-19.93	85.8
SD5	15	BV _p	0.93	-2.7	23.95
SD5	15	BK _a	0.94	-5.72	21.21
SD5	15	RUV	1.04	5.2	11.96
SD5	30	CL	1	0.71	4.27
SD5	30	V	1.07	7.46	46.43
SD5	30	Q	0.98	22.89	127.27
SD5	30	V _p	0.98	-1.35	30.42
SD5	30	K _a	1.02	3.47	18.18
SD5	30	BCL	0.99	-0.21	7.51
SD5	30	BV	1	17.2	130.33
SD5	30	BQ	0.88	-2.86	90.25
SD5	30	BV _p	0.98	4.42	31.97

continued on next page

Study design	Level	Parameter	Median	rBias	rRMSE
SD5	30	BKa	1.05	5.09	24.01
SD5	30	RUV	1.18	18.85	21.35
SD4	5	CL	1	0.16	3.06
SD4	5	V	0.98	0.76	44.35
SD4	5	Q	0.84	-6.7	40.89
SD4	5	Vp	1.03	1.19	28.49
SD4	5	Ka	0.95	-4.87	18.26
SD4	5	BCL	0.99	-0.74	6.64
SD4	5	BV	1.13	24.14	108.49
SD4	5	BQ	0.54	-39.03	71.01
SD4	5	BVp	0.93	-0.62	28.59
SD4	5	BKa	0.92	-9.55	22.75
SD4	5	RUV	1	-0.4	7.07
SD4	10	CL	1	0.21	3.13
SD4	10	V	0.97	0.41	44.73
SD4	10	Q	0.85	-4.91	44.46
SD4	10	Vp	1.03	1.49	28.89
SD4	10	Ka	0.95	-4.65	18.36
SD4	10	BCL	0.99	-0.74	6.63

continued on next page

Study design	Level	Parameter	Median	rBias	rRMSE
SD4	10	BV	1.1	19.78	89.69
SD4	10	BQ	0.57	-36.77	71.71
SD4	10	BVp	0.92	-0.45	29.77
SD4	10	BKa	0.92	-9.06	22.49
SD4	10	RUV	1.01	1.14	7.23
SD4	15	CL	1	0.21	3.15
SD4	15	V	0.97	-0.88	45.2
SD4	15	Q	0.89	-0.75	50.79
SD4	15	Vp	1.02	2.52	29.4
SD4	15	Ka	0.96	-4.12	18.36
SD4	15	BCL	0.99	-0.74	6.7
SD4	15	BV	1.11	23.7	105
SD4	15	BQ	0.64	-30.62	71.77
SD4	15	BVp	0.91	-0.83	30.1
SD4	15	BKa	0.93	-7.78	22.65
SD4	15	RUV	1.04	3.65	8.17
SD4	30	CL	1	0.41	3.16
SD4	30	V	0.94	-6.35	50.69
SD4	30	Q	1.07	24.07	75.89

continued on next page

Study design	Level	Parameter	Median	rBias	rRMSE
SD4	30	Vp	1.07	7.41	34.14
SD4	30	Ka	1.01	-0.24	18.87
SD4	30	BCL	0.99	-0.77	6.71
SD4	30	BV	1.1	43.33	179.03
SD4	30	BQ	0.94	-5.01	82.63
SD4	30	BVp	0.9	-1.49	33.2
SD4	30	BKa	1.05	4.19	23.53
SD4	30	RUV	1.17	16.8	19.16

Pharmacokinetic Model Misspecification - Technical execution

Study design	Level	Parameter	Median	rBias	rRMSE
SD9	M	CL	1	0.29	3.08
SD9	M	V	1.07	7.19	7.53
SD9	M	Ka	2.28	127.44	128.01
SD9	M	BCL	0.99	-1.06	6.56
SD9	M	BV	0.69	-31.1	31.53
SD9	M	BKa	1.7	70.31	71.79
SD9	M	RUV	1.37	37.17	37.86
SD7	M	CL	1	0.17	3.07
SD7	M	V	1.06	6.35	6.74
SD7	M	Ka	2.08	108.87	109.67
SD7	M	BCL	0.99	-1.22	6.57
SD7	M	BV	0.69	-30.78	31.22
SD7	M	BKa	1.91	90.55	92.2
SD7	M	RUV	1.27	27.97	29.44
SD5	M	CL	1.01	0.73	3.2
SD5	M	V	1.07	6.76	7.14

continued on next page

Study design	Level	Parameter	Median	rBias	rRMSE
SD5	M	Ka	1.71	71.52	72.4
SD5	M	BCL	0.99	-0.69	6.51
SD5	M	BV	0.69	-30.91	31.35
SD5	M	BKa	1.61	61.27	63.65
SD5	M	RUV	1.2	20.91	22.96
SD4	M	CL	1.01	0.63	3.17
SD4	M	V	1.06	6.31	6.72
SD4	M	Ka	1.65	65.91	66.77
SD4	M	BCL	0.99	-1.19	6.58
SD4	M	BV	0.67	-32.78	33.2
SD4	M	BKa	1.47	48.22	51.08
SD4	M	RUV	1.28	28.41	30.97

Residual Model Misspecification - Technical execution

Study design	Level	Parameter	Median	rBias	rRMSE
SD9	A1	CL	1	0.05	3.14
SD9	A1	V	0.87	-14.23	22.39
SD9	A1	Q	0.83	-17.56	25.43
SD9	A1	Vp	1.08	7.62	10.61
SD9	A1	Ka	0.83	-17.6	25.36
SD9	A1	BCL	0.98	-1.91	6.63
SD9	A1	BV	1.13	13.35	23.93
SD9	A1	BQ	0.52	-41.54	70.78
SD9	A1	BVp	0.97	-2.99	9.7
SD9	A1	BKa	0.91	-8.64	17.76
SD9	A1	RUV	1.33	36.15	38.85
SD9	A2	CL	1	-0.1	3.04
SD9	A2	V	0.63	-36.92	45.42
SD9	A2	Q	0.57	-42.11	49.86
SD9	A2	Vp	1.13	11.54	14.61
SD9	A2	Ka	0.59	-40.84	48.53

continued on next page

Study design	Level	Parameter	Median	rBias	rRMSE
SD9	A2	BCL	0.97	-3.24	7.43
SD9	A2	BV	1.24	22.44	31.66
SD9	A2	BQ	0.01	-70.67	87.52
SD9	A2	BVp	0.99	0.93	12.69
SD9	A2	BKa	0.8	-20.04	28.08
SD9	A2	RUV	1.71	71.74	73.76
SD9	A3	CL	0.99	-0.98	3.15
SD9	A3	V	0.26	-65.58	69.35
SD9	A3	Q	0.19	-72.71	76.04
SD9	A3	Vp	1.06	5.46	12.3
SD9	A3	Ka	0.23	-68.98	72.23
SD9	A3	BCL	0.94	-5.53	8.64
SD9	A3	BV	1.39	36.43	42.28
SD9	A3	BQ	0.01	-72.16	87.33
SD9	A3	BVp	1.27	28.94	39.02
SD9	A3	BKa	0.71	-29.96	34.16
SD9	A3	RUV	2.26	126.5	128.55
SD7	A1	CL	1	0.31	3.32
SD7	A1	V	0.78	-20.13	30.66

continued on next page

Study design	Level	Parameter	Median	rBias	rRMSE
SD7	A1	Q	0.72	-27.14	35.55
SD7	A1	Vp	1.12	9.61	13.92
SD7	A1	Ka	0.73	-25.89	34.33
SD7	A1	BCL	0.98	-1.84	6.62
SD7	A1	BV	1.29	25.88	37.96
SD7	A1	BQ	0.01	-57.42	93.46
SD7	A1	BVp	0.94	-5.85	12.14
SD7	A1	BKa	0.81	-17.95	25.38
SD7	A1	RUV	1.41	44.71	48.07
SD7	A2	CL	1	0.23	3.09
SD7	A2	V	0.48	-44.89	50.66
SD7	A2	Q	0.4	-53.27	58.57
SD7	A2	Vp	1.15	13.29	16.02
SD7	A2	Ka	0.41	-51.1	55.74
SD7	A2	BCL	0.97	-3.18	7.21
SD7	A2	BV	1.39	36.17	44.92
SD7	A2	BQ	0.01	-80.17	92.88
SD7	A2	BVp	0.96	-1.87	13.03
SD7	A2	BKa	0.67	-31.07	36.1

continued on next page

Study design	Level	Parameter	Median	rBias	rRMSE
SD7	A2	RUV	1.87	87.18	89.86
SD7	A3	CL	0.99	-0.53	3.13
SD7	A3	V	0.29	-67.05	69.4
SD7	A3	Q	0.19	-77.28	78.82
SD7	A3	V _p	1.08	7.08	12.67
SD7	A3	K _a	0.23	-72.93	74.61
SD7	A3	BCL	0.95	-5.36	8.55
SD7	A3	BV	1.35	28.4	45.94
SD7	A3	BQ	0.01	-63.04	87.24
SD7	A3	BV _p	1.26	28.24	40.37
SD7	A3	BK _a	0.64	-39.14	43.74
SD7	A3	RUV	2.49	149.49	152.22
SD5	A1	CL	1	0.09	3.44
SD5	A1	V	0.53	-40	63.37
SD5	A1	Q	0.65	-26.27	45.54
SD5	A1	V _p	1.21	20.78	34.95
SD5	A1	K _a	0.61	-32.01	40.07
SD5	A1	BCL	0.97	-2.32	7.43
SD5	A1	BV	1.78	203.75	373.83

continued on next page

Study design	Level	Parameter	Median	rBias	rRMSE
SD5	A1	BQ	0.01	-53.15	106.75
SD5	A1	BVp	0.85	-11.41	24.59
SD5	A1	BKa	0.72	-28.85	40.08
SD5	A1	RUV	1.58	63.39	68.31
SD5	A2	CL	1	0.23	3.22
SD5	A2	V	0.38	-57.67	71.95
SD5	A2	Q	0.42	-10.99	787.83
SD5	A2	Vp	1.21	22.47	33.95
SD5	A2	Ka	0.41	-50.71	56.99
SD5	A2	BCL	0.96	-4.2	7.86
SD5	A2	BV	1.71	200.35	381.12
SD5	A2	BQ	0.01	-63.81	101.36
SD5	A2	BVp	0.9	-4.22	34.71
SD5	A2	BKa	0.58	-49.52	58.02
SD5	A2	RUV	2.17	119.64	124.37
SD5	A3	CL	1	-0.06	3.99
SD5	A3	V	0.35	-57.46	70.8
SD5	A3	Q	0.19	10072384.75	225226600.92
SD5	A3	Vp	1.07	18.98	95.33

continued on next page

Study design	Level	Parameter	Median	rBias	rRMSE
SD5	A3	Ka	0.25	-60.02	69.98
SD5	A3	BCL	0.93	-6.57	9.73
SD5	A3	BV	0.01	-15.7	220.54
SD5	A3	BQ	0.01	-55.15	100.78
SD5	A3	BVp	1.3	40.64	99.16
SD5	A3	BKa	0.51	-58.75	65.71
SD5	A3	RUV	2.97	202.59	207.87
SD4	A1	CL	1	0.16	3.23
SD4	A1	V	0.41	-42.42	72.91
SD4	A1	Q	0.66	7.96	349.85
SD4	A1	Vp	1.3	22.14	42.4
SD4	A1	Ka	0.61	-29.51	41.51
SD4	A1	BCL	0.97	-2.98	7.17
SD4	A1	BV	1.99	252.55	439.56
SD4	A1	BQ	0.01	-46.55	121.4
SD4	A1	BVp	0.83	-9.77	30.24
SD4	A1	BKa	0.71	-33.92	48.53
SD4	A1	RUV	1.72	80.62	88.77
SD4	A2	CL	1	0.41	3.2

continued on next page

Study design	Level	Parameter	Median	rBias	rRMSE
SD4	A2	V	0.33	-45.71	76.56
SD4	A2	Q	0.47	15240.56	240280.52
SD4	A2	V _p	1.28	19.05	41
SD4	A2	K _a	0.47	-39	50.83
SD4	A2	BCL	0.95	-5.12	8.46
SD4	A2	BV	1.48	199.05	408.51
SD4	A2	BQ	0.01	-38.55	249.51
SD4	A2	BV _p	0.9	0.22	41.86
SD4	A2	BK _a	0.35	-64.41	73.17
SD4	A2	RUV	2.45	154.57	162.08
SD4	A3	CL	1	-0.91	5.66
SD4	A3	V	0.42	-48.16	70.87
SD4	A3	Q	0.26	13634963.03	226506977.79
SD4	A3	V _p	1.1	11481657.98	256736823.65
SD4	A3	K _a	0.29	-50.86	64.19
SD4	A3	BCL	0.92	-8.23	11.25
SD4	A3	BV	0.02	13.25	265.04
SD4	A3	BQ	0.01	-53.65	110.08
SD4	A3	BV _p	1.16	42.29	121.45

continued on next page

Study design	Level	Parameter	Median	rBias	rRMSE
SD4	A3	BKa	0.01	-77.16	81.68
SD4	A3	RUV	3.59	259.63	266.85

Pharmacokinetic Model Misspecification - Technical execution

Study design	Level	Parameter	Median	rBias	rRMSE
SD9	M	CL	1	0.29	3.08
SD9	M	V	1.07	7.19	7.53
SD9	M	Ka	2.28	127.44	128.01
SD9	M	BCL	0.99	-1.06	6.56
SD9	M	BV	0.69	-31.1	31.53
SD9	M	BKa	1.7	70.31	71.79
SD9	M	RUV	1.37	37.17	37.86
SD7	M	CL	1	0.17	3.07
SD7	M	V	1.06	6.35	6.74
SD7	M	Ka	2.08	108.87	109.67
SD7	M	BCL	0.99	-1.22	6.57
SD7	M	BV	0.69	-30.78	31.22
SD7	M	BKa	1.91	90.55	92.2
SD7	M	RUV	1.27	27.97	29.44
SD5	M	CL	1.01	0.73	3.2
SD5	M	V	1.07	6.76	7.14

continued on next page

Study design	Level	Parameter	Median	rBias	rRMSE
SD5	M	Ka	1.71	71.52	72.4
SD5	M	BCL	0.99	-0.69	6.51
SD5	M	BV	0.69	-30.91	31.35
SD5	M	BKa	1.61	61.27	63.65
SD5	M	RUV	1.2	20.91	22.96
SD4	M	CL	1.01	0.63	3.17
SD4	M	V	1.06	6.31	6.72
SD4	M	Ka	1.65	65.91	66.77
SD4	M	BCL	0.99	-1.19	6.58
SD4	M	BV	0.67	-32.78	33.2
SD4	M	BKa	1.47	48.22	51.08
SD4	M	RUV	1.28	28.41	30.97

Combined scenarios

Study design	Parameter	Median	rBias	rRMSE
SD9	CL	1	-0.19	2.99
SD9	V	1.1	10.27	10.62
SD9	Ka	2.23	123.49	124.13
SD9	BCL	0.98	-2.4	6.94
SD9	BV	0.75	-25.04	25.79
SD9	BKa	1.66	65.63	67.68
SD9	RUV	2.81	181.4	182.5
SD7	CL	1	0.19	3.07
SD7	V	1.12	12.08	12.78
SD7	Ka	2.22	1.254396e+50	2.80491472670383e+51
SD7	BCL	0.96	-3.42	7.77
SD7	BV	0.74	-26.3	27.28
SD7	BKa	1.71	320.99	2088.81
SD7	RUV	3.14	234.66	240.74
SD5	CL	1.01	1.14	3.65
SD5	V	1.11	11.32	11.68
SD5	Ka	1.74	2500520096079270	55913326990977800
SD5	BCL	0.95	-5.22	8.56

continued on next page

Study design	Parameter	Median	rBias	rRMSE
SD5	BV	0.69	-31.63	32.5
SD5	BKa	0.01	3964.45	73614
SD5	RUV	3.7	268.56	270.2
SD4	CL	1.02	1.63	4.47
SD4	V	1.12	11.33	12.32
SD4	Ka	1.73	7.74051228000844e+22	1.72950070574194e+24
SD4	BCL	0.91	-8.96	11.35
SD4	BV	0.57	-43.45	44.99
SD4	BKa	0.01	13442.68	177381.91
SD4	RUV	4.28	331.71	334.43

Appendix B

The impact of unrecorded time deviation in nonlinear mixed-effect analyses

Part I - numerical values for relative bias

Study	Magnitude of perturbation	kappa	γ	variable	Bias
I	5	0	1	THETA1_BiasCL	2.16
I	5	0	0.5	THETA1_BiasCL	2.07
I	5	0	0.2	THETA1_BiasCL	2.02
I	5	1	1	THETA1_BiasCL	2.02
I	5	1	0.5	THETA1_BiasCL	1.99
I	5	1	0.2	THETA1_BiasCL	1.94
I	10	0	1	THETA1_BiasCL	2.86

continued on next page

Study	Magnitude of perturbation	kappa	γ	variable	Bias
I	10	0	0.5	THETA1_BiasCL	2.44
I	10	0	0.2	THETA1_BiasCL	2.14
I	10	1	1	THETA1_BiasCL	2.16
I	10	1	0.5	THETA1_BiasCL	2.09
I	10	1	0.2	THETA1_BiasCL	1.97
I	15	0	1	THETA1_BiasCL	3.62
I	15	0	0.5	THETA1_BiasCL	2.87
I	15	0	0.2	THETA1_BiasCL	2.33
I	15	1	1	THETA1_BiasCL	2.29
I	15	1	0.5	THETA1_BiasCL	2.15
I	15	1	0.2	THETA1_BiasCL	2.02
I	30	0	1	THETA1_BiasCL	4.45
I	30	0	0.5	THETA1_BiasCL	3.33
I	30	0	0.2	THETA1_BiasCL	2.54
I	30	1	1	THETA1_BiasCL	2.57
I	30	1	0.5	THETA1_BiasCL	2.35
I	30	1	0.2	THETA1_BiasCL	2.12
M	5	0	1	THETA1_BiasCL	2.54
M	5	0	0.5	THETA1_BiasCL	2.45

continued on next page

Study	Magnitude of perturbation	kappa	γ	variable	Bias
M	5	0	0.2	THETA1_BiasCL	2.42
M	5	1	1	THETA1_BiasCL	2.48
M	5	1	0.5	THETA1_BiasCL	2.42
M	5	1	0.2	THETA1_BiasCL	2.41
M	10	0	1	THETA1_BiasCL	3.19
M	10	0	0.5	THETA1_BiasCL	2.73
M	10	0	0.2	THETA1_BiasCL	2.53
M	10	1	1	THETA1_BiasCL	2.66
M	10	1	0.5	THETA1_BiasCL	2.52
M	10	1	0.2	THETA1_BiasCL	2.45
M	15	0	1	THETA1_BiasCL	4
M	15	0	0.5	THETA1_BiasCL	3.18
M	15	0	0.2	THETA1_BiasCL	2.74
M	15	1	1	THETA1_BiasCL	2.8
M	15	1	0.5	THETA1_BiasCL	2.62
M	15	1	0.2	THETA1_BiasCL	2.51
M	30	0	1	THETA1_BiasCL	4.64
M	30	0	0.5	THETA1_BiasCL	3.62
M	30	0	0.2	THETA1_BiasCL	2.97

continued on next page

Study	Magnitude of perturbation	kappa	γ	variable	Bias
M	30	1	1	THETA1_BiasCL	3.17
M	30	1	0.5	THETA1_BiasCL	2.84
M	30	1	0.2	THETA1_BiasCL	2.63
S	5	0	1	THETA1_BiasCL	2.38
S	5	0	0.5	THETA1_BiasCL	2.59
S	5	0	0.2	THETA1_BiasCL	2.71
S	5	1	1	THETA1_BiasCL	2.69
S	5	1	0.5	THETA1_BiasCL	2.76
S	5	1	0.2	THETA1_BiasCL	2.8
S	10	0	1	THETA1_BiasCL	2.52
S	10	0	0.5	THETA1_BiasCL	2.99
S	10	0	0.2	THETA1_BiasCL	3.07
S	10	1	1	THETA1_BiasCL	2.61
S	10	1	0.5	THETA1_BiasCL	2.87
S	10	1	0.2	THETA1_BiasCL	2.96
S	15	0	1	THETA1_BiasCL	4.3
S	15	0	0.5	THETA1_BiasCL	4.48
S	15	0	0.2	THETA1_BiasCL	3.97
S	15	1	1	THETA1_BiasCL	2.55

continued on next page

Study	Magnitude of perturbation	kappa	γ	variable	Bias
S	15	1	0.5	THETA1_BiasCL	2.94
S	15	1	0.2	THETA1_BiasCL	3.05
S	30	0	1	THETA1_BiasCL	7.81
S	30	0	0.5	THETA1_BiasCL	6.43
S	30	0	0.2	THETA1_BiasCL	4.85
S	30	1	1	THETA1_BiasCL	5.05
S	30	1	0.5	THETA1_BiasCL	4.31
S	30	1	0.2	THETA1_BiasCL	3.67
I	5	0	1	THETA2_BiasV	12.33
I	5	0	0.5	THETA2_BiasV	11.47
I	5	0	0.2	THETA2_BiasV	11.08
I	5	1	1	THETA2_BiasV	10.92
I	5	1	0.5	THETA2_BiasV	10.74
I	5	1	0.2	THETA2_BiasV	10.41
I	10	0	1	THETA2_BiasV	16.48
I	10	0	0.5	THETA2_BiasV	13.62
I	10	0	0.2	THETA2_BiasV	12.05
I	10	1	1	THETA2_BiasV	8.1
I	10	1	0.5	THETA2_BiasV	9.7

continued on next page

Study	Magnitude of perturbation	kappa	γ	variable	Bias
I	10	1	0.2	THETA2_BiasV	10.54
I	15	0	1	THETA2_BiasV	19.46
I	15	0	0.5	THETA2_BiasV	16.4
I	15	0	0.2	THETA2_BiasV	13.27
I	15	1	1	THETA2_BiasV	7.55
I	15	1	0.5	THETA2_BiasV	9.07
I	15	1	0.2	THETA2_BiasV	10.35
I	30	0	1	THETA2_BiasV	30.05
I	30	0	0.5	THETA2_BiasV	22.53
I	30	0	0.2	THETA2_BiasV	16.13
I	30	1	1	THETA2_BiasV	14.21
I	30	1	0.5	THETA2_BiasV	12.39
I	30	1	0.2	THETA2_BiasV	11.82
M	5	0	1	THETA2_BiasV	9.94
M	5	0	0.5	THETA2_BiasV	8.59
M	5	0	0.2	THETA2_BiasV	7.65
M	5	1	1	THETA2_BiasV	8.2
M	5	1	0.5	THETA2_BiasV	7.92
M	5	1	0.2	THETA2_BiasV	6.76

continued on next page

Study	Magnitude of perturbation	kappa	γ	variable	Bias
M	10	0	1	THETA2_BiasV	14.61
M	10	0	0.5	THETA2_BiasV	11.81
M	10	0	0.2	THETA2_BiasV	8.78
M	10	1	1	THETA2_BiasV	5.85
M	10	1	0.5	THETA2_BiasV	7.7
M	10	1	0.2	THETA2_BiasV	7.38
M	15	0	1	THETA2_BiasV	18.54
M	15	0	0.5	THETA2_BiasV	14.2
M	15	0	0.2	THETA2_BiasV	9.2
M	15	1	1	THETA2_BiasV	4.62
M	15	1	0.5	THETA2_BiasV	6.57
M	15	1	0.2	THETA2_BiasV	6.9
M	30	0	1	THETA2_BiasV	31.91
M	30	0	0.5	THETA2_BiasV	21.32
M	30	0	0.2	THETA2_BiasV	12.3
M	30	1	1	THETA2_BiasV	17.13
M	30	1	0.5	THETA2_BiasV	12.26
M	30	1	0.2	THETA2_BiasV	8.9
S	5	0	1	THETA2_BiasV	9.79

continued on next page

Study	Magnitude of perturbation	kappa	γ	variable	Bias
S	5	0	0.5	THETA2_BiasV	8.51
S	5	0	0.2	THETA2_BiasV	6.76
S	5	1	1	THETA2_BiasV	2.62
S	5	1	0.5	THETA2_BiasV	3.51
S	5	1	0.2	THETA2_BiasV	3.11
S	10	0	1	THETA2_BiasV	12.78
S	10	0	0.5	THETA2_BiasV	7.29
S	10	0	0.2	THETA2_BiasV	5.63
S	10	1	1	THETA2_BiasV	-2.76
S	10	1	0.5	THETA2_BiasV	0.28
S	10	1	0.2	THETA2_BiasV	1.9
S	15	0	1	THETA2_BiasV	14.9
S	15	0	0.5	THETA2_BiasV	0.03
S	15	0	0.2	THETA2_BiasV	-1.31
S	15	1	1	THETA2_BiasV	-5.59
S	15	1	0.5	THETA2_BiasV	-1.7
S	15	1	0.2	THETA2_BiasV	0.72
S	30	0	1	THETA2_BiasV	15.17
S	30	0	0.5	THETA2_BiasV	-0.17

continued on next page

Study	Magnitude of perturbation	kappa	γ	variable	Bias
S	30	0	0.2	THETA2_BiasV	-3.63
S	30	1	1	THETA2_BiasV	2.26
S	30	1	0.5	THETA2_BiasV	1.26
S	30	1	0.2	THETA2_BiasV	2.46
I	5	0	1	THETA3_BiasKa	9.49
I	5	0	0.5	THETA3_BiasKa	8.85
I	5	0	0.2	THETA3_BiasKa	8.68
I	5	1	1	THETA3_BiasKa	7.76
I	5	1	0.5	THETA3_BiasKa	7.94
I	5	1	0.2	THETA3_BiasKa	7.9
I	10	0	1	THETA3_BiasKa	12.26
I	10	0	0.5	THETA3_BiasKa	10.32
I	10	0	0.2	THETA3_BiasKa	9.42
I	10	1	1	THETA3_BiasKa	3.08
I	10	1	0.5	THETA3_BiasKa	5.7
I	10	1	0.2	THETA3_BiasKa	7.53
I	15	0	1	THETA3_BiasKa	14.35
I	15	0	0.5	THETA3_BiasKa	12.77
I	15	0	0.2	THETA3_BiasKa	10.53

continued on next page

Study	Magnitude of perturbation	kappa	γ	variable	Bias
I	15	1	1	THETA3_BiasKa	1.2
I	15	1	0.5	THETA3_BiasKa	4.23
I	15	1	0.2	THETA3_BiasKa	6.87
I	30	0	1	THETA3_BiasKa	26.08
I	30	0	0.5	THETA3_BiasKa	19.99
I	30	0	0.2	THETA3_BiasKa	13.81
I	30	1	1	THETA3_BiasKa	7.23
I	30	1	0.5	THETA3_BiasKa	7.49
I	30	1	0.2	THETA3_BiasKa	8.27
M	5	0	1	THETA3_BiasKa	6.07
M	5	0	0.5	THETA3_BiasKa	5.07
M	5	0	0.2	THETA3_BiasKa	4.6
M	5	1	1	THETA3_BiasKa	4.21
M	5	1	0.5	THETA3_BiasKa	4.35
M	5	1	0.2	THETA3_BiasKa	3.7
M	10	0	1	THETA3_BiasKa	8.07
M	10	0	0.5	THETA3_BiasKa	6.62
M	10	0	0.2	THETA3_BiasKa	5.13
M	10	1	1	THETA3_BiasKa	-0.48

continued on next page

Study	Magnitude of perturbation	kappa	γ	variable	Bias
M	10	1	0.5	THETA3_BiasKa	2.59
M	10	1	0.2	THETA3_BiasKa	3.61
M	15	0	1	THETA3_BiasKa	10.82
M	15	0	0.5	THETA3_BiasKa	8.31
M	15	0	0.2	THETA3_BiasKa	5.22
M	15	1	1	THETA3_BiasKa	-2.79
M	15	1	0.5	THETA3_BiasKa	0.81
M	15	1	0.2	THETA3_BiasKa	2.69
M	30	0	1	THETA3_BiasKa	31.24
M	30	0	0.5	THETA3_BiasKa	19.42
M	30	0	0.2	THETA3_BiasKa	9.73
M	30	1	1	THETA3_BiasKa	11.57
M	30	1	0.5	THETA3_BiasKa	8.61
M	30	1	0.2	THETA3_BiasKa	5.69
S	5	0	1	THETA3_BiasKa	5.09
S	5	0	0.5	THETA3_BiasKa	4.57
S	5	0	0.2	THETA3_BiasKa	3.53
S	5	1	1	THETA3_BiasKa	-1.2
S	5	1	0.5	THETA3_BiasKa	0.18

continued on next page

Study	Magnitude of perturbation	kappa	γ	variable	Bias
S	5	1	0.2	THETA3_BiasKa	0.31
S	10	0	1	THETA3_BiasKa	3.45
S	10	0	0.5	THETA3_BiasKa	0.83
S	10	0	0.2	THETA3_BiasKa	1.31
S	10	1	1	THETA3_BiasKa	-9.1
S	10	1	0.5	THETA3_BiasKa	-4.53
S	10	1	0.2	THETA3_BiasKa	-1.46
S	15	0	1	THETA3_BiasKa	4.29
S	15	0	0.5	THETA3_BiasKa	-6.61
S	15	0	0.2	THETA3_BiasKa	-5.87
S	15	1	1	THETA3_BiasKa	-13.21
S	15	1	0.5	THETA3_BiasKa	-7.09
S	15	1	0.2	THETA3_BiasKa	-2.78
S	30	0	1	THETA3_BiasKa	15.6
S	30	0	0.5	THETA3_BiasKa	-1.88
S	30	0	0.2	THETA3_BiasKa	-6.35
S	30	1	1	THETA3_BiasKa	3.76
S	30	1	0.5	THETA3_BiasKa	0.65
S	30	1	0.2	THETA3_BiasKa	0.82

continued on next page

Study	Magnitude of perturbation	kappa	γ	variable	Bias
I	5	0	1	THETA4_BiasQ	-4.92
I	5	0	0.5	THETA4_BiasQ	-4.2
I	5	0	0.2	THETA4_BiasQ	-3.82
I	5	1	1	THETA4_BiasQ	-3.54
I	5	1	0.5	THETA4_BiasQ	-3.48
I	5	1	0.2	THETA4_BiasQ	-3.38
I	10	0	1	THETA4_BiasQ	-8.22
I	10	0	0.5	THETA4_BiasQ	-5.92
I	10	0	0.2	THETA4_BiasQ	-4.55
I	10	1	1	THETA4_BiasQ	-1.77
I	10	1	0.5	THETA4_BiasQ	-2.63
I	10	1	0.2	THETA4_BiasQ	-3.17
I	15	0	1	THETA4_BiasQ	-10.63
I	15	0	0.5	THETA4_BiasQ	-7.91
I	15	0	0.2	THETA4_BiasQ	-5.42
I	15	1	1	THETA4_BiasQ	-1.29
I	15	1	0.5	THETA4_BiasQ	-2.2
I	15	1	0.2	THETA4_BiasQ	-2.9
I	30	0	1	THETA4_BiasQ	-17.32

continued on next page

Study	Magnitude of perturbation	kappa	γ	variable	Bias
I	30	0	0.5	THETA4_BiasQ	-12.21
I	30	0	0.2	THETA4_BiasQ	-7.32
I	30	1	1	THETA4_BiasQ	-4.8
I	30	1	0.5	THETA4_BiasQ	-4.15
I	30	1	0.2	THETA4_BiasQ	-3.64
M	5	0	1	THETA4_BiasQ	-2.98
M	5	0	0.5	THETA4_BiasQ	-1.84
M	5	0	0.2	THETA4_BiasQ	-0.95
M	5	1	1	THETA4_BiasQ	-0.93
M	5	1	0.5	THETA4_BiasQ	-0.98
M	5	1	0.2	THETA4_BiasQ	-0.35
M	10	0	1	THETA4_BiasQ	-7.73
M	10	0	0.5	THETA4_BiasQ	-4.91
M	10	0	0.2	THETA4_BiasQ	-2.04
M	10	1	1	THETA4_BiasQ	0.74
M	10	1	0.5	THETA4_BiasQ	-0.56
M	10	1	0.2	THETA4_BiasQ	-0.34
M	15	0	1	THETA4_BiasQ	-10.66
M	15	0	0.5	THETA4_BiasQ	-6.95

continued on next page

Study	Magnitude of perturbation	kappa	γ	variable	Bias
M	15	0	0.2	THETA4_BiasQ	-2.58
M	15	1	1	THETA4_BiasQ	1.57
M	15	1	0.5	THETA4_BiasQ	0.22
M	15	1	0.2	THETA4_BiasQ	0.26
M	30	0	1	THETA4_BiasQ	-18.06
M	30	0	0.5	THETA4_BiasQ	-10.46
M	30	0	0.2	THETA4_BiasQ	-3.86
M	30	1	1	THETA4_BiasQ	-4.23
M	30	1	0.5	THETA4_BiasQ	-2.33
M	30	1	0.2	THETA4_BiasQ	-0.27
S	5	0	1	THETA4_BiasQ	-7.54
S	5	0	0.5	THETA4_BiasQ	-4.47
S	5	0	0.2	THETA4_BiasQ	-2.02
S	5	1	1	THETA4_BiasQ	1.52
S	5	1	0.5	THETA4_BiasQ	1.85
S	5	1	0.2	THETA4_BiasQ	2.36
S	10	0	1	THETA4_BiasQ	-14.29
S	10	0	0.5	THETA4_BiasQ	-6.37
S	10	0	0.2	THETA4_BiasQ	-2.1

continued on next page

Study	Magnitude of perturbation	kappa	γ	variable	Bias
S	10	1	1	THETA4_BiasQ	4.08
S	10	1	0.5	THETA4_BiasQ	5.24
S	10	1	0.2	THETA4_BiasQ	4.99
S	15	0	1	THETA4_BiasQ	-8.7
S	15	0	0.5	THETA4_BiasQ	3.69
S	15	0	0.2	THETA4_BiasQ	4.1
S	15	1	1	THETA4_BiasQ	4.95
S	15	1	0.5	THETA4_BiasQ	7.3
S	15	1	0.2	THETA4_BiasQ	7.21
S	30	0	1	THETA4_BiasQ	12.93
S	30	0	0.5	THETA4_BiasQ	18.13
S	30	0	0.2	THETA4_BiasQ	10.86
S	30	1	1	THETA4_BiasQ	18.35
S	30	1	0.5	THETA4_BiasQ	15.49
S	30	1	0.2	THETA4_BiasQ	10.66
I	5	0	1	THETA5_BiasVp	-4.29
I	5	0	0.5	THETA5_BiasVp	-3.95
I	5	0	0.2	THETA5_BiasVp	-3.81
I	5	1	1	THETA5_BiasVp	-3.63

continued on next page

Study	Magnitude of perturbation	kappa	γ	variable	Bias
I	5	1	0.5	THETA5_BiasVp	-3.61
I	5	1	0.2	THETA5_BiasVp	-3.53
I	10	0	1	THETA5_BiasVp	-5.76
I	10	0	0.5	THETA5_BiasVp	-4.73
I	10	0	0.2	THETA5_BiasVp	-4.19
I	10	1	1	THETA5_BiasVp	-2.1
I	10	1	0.5	THETA5_BiasVp	-2.96
I	10	1	0.2	THETA5_BiasVp	-3.48
I	15	0	1	THETA5_BiasVp	-6.6
I	15	0	0.5	THETA5_BiasVp	-5.76
I	15	0	0.2	THETA5_BiasVp	-4.67
I	15	1	1	THETA5_BiasVp	-1.63
I	15	1	0.5	THETA5_BiasVp	-2.54
I	15	1	0.2	THETA5_BiasVp	-3.32
I	30	0	1	THETA5_BiasVp	-10.79
I	30	0	0.5	THETA5_BiasVp	-8.32
I	30	0	0.2	THETA5_BiasVp	-5.89
I	30	1	1	THETA5_BiasVp	-4.36
I	30	1	0.5	THETA5_BiasVp	-3.89

continued on next page

Study	Magnitude of perturbation	kappa	γ	variable	Bias
I	30	1	0.2	THETA5_BiasVp	-3.89
M	5	0	1	THETA5_BiasVp	-2.18
M	5	0	0.5	THETA5_BiasVp	-1.55
M	5	0	0.2	THETA5_BiasVp	-1.07
M	5	1	1	THETA5_BiasVp	-1.15
M	5	1	0.5	THETA5_BiasVp	-1.14
M	5	1	0.2	THETA5_BiasVp	-0.64
M	10	0	1	THETA5_BiasVp	-4.42
M	10	0	0.5	THETA5_BiasVp	-3.13
M	10	0	0.2	THETA5_BiasVp	-1.62
M	10	1	1	THETA5_BiasVp	0.27
M	10	1	0.5	THETA5_BiasVp	-0.81
M	10	1	0.2	THETA5_BiasVp	-0.78
M	15	0	1	THETA5_BiasVp	-5.96
M	15	0	0.5	THETA5_BiasVp	-4.15
M	15	0	0.2	THETA5_BiasVp	-1.78
M	15	1	1	THETA5_BiasVp	1.06
M	15	1	0.5	THETA5_BiasVp	-0.12
M	15	1	0.2	THETA5_BiasVp	-0.41

continued on next page

Study	Magnitude of perturbation	kappa	γ	variable	Bias
M	30	0	1	THETA5_BiasVp	-11.82
M	30	0	0.5	THETA5_BiasVp	-7.07
M	30	0	0.2	THETA5_BiasVp	-2.93
M	30	1	1	THETA5_BiasVp	-4.2
M	30	1	0.5	THETA5_BiasVp	-2.4
M	30	1	0.2	THETA5_BiasVp	-1.06
S	5	0	1	THETA5_BiasVp	-3.01
S	5	0	0.5	THETA5_BiasVp	-1.28
S	5	0	0.2	THETA5_BiasVp	0.24
S	5	1	1	THETA5_BiasVp	2.72
S	5	1	0.5	THETA5_BiasVp	2.6
S	5	1	0.2	THETA5_BiasVp	2.93
S	10	0	1	THETA5_BiasVp	-7.78
S	10	0	0.5	THETA5_BiasVp	-2.05
S	10	0	0.2	THETA5_BiasVp	0.65
S	10	1	1	THETA5_BiasVp	5.28
S	10	1	0.5	THETA5_BiasVp	4.89
S	10	1	0.2	THETA5_BiasVp	4.35
S	15	0	1	THETA5_BiasVp	-6.78

continued on next page

Study	Magnitude of perturbation	kappa	γ	variable	Bias
S	15	0	0.5	THETA5_BiasVp	3.24
S	15	0	0.2	THETA5_BiasVp	4.97
S	15	1	1	THETA5_BiasVp	6.48
S	15	1	0.5	THETA5_BiasVp	6.29
S	15	1	0.2	THETA5_BiasVp	5.55
S	30	0	1	THETA5_BiasVp	3
S	30	0	0.5	THETA5_BiasVp	8.8
S	30	0	0.2	THETA5_BiasVp	8.19
S	30	1	1	THETA5_BiasVp	10.39
S	30	1	0.5	THETA5_BiasVp	9.07
S	30	1	0.2	THETA5_BiasVp	6.61
I	5	0	1	OMEGA(1,1)_BiasOM	-2.61
I	5	0	0.5	OMEGA(1,1)_BiasOM	-2.49
I	5	0	0.2	OMEGA(1,1)_BiasOM	-2.32
I	5	1	1	OMEGA(1,1)_BiasOM	-2.24
I	5	1	0.5	OMEGA(1,1)_BiasOM	-2.28
I	5	1	0.2	OMEGA(1,1)_BiasOM	-2.35
I	10	0	1	OMEGA(1,1)_BiasOM	-3.6
I	10	0	0.5	OMEGA(1,1)_BiasOM	-3.04

continued on next page

Study	Magnitude of perturbation	kappa	γ	variable	Bias
I	10	0	0.2	OMEGA(1,1)_BiasOM	-2.64
I	10	1	1	OMEGA(1,1)_BiasOM	-1.93
I	10	1	0.5	OMEGA(1,1)_BiasOM	-2.08
I	10	1	0.2	OMEGA(1,1)_BiasOM	-2.26
I	15	0	1	OMEGA(1,1)_BiasOM	-4.58
I	15	0	0.5	OMEGA(1,1)_BiasOM	-3.66
I	15	0	0.2	OMEGA(1,1)_BiasOM	-2.96
I	15	1	1	OMEGA(1,1)_BiasOM	-1.75
I	15	1	0.5	OMEGA(1,1)_BiasOM	-1.94
I	15	1	0.2	OMEGA(1,1)_BiasOM	-2.16
I	30	0	1	OMEGA(1,1)_BiasOM	-5.58
I	30	0	0.5	OMEGA(1,1)_BiasOM	-4.27
I	30	0	0.2	OMEGA(1,1)_BiasOM	-3.25
I	30	1	1	OMEGA(1,1)_BiasOM	-1.84
I	30	1	0.5	OMEGA(1,1)_BiasOM	-1.93
I	30	1	0.2	OMEGA(1,1)_BiasOM	-2.12
M	5	0	1	OMEGA(1,1)_BiasOM	-2.3
M	5	0	0.5	OMEGA(1,1)_BiasOM	-2.04
M	5	0	0.2	OMEGA(1,1)_BiasOM	-1.94

continued on next page

Study	Magnitude of perturbation	kappa	γ	variable	Bias
M	5	1	1	OMEGA(1,1)_BiasOM	-1.73
M	5	1	0.5	OMEGA(1,1)_BiasOM	-1.8
M	5	1	0.2	OMEGA(1,1)_BiasOM	-1.78
M	10	0	1	OMEGA(1,1)_BiasOM	-3.89
M	10	0	0.5	OMEGA(1,1)_BiasOM	-2.87
M	10	0	0.2	OMEGA(1,1)_BiasOM	-2.28
M	10	1	1	OMEGA(1,1)_BiasOM	-1.28
M	10	1	0.5	OMEGA(1,1)_BiasOM	-1.55
M	10	1	0.2	OMEGA(1,1)_BiasOM	-1.69
M	15	0	1	OMEGA(1,1)_BiasOM	-5.49
M	15	0	0.5	OMEGA(1,1)_BiasOM	-3.87
M	15	0	0.2	OMEGA(1,1)_BiasOM	-2.74
M	15	1	1	OMEGA(1,1)_BiasOM	-1.02
M	15	1	0.5	OMEGA(1,1)_BiasOM	-1.33
M	15	1	0.2	OMEGA(1,1)_BiasOM	-1.54
M	30	0	1	OMEGA(1,1)_BiasOM	-7.01
M	30	0	0.5	OMEGA(1,1)_BiasOM	-4.89
M	30	0	0.2	OMEGA(1,1)_BiasOM	-3.19
M	30	1	1	OMEGA(1,1)_BiasOM	-1.38

continued on next page

Study	Magnitude of perturbation	kappa	γ	variable	Bias
M	30	1	0.5	OMEGA(1,1)_BiasOM	-1.54
M	30	1	0.2	OMEGA(1,1)_BiasOM	-1.57
S	5	0	1	OMEGA(1,1)_BiasOM	-2.54
S	5	0	0.5	OMEGA(1,1)_BiasOM	-1.87
S	5	0	0.2	OMEGA(1,1)_BiasOM	-1.29
S	5	1	1	OMEGA(1,1)_BiasOM	0.06
S	5	1	0.5	OMEGA(1,1)_BiasOM	0
S	5	1	0.2	OMEGA(1,1)_BiasOM	0.1
S	10	0	1	OMEGA(1,1)_BiasOM	-5.53
S	10	0	0.5	OMEGA(1,1)_BiasOM	-3.89
S	10	0	0.2	OMEGA(1,1)_BiasOM	-2.23
S	10	1	1	OMEGA(1,1)_BiasOM	1.39
S	10	1	0.5	OMEGA(1,1)_BiasOM	1.26
S	10	1	0.2	OMEGA(1,1)_BiasOM	0.97
S	15	0	1	OMEGA(1,1)_BiasOM	-4.22
S	15	0	0.5	OMEGA(1,1)_BiasOM	-4.33
S	15	0	0.2	OMEGA(1,1)_BiasOM	-2.88
S	15	1	1	OMEGA(1,1)_BiasOM	2.12
S	15	1	0.5	OMEGA(1,1)_BiasOM	2.05

continued on next page

Study	Magnitude of perturbation	kappa	γ	variable	Bias
S	15	1	0.2	OMEGA(1,1)_BiasOM	1.87
S	30	0	1	OMEGA(1,1)_BiasOM	-2.48
S	30	0	0.5	OMEGA(1,1)_BiasOM	-3.39
S	30	0	0.2	OMEGA(1,1)_BiasOM	-3.09
S	30	1	1	OMEGA(1,1)_BiasOM	2.74
S	30	1	0.5	OMEGA(1,1)_BiasOM	2.39
S	30	1	0.2	OMEGA(1,1)_BiasOM	1.93
I	5	0	1	OMEGA(2,2)_BiasOM	-7.61
I	5	0	0.5	OMEGA(2,2)_BiasOM	-5.93
I	5	0	0.2	OMEGA(2,2)_BiasOM	-4.98
I	5	1	1	OMEGA(2,2)_BiasOM	-4.95
I	5	1	0.5	OMEGA(2,2)_BiasOM	-4.48
I	5	1	0.2	OMEGA(2,2)_BiasOM	-4.02
I	10	0	1	OMEGA(2,2)_BiasOM	-14.96
I	10	0	0.5	OMEGA(2,2)_BiasOM	-9.75
I	10	0	0.2	OMEGA(2,2)_BiasOM	-6.56
I	10	1	1	OMEGA(2,2)_BiasOM	-0.84
I	10	1	0.5	OMEGA(2,2)_BiasOM	-3.08
I	10	1	0.2	OMEGA(2,2)_BiasOM	-4.04

continued on next page

Study	Magnitude of perturbation	kappa	γ	variable	Bias
I	15	0	1	OMEGA(2,2)_BiasOM	-18.03
I	15	0	0.5	OMEGA(2,2)_BiasOM	-13.36
I	15	0	0.2	OMEGA(2,2)_BiasOM	-7.95
I	15	1	1	OMEGA(2,2)_BiasOM	0.19
I	15	1	0.5	OMEGA(2,2)_BiasOM	-2.03
I	15	1	0.2	OMEGA(2,2)_BiasOM	-3.54
I	30	0	1	OMEGA(2,2)_BiasOM	-30.24
I	30	0	0.5	OMEGA(2,2)_BiasOM	-18.9
I	30	0	0.2	OMEGA(2,2)_BiasOM	-10.57
I	30	1	1	OMEGA(2,2)_BiasOM	-7.96
I	30	1	0.5	OMEGA(2,2)_BiasOM	-4.92
I	30	1	0.2	OMEGA(2,2)_BiasOM	-4.73
M	5	0	1	OMEGA(2,2)_BiasOM	-9.07
M	5	0	0.5	OMEGA(2,2)_BiasOM	-5.9
M	5	0	0.2	OMEGA(2,2)_BiasOM	-3.54
M	5	1	1	OMEGA(2,2)_BiasOM	-3.59
M	5	1	0.5	OMEGA(2,2)_BiasOM	-3.46
M	5	1	0.2	OMEGA(2,2)_BiasOM	-1.29
M	10	0	1	OMEGA(2,2)_BiasOM	-23.03

continued on next page

Study	Magnitude of perturbation	kappa	γ	variable	Bias
M	10	0	0.5	OMEGA(2,2)_BiasOM	-15.76
M	10	0	0.2	OMEGA(2,2)_BiasOM	-6.97
M	10	1	1	OMEGA(2,2)_BiasOM	0.18
M	10	1	0.5	OMEGA(2,2)_BiasOM	-3.14
M	10	1	0.2	OMEGA(2,2)_BiasOM	-2.11
M	15	0	1	OMEGA(2,2)_BiasOM	-32.13
M	15	0	0.5	OMEGA(2,2)_BiasOM	-21.81
M	15	0	0.2	OMEGA(2,2)_BiasOM	-8.44
M	15	1	1	OMEGA(2,2)_BiasOM	2.65
M	15	1	0.5	OMEGA(2,2)_BiasOM	-0.62
M	15	1	0.2	OMEGA(2,2)_BiasOM	-1.1
M	30	0	1	OMEGA(2,2)_BiasOM	-41.23
M	30	0	0.5	OMEGA(2,2)_BiasOM	-28.64
M	30	0	0.2	OMEGA(2,2)_BiasOM	-12.62
M	30	1	1	OMEGA(2,2)_BiasOM	-8.19
M	30	1	0.5	OMEGA(2,2)_BiasOM	-4.68
M	30	1	0.2	OMEGA(2,2)_BiasOM	-2.32
S	5	0	1	OMEGA(2,2)_BiasOM	-11.13
S	5	0	0.5	OMEGA(2,2)_BiasOM	-6.4

continued on next page

Study	Magnitude of perturbation	kappa	γ	variable	Bias
S	5	0	0.2	OMEGA(2,2)_BiasOM	0.24
S	5	1	1	OMEGA(2,2)_BiasOM	15.47
S	5	1	0.5	OMEGA(2,2)_BiasOM	13.49
S	5	1	0.2	OMEGA(2,2)_BiasOM	14.87
S	10	0	1	OMEGA(2,2)_BiasOM	-41.13
S	10	0	0.5	OMEGA(2,2)_BiasOM	-20.97
S	10	0	0.2	OMEGA(2,2)_BiasOM	-5.75
S	10	1	1	OMEGA(2,2)_BiasOM	27.31
S	10	1	0.5	OMEGA(2,2)_BiasOM	23.21
S	10	1	0.2	OMEGA(2,2)_BiasOM	20.73
S	15	0	1	OMEGA(2,2)_BiasOM	-52.7
S	15	0	0.5	OMEGA(2,2)_BiasOM	-12.93
S	15	0	0.2	OMEGA(2,2)_BiasOM	0.7
S	15	1	1	OMEGA(2,2)_BiasOM	32.52
S	15	1	0.5	OMEGA(2,2)_BiasOM	29.18
S	15	1	0.2	OMEGA(2,2)_BiasOM	26.84
S	30	0	1	OMEGA(2,2)_BiasOM	-37.58
S	30	0	0.5	OMEGA(2,2)_BiasOM	-6.45
S	30	0	0.2	OMEGA(2,2)_BiasOM	6.25

continued on next page

Study	Magnitude of perturbation	kappa	γ	variable	Bias
S	30	1	1	OMEGA(2,2)_BiasOM	35.58
S	30	1	0.5	OMEGA(2,2)_BiasOM	30.45
S	30	1	0.2	OMEGA(2,2)_BiasOM	27.42
I	5	0	1	OMEGA(3,3)_BiasOM	15.56
I	5	0	0.5	OMEGA(3,3)_BiasOM	11.13
I	5	0	0.2	OMEGA(3,3)_BiasOM	8.65
I	5	1	1	OMEGA(3,3)_BiasOM	8.35
I	5	1	0.5	OMEGA(3,3)_BiasOM	7.34
I	5	1	0.2	OMEGA(3,3)_BiasOM	6.71
I	10	0	1	OMEGA(3,3)_BiasOM	30.25
I	10	0	0.5	OMEGA(3,3)_BiasOM	17.92
I	10	0	0.2	OMEGA(3,3)_BiasOM	11.55
I	10	1	1	OMEGA(3,3)_BiasOM	0.4
I	10	1	0.5	OMEGA(3,3)_BiasOM	3.3
I	10	1	0.2	OMEGA(3,3)_BiasOM	5.31
I	15	0	1	OMEGA(3,3)_BiasOM	38.99
I	15	0	0.5	OMEGA(3,3)_BiasOM	23.52
I	15	0	0.2	OMEGA(3,3)_BiasOM	13.32
I	15	1	1	OMEGA(3,3)_BiasOM	-1.58

continued on next page

Study	Magnitude of perturbation	kappa	γ	variable	Bias
I	15	1	0.5	OMEGA(3,3)_BiasOM	1.3
I	15	1	0.2	OMEGA(3,3)_BiasOM	3.9
I	30	0	1	OMEGA(3,3)_BiasOM	80.24
I	30	0	0.5	OMEGA(3,3)_BiasOM	44.75
I	30	0	0.2	OMEGA(3,3)_BiasOM	20.89
I	30	1	1	OMEGA(3,3)_BiasOM	18.63
I	30	1	0.5	OMEGA(3,3)_BiasOM	12.64
I	30	1	0.2	OMEGA(3,3)_BiasOM	7.84
M	5	0	1	OMEGA(3,3)_BiasOM	20.41
M	5	0	0.5	OMEGA(3,3)_BiasOM	13.98
M	5	0	0.2	OMEGA(3,3)_BiasOM	7.07
M	5	1	1	OMEGA(3,3)_BiasOM	5.83
M	5	1	0.5	OMEGA(3,3)_BiasOM	7.7
M	5	1	0.2	OMEGA(3,3)_BiasOM	2.74
M	10	0	1	OMEGA(3,3)_BiasOM	53.88
M	10	0	0.5	OMEGA(3,3)_BiasOM	38.88
M	10	0	0.2	OMEGA(3,3)_BiasOM	16.63
M	10	1	1	OMEGA(3,3)_BiasOM	-4.14
M	10	1	0.5	OMEGA(3,3)_BiasOM	7.04

continued on next page

Study	Magnitude of perturbation	kappa	γ	variable	Bias
M	10	1	0.2	OMEGA(3,3)_BiasOM	3.8
M	15	0	1	OMEGA(3,3)_BiasOM	77.71
M	15	0	0.5	OMEGA(3,3)_BiasOM	54.23
M	15	0	0.2	OMEGA(3,3)_BiasOM	21.67
M	15	1	1	OMEGA(3,3)_BiasOM	-9.51
M	15	1	0.5	OMEGA(3,3)_BiasOM	2.94
M	15	1	0.2	OMEGA(3,3)_BiasOM	0.89
M	30	0	1	OMEGA(3,3)_BiasOM	129.74
M	30	0	0.5	OMEGA(3,3)_BiasOM	82.46
M	30	0	0.2	OMEGA(3,3)_BiasOM	33.12
M	30	1	1	OMEGA(3,3)_BiasOM	19.09
M	30	1	0.5	OMEGA(3,3)_BiasOM	20.98
M	30	1	0.2	OMEGA(3,3)_BiasOM	7.31
S	5	0	1	OMEGA(3,3)_BiasOM	29.24
S	5	0	0.5	OMEGA(3,3)_BiasOM	16.55
S	5	0	0.2	OMEGA(3,3)_BiasOM	5.61
S	5	1	1	OMEGA(3,3)_BiasOM	-12.59
S	5	1	0.5	OMEGA(3,3)_BiasOM	-13.43
S	5	1	0.2	OMEGA(3,3)_BiasOM	-15.82

continued on next page

Study	Magnitude of perturbation	kappa	γ	variable	Bias
S	10	0	1	OMEGA(3,3)_BiasOM	83.68
S	10	0	0.5	OMEGA(3,3)_BiasOM	39.97
S	10	0	0.2	OMEGA(3,3)_BiasOM	13.81
S	10	1	1	OMEGA(3,3)_BiasOM	-30.77
S	10	1	0.5	OMEGA(3,3)_BiasOM	-31.72
S	10	1	0.2	OMEGA(3,3)_BiasOM	-28.12
S	15	0	1	OMEGA(3,3)_BiasOM	105.49
S	15	0	0.5	OMEGA(3,3)_BiasOM	27.66
S	15	0	0.2	OMEGA(3,3)_BiasOM	3.35
S	15	1	1	OMEGA(3,3)_BiasOM	-38.97
S	15	1	0.5	OMEGA(3,3)_BiasOM	-41.94
S	15	1	0.2	OMEGA(3,3)_BiasOM	-39.99
S	30	0	1	OMEGA(3,3)_BiasOM	111.18
S	30	0	0.5	OMEGA(3,3)_BiasOM	27.72
S	30	0	0.2	OMEGA(3,3)_BiasOM	-0.78
S	30	1	1	OMEGA(3,3)_BiasOM	-27.7
S	30	1	0.5	OMEGA(3,3)_BiasOM	-35.64
S	30	1	0.2	OMEGA(3,3)_BiasOM	-37.92
I	5	0	1	OMEGA(4,4)_BiasOM	-20.18

continued on next page

Study	Magnitude of perturbation	kappa	γ	variable	Bias
I	5	0	0.5	OMEGA(4,4)_BiasOM	-16.84
I	5	0	0.2	OMEGA(4,4)_BiasOM	-14.27
I	5	1	1	OMEGA(4,4)_BiasOM	-13.18
I	5	1	0.5	OMEGA(4,4)_BiasOM	-13.01
I	5	1	0.2	OMEGA(4,4)_BiasOM	-12.68
I	10	0	1	OMEGA(4,4)_BiasOM	-44.06
I	10	0	0.5	OMEGA(4,4)_BiasOM	-30.96
I	10	0	0.2	OMEGA(4,4)_BiasOM	-19.94
I	10	1	1	OMEGA(4,4)_BiasOM	-13.29
I	10	1	0.5	OMEGA(4,4)_BiasOM	-13.21
I	10	1	0.2	OMEGA(4,4)_BiasOM	-12.22
I	15	0	1	OMEGA(4,4)_BiasOM	-64.61
I	15	0	0.5	OMEGA(4,4)_BiasOM	-45.31
I	15	0	0.2	OMEGA(4,4)_BiasOM	-26.84
I	15	1	1	OMEGA(4,4)_BiasOM	-13.24
I	15	1	0.5	OMEGA(4,4)_BiasOM	-13.55
I	15	1	0.2	OMEGA(4,4)_BiasOM	-12.05
I	30	0	1	OMEGA(4,4)_BiasOM	-76.54
I	30	0	0.5	OMEGA(4,4)_BiasOM	-56.05

continued on next page

Study	Magnitude of perturbation	kappa	γ	variable	Bias
I	30	0	0.2	OMEGA(4,4)_BiasOM	-32.53
I	30	1	1	OMEGA(4,4)_BiasOM	-8.62
I	30	1	0.5	OMEGA(4,4)_BiasOM	-12.91
I	30	1	0.2	OMEGA(4,4)_BiasOM	-11.73
M	5	0	1	OMEGA(4,4)_BiasOM	-12.87
M	5	0	0.5	OMEGA(4,4)_BiasOM	-7.73
M	5	0	0.2	OMEGA(4,4)_BiasOM	-6.01
M	5	1	1	OMEGA(4,4)_BiasOM	-5.91
M	5	1	0.5	OMEGA(4,4)_BiasOM	-4.84
M	5	1	0.2	OMEGA(4,4)_BiasOM	-4.89
M	10	0	1	OMEGA(4,4)_BiasOM	-42.13
M	10	0	0.5	OMEGA(4,4)_BiasOM	-21.65
M	10	0	0.2	OMEGA(4,4)_BiasOM	-11.29
M	10	1	1	OMEGA(4,4)_BiasOM	-6.92
M	10	1	0.5	OMEGA(4,4)_BiasOM	-4.5
M	10	1	0.2	OMEGA(4,4)_BiasOM	-4.01
M	15	0	1	OMEGA(4,4)_BiasOM	-68.46
M	15	0	0.5	OMEGA(4,4)_BiasOM	-40.11
M	15	0	0.2	OMEGA(4,4)_BiasOM	-19.81

continued on next page

Study	Magnitude of perturbation	kappa	γ	variable	Bias
M	15	1	1	OMEGA(4,4)_BiasOM	-7.52
M	15	1	0.5	OMEGA(4,4)_BiasOM	-5.01
M	15	1	0.2	OMEGA(4,4)_BiasOM	-3.39
M	30	0	1	OMEGA(4,4)_BiasOM	-79.48
M	30	0	0.5	OMEGA(4,4)_BiasOM	-49.48
M	30	0	0.2	OMEGA(4,4)_BiasOM	-25.09
M	30	1	1	OMEGA(4,4)_BiasOM	-2.31
M	30	1	0.5	OMEGA(4,4)_BiasOM	-3.61
M	30	1	0.2	OMEGA(4,4)_BiasOM	-2.56
S	5	0	1	OMEGA(4,4)_BiasOM	7.17
S	5	0	0.5	OMEGA(4,4)_BiasOM	14.45
S	5	0	0.2	OMEGA(4,4)_BiasOM	18.54
S	5	1	1	OMEGA(4,4)_BiasOM	32.83
S	5	1	0.5	OMEGA(4,4)_BiasOM	33.51
S	5	1	0.2	OMEGA(4,4)_BiasOM	32.14
S	10	0	1	OMEGA(4,4)_BiasOM	-74.54
S	10	0	0.5	OMEGA(4,4)_BiasOM	-38.66
S	10	0	0.2	OMEGA(4,4)_BiasOM	-4.85
S	10	1	1	OMEGA(4,4)_BiasOM	39.47

continued on next page

Study	Magnitude of perturbation	kappa	γ	variable	Bias
S	10	1	0.5	OMEGA(4,4)_BiasOM	43.52
S	10	1	0.2	OMEGA(4,4)_BiasOM	39.72
S	15	0	1	OMEGA(4,4)_BiasOM	-99.8
S	15	0	0.5	OMEGA(4,4)_BiasOM	-89.6
S	15	0	0.2	OMEGA(4,4)_BiasOM	-46.24
S	15	1	1	OMEGA(4,4)_BiasOM	40.89
S	15	1	0.5	OMEGA(4,4)_BiasOM	49.08
S	15	1	0.2	OMEGA(4,4)_BiasOM	46.74
S	30	0	1	OMEGA(4,4)_BiasOM	-99.94
S	30	0	0.5	OMEGA(4,4)_BiasOM	-97.12
S	30	0	0.2	OMEGA(4,4)_BiasOM	-61.09
S	30	1	1	OMEGA(4,4)_BiasOM	66.56
S	30	1	0.5	OMEGA(4,4)_BiasOM	64.06
S	30	1	0.2	OMEGA(4,4)_BiasOM	52.21
I	5	0	1	OMEGA(5,5)_BiasOM	2.83
I	5	0	0.5	OMEGA(5,5)_BiasOM	2.83
I	5	0	0.2	OMEGA(5,5)_BiasOM	2.91
I	5	1	1	OMEGA(5,5)_BiasOM	2.97
I	5	1	0.5	OMEGA(5,5)_BiasOM	2.97

continued on next page

Study	Magnitude of perturbation	kappa	γ	variable	Bias
I	5	1	0.2	OMEGA(5,5)_BiasOM	2.85
I	10	0	1	OMEGA(5,5)_BiasOM	0.95
I	10	0	0.5	OMEGA(5,5)_BiasOM	1.59
I	10	0	0.2	OMEGA(5,5)_BiasOM	2.53
I	10	1	1	OMEGA(5,5)_BiasOM	0.72
I	10	1	0.5	OMEGA(5,5)_BiasOM	2.08
I	10	1	0.2	OMEGA(5,5)_BiasOM	2.73
I	15	0	1	OMEGA(5,5)_BiasOM	-1.54
I	15	0	0.5	OMEGA(5,5)_BiasOM	0.76
I	15	0	0.2	OMEGA(5,5)_BiasOM	2.03
I	15	1	1	OMEGA(5,5)_BiasOM	0.27
I	15	1	0.5	OMEGA(5,5)_BiasOM	1.57
I	15	1	0.2	OMEGA(5,5)_BiasOM	2.55
I	30	0	1	OMEGA(5,5)_BiasOM	2.65
I	30	0	0.5	OMEGA(5,5)_BiasOM	4.03
I	30	0	0.2	OMEGA(5,5)_BiasOM	3.37
I	30	1	1	OMEGA(5,5)_BiasOM	5.78
I	30	1	0.5	OMEGA(5,5)_BiasOM	4.47
I	30	1	0.2	OMEGA(5,5)_BiasOM	3.86

continued on next page

Study	Magnitude of perturbation	kappa	γ	variable	Bias
M	5	0	1	OMEGA(5,5)_BiasOM	-0.6
M	5	0	0.5	OMEGA(5,5)_BiasOM	0.05
M	5	0	0.2	OMEGA(5,5)_BiasOM	-0.1
M	5	1	1	OMEGA(5,5)_BiasOM	0.53
M	5	1	0.5	OMEGA(5,5)_BiasOM	0.55
M	5	1	0.2	OMEGA(5,5)_BiasOM	0.04
M	10	0	1	OMEGA(5,5)_BiasOM	-6.67
M	10	0	0.5	OMEGA(5,5)_BiasOM	-2.58
M	10	0	0.2	OMEGA(5,5)_BiasOM	-1.35
M	10	1	1	OMEGA(5,5)_BiasOM	-0.86
M	10	1	0.5	OMEGA(5,5)_BiasOM	0.49
M	10	1	0.2	OMEGA(5,5)_BiasOM	0.34
M	15	0	1	OMEGA(5,5)_BiasOM	-13.98
M	15	0	0.5	OMEGA(5,5)_BiasOM	-7.02
M	15	0	0.2	OMEGA(5,5)_BiasOM	-3.97
M	15	1	1	OMEGA(5,5)_BiasOM	-1.65
M	15	1	0.5	OMEGA(5,5)_BiasOM	0.02
M	15	1	0.2	OMEGA(5,5)_BiasOM	0.18
M	30	0	1	OMEGA(5,5)_BiasOM	-12.37

continued on next page

Study	Magnitude of perturbation	kappa	γ	variable	Bias
M	30	0	0.5	OMEGA(5,5)_BiasOM	-6.57
M	30	0	0.2	OMEGA(5,5)_BiasOM	-4.03
M	30	1	1	OMEGA(5,5)_BiasOM	7.2
M	30	1	0.5	OMEGA(5,5)_BiasOM	4.33
M	30	1	0.2	OMEGA(5,5)_BiasOM	1.59
S	5	0	1	OMEGA(5,5)_BiasOM	-3.73
S	5	0	0.5	OMEGA(5,5)_BiasOM	-0.56
S	5	0	0.2	OMEGA(5,5)_BiasOM	2.27
S	5	1	1	OMEGA(5,5)_BiasOM	7.91
S	5	1	0.5	OMEGA(5,5)_BiasOM	8.26
S	5	1	0.2	OMEGA(5,5)_BiasOM	8.75
S	10	0	1	OMEGA(5,5)_BiasOM	-35.12
S	10	0	0.5	OMEGA(5,5)_BiasOM	-23.24
S	10	0	0.2	OMEGA(5,5)_BiasOM	-9.16
S	10	1	1	OMEGA(5,5)_BiasOM	10.86
S	10	1	0.5	OMEGA(5,5)_BiasOM	11.88
S	10	1	0.2	OMEGA(5,5)_BiasOM	11.93
S	15	0	1	OMEGA(5,5)_BiasOM	-76.47
S	15	0	0.5	OMEGA(5,5)_BiasOM	-51.89

continued on next page

Study	Magnitude of perturbation	kappa	γ	variable	Bias
S	15	0	0.2	OMEGA(5,5)_BiasOM	-26.16
S	15	1	1	OMEGA(5,5)_BiasOM	11.86
S	15	1	0.5	OMEGA(5,5)_BiasOM	13.88
S	15	1	0.2	OMEGA(5,5)_BiasOM	15.87
S	30	0	1	OMEGA(5,5)_BiasOM	-90.98
S	30	0	0.5	OMEGA(5,5)_BiasOM	-68.6
S	30	0	0.2	OMEGA(5,5)_BiasOM	-35.09
S	30	1	1	OMEGA(5,5)_BiasOM	10.76
S	30	1	0.5	OMEGA(5,5)_BiasOM	12.02
S	30	1	0.2	OMEGA(5,5)_BiasOM	14.49
I	5	0	1	SIGMA(1,1)_BiasRUV	8.95
I	5	0	0.5	SIGMA(1,1)_BiasRUV	5.02
I	5	0	0.2	SIGMA(1,1)_BiasRUV	2.18
I	5	1	1	SIGMA(1,1)_BiasRUV	0.79
I	5	1	0.5	SIGMA(1,1)_BiasRUV	0.61
I	5	1	0.2	SIGMA(1,1)_BiasRUV	0.39
I	10	0	1	SIGMA(1,1)_BiasRUV	40.46
I	10	0	0.5	SIGMA(1,1)_BiasRUV	21.65
I	10	0	0.2	SIGMA(1,1)_BiasRUV	8.7

continued on next page

Study	Magnitude of perturbation	kappa	γ	variable	Bias
I	10	1	1	SIGMA(1,1)_BiasRUV	0.16
I	10	1	0.5	SIGMA(1,1)_BiasRUV	-0.13
I	10	1	0.2	SIGMA(1,1)_BiasRUV	0.05
I	15	0	1	SIGMA(1,1)_BiasRUV	77.65
I	15	0	0.5	SIGMA(1,1)_BiasRUV	41.78
I	15	0	0.2	SIGMA(1,1)_BiasRUV	17.35
I	15	1	1	SIGMA(1,1)_BiasRUV	1.09
I	15	1	0.5	SIGMA(1,1)_BiasRUV	0.26
I	15	1	0.2	SIGMA(1,1)_BiasRUV	-0.17
I	30	0	1	SIGMA(1,1)_BiasRUV	121.19
I	30	0	0.5	SIGMA(1,1)_BiasRUV	65.2
I	30	0	0.2	SIGMA(1,1)_BiasRUV	27.51
I	30	1	1	SIGMA(1,1)_BiasRUV	11.25
I	30	1	0.5	SIGMA(1,1)_BiasRUV	6.04
I	30	1	0.2	SIGMA(1,1)_BiasRUV	2.3
M	5	0	1	SIGMA(1,1)_BiasRUV	7.74
M	5	0	0.5	SIGMA(1,1)_BiasRUV	2.34
M	5	0	0.2	SIGMA(1,1)_BiasRUV	0.45
M	5	1	1	SIGMA(1,1)_BiasRUV	-0.81

continued on next page

Study	Magnitude of perturbation	kappa	γ	variable	Bias
M	5	1	0.5	SIGMA(1,1)_BiasRUV	-1.18
M	5	1	0.2	SIGMA(1,1)_BiasRUV	-1.54
M	10	0	1	SIGMA(1,1)_BiasRUV	45.47
M	10	0	0.5	SIGMA(1,1)_BiasRUV	19.17
M	10	0	0.2	SIGMA(1,1)_BiasRUV	6.78
M	10	1	1	SIGMA(1,1)_BiasRUV	-1.82
M	10	1	0.5	SIGMA(1,1)_BiasRUV	-2.21
M	10	1	0.2	SIGMA(1,1)_BiasRUV	-2.17
M	15	0	1	SIGMA(1,1)_BiasRUV	94.05
M	15	0	0.5	SIGMA(1,1)_BiasRUV	44.4
M	15	0	0.2	SIGMA(1,1)_BiasRUV	17.14
M	15	1	1	SIGMA(1,1)_BiasRUV	-1.38
M	15	1	0.5	SIGMA(1,1)_BiasRUV	-2.22
M	15	1	0.2	SIGMA(1,1)_BiasRUV	-2.83
M	30	0	1	SIGMA(1,1)_BiasRUV	138.41
M	30	0	0.5	SIGMA(1,1)_BiasRUV	69.04
M	30	0	0.2	SIGMA(1,1)_BiasRUV	27.79
M	30	1	1	SIGMA(1,1)_BiasRUV	8.38
M	30	1	0.5	SIGMA(1,1)_BiasRUV	3.72

continued on next page

Study	Magnitude of perturbation	kappa	γ	variable	Bias
M	30	1	0.2	SIGMA(1,1)_BiasRUV	-0.06
S	5	0	1	SIGMA(1,1)_BiasRUV	8.02
S	5	0	0.5	SIGMA(1,1)_BiasRUV	1.42
S	5	0	0.2	SIGMA(1,1)_BiasRUV	-3.74
S	5	1	1	SIGMA(1,1)_BiasRUV	-15.95
S	5	1	0.5	SIGMA(1,1)_BiasRUV	-15.56
S	5	1	0.2	SIGMA(1,1)_BiasRUV	-15.96
S	10	0	1	SIGMA(1,1)_BiasRUV	81.23
S	10	0	0.5	SIGMA(1,1)_BiasRUV	46.19
S	10	0	0.2	SIGMA(1,1)_BiasRUV	15.62
S	10	1	1	SIGMA(1,1)_BiasRUV	-25.61
S	10	1	0.5	SIGMA(1,1)_BiasRUV	-24.09
S	10	1	0.2	SIGMA(1,1)_BiasRUV	-21.67
S	15	0	1	SIGMA(1,1)_BiasRUV	173.31
S	15	0	0.5	SIGMA(1,1)_BiasRUV	106.17
S	15	0	0.2	SIGMA(1,1)_BiasRUV	46.14
S	15	1	1	SIGMA(1,1)_BiasRUV	-30.11
S	15	1	0.5	SIGMA(1,1)_BiasRUV	-28.81
S	15	1	0.2	SIGMA(1,1)_BiasRUV	-27.72

continued on next page

Study	Magnitude of perturbation	kappa	γ	variable	Bias
S	30	0	1	SIGMA(1,1)_BiasRUV	228.05
S	30	0	0.5	SIGMA(1,1)_BiasRUV	141.69
S	30	0	0.2	SIGMA(1,1)_BiasRUV	63.56
S	30	1	1	SIGMA(1,1)_BiasRUV	-17.19
S	30	1	0.5	SIGMA(1,1)_BiasRUV	-21.15
S	30	1	0.2	SIGMA(1,1)_BiasRUV	-23.43

Part I - Numerical values for relative RMSE

Study	Magnitude of perturbation	kappa	γ	variable	RMSE[%]
I	5	0	1	THETA1_RMCL	2.5
I	5	0	0.5	THETA1_RMCL	2.42
I	5	0	0.2	THETA1_RMCL	2.36
I	5	1	1	THETA1_RMCL	2.39
I	5	1	0.5	THETA1_RMCL	2.36
I	5	1	0.2	THETA1_RMCL	2.33
I	10	0	1	THETA1_RMCL	3.13
I	10	0	0.5	THETA1_RMCL	2.75
I	10	0	0.2	THETA1_RMCL	2.49
I	10	1	1	THETA1_RMCL	2.51
I	10	1	0.5	THETA1_RMCL	2.45
I	10	1	0.2	THETA1_RMCL	2.35
I	15	0	1	THETA1_RMCL	3.85
I	15	0	0.5	THETA1_RMCL	3.14
I	15	0	0.2	THETA1_RMCL	2.65
I	15	1	1	THETA1_RMCL	2.62
I	15	1	0.5	THETA1_RMCL	2.5
I	15	1	0.2	THETA1_RMCL	2.39

continued on next page

Study	Magnitude of perturbation	kappa	γ	variable	RMSE[%]
I	30	0	1	THETA1_RMCL	4.63
I	30	0	0.5	THETA1_RMCL	3.58
I	30	0	0.2	THETA1_RMCL	2.85
I	30	1	1	THETA1_RMCL	2.88
I	30	1	0.5	THETA1_RMCL	2.67
I	30	1	0.2	THETA1_RMCL	2.47
M	5	0	1	THETA1_RMCL	2.87
M	5	0	0.5	THETA1_RMCL	2.78
M	5	0	0.2	THETA1_RMCL	2.76
M	5	1	1	THETA1_RMCL	2.82
M	5	1	0.5	THETA1_RMCL	2.76
M	5	1	0.2	THETA1_RMCL	2.75
M	10	0	1	THETA1_RMCL	3.46
M	10	0	0.5	THETA1_RMCL	3.03
M	10	0	0.2	THETA1_RMCL	2.86
M	10	1	1	THETA1_RMCL	2.98
M	10	1	0.5	THETA1_RMCL	2.84
M	10	1	0.2	THETA1_RMCL	2.79
M	15	0	1	THETA1_RMCL	4.23

continued on next page

Study	Magnitude of perturbation	kappa	γ	variable	RMSE[%]
M	15	0	0.5	THETA1_RMCL	3.45
M	15	0	0.2	THETA1_RMCL	3.05
M	15	1	1	THETA1_RMCL	3.11
M	15	1	0.5	THETA1_RMCL	2.94
M	15	1	0.2	THETA1_RMCL	2.84
M	30	0	1	THETA1_RMCL	4.84
M	30	0	0.5	THETA1_RMCL	3.87
M	30	0	0.2	THETA1_RMCL	3.26
M	30	1	1	THETA1_RMCL	3.46
M	30	1	0.5	THETA1_RMCL	3.15
M	30	1	0.2	THETA1_RMCL	2.95
S	5	0	1	THETA1_RMCL	2.96
S	5	0	0.5	THETA1_RMCL	3.12
S	5	0	0.2	THETA1_RMCL	3.22
S	5	1	1	THETA1_RMCL	3.17
S	5	1	0.5	THETA1_RMCL	3.21
S	5	1	0.2	THETA1_RMCL	3.26
S	10	0	1	THETA1_RMCL	3.22
S	10	0	0.5	THETA1_RMCL	3.47

continued on next page

Study	Magnitude of perturbation	kappa	γ	variable	RMSE[%]
S	10	0	0.2	THETA1_RMCL	3.51
S	10	1	1	THETA1_RMCL	3.09
S	10	1	0.5	THETA1_RMCL	3.27
S	10	1	0.2	THETA1_RMCL	3.36
S	15	0	1	THETA1_RMCL	4.65
S	15	0	0.5	THETA1_RMCL	4.73
S	15	0	0.2	THETA1_RMCL	4.27
S	15	1	1	THETA1_RMCL	3.07
S	15	1	0.5	THETA1_RMCL	3.31
S	15	1	0.2	THETA1_RMCL	3.43
S	30	0	1	THETA1_RMCL	8.02
S	30	0	0.5	THETA1_RMCL	6.57
S	30	0	0.2	THETA1_RMCL	5.1
S	30	1	1	THETA1_RMCL	5.4
S	30	1	0.5	THETA1_RMCL	4.61
S	30	1	0.2	THETA1_RMCL	4.01
I	5	0	1	THETA2_RMV	13.91
I	5	0	0.5	THETA2_RMV	13.3
I	5	0	0.2	THETA2_RMV	13.04

continued on next page

Study	Magnitude of perturbation	kappa	γ	variable	RMSE[%]
I	5	1	1	THETA2_RMV	12.45
I	5	1	0.5	THETA2_RMV	12.59
I	5	1	0.2	THETA2_RMV	13.03
I	10	0	1	THETA2_RMV	17.19
I	10	0	0.5	THETA2_RMV	15.06
I	10	0	0.2	THETA2_RMV	13.64
I	10	1	1	THETA2_RMV	12.01
I	10	1	0.5	THETA2_RMV	11.94
I	10	1	0.2	THETA2_RMV	12.25
I	15	0	1	THETA2_RMV	21.38
I	15	0	0.5	THETA2_RMV	17.71
I	15	0	0.2	THETA2_RMV	14.88
I	15	1	1	THETA2_RMV	11.96
I	15	1	0.5	THETA2_RMV	12.21
I	15	1	0.2	THETA2_RMV	12.16
I	30	0	1	THETA2_RMV	30.37
I	30	0	0.5	THETA2_RMV	24.2
I	30	0	0.2	THETA2_RMV	17.77
I	30	1	1	THETA2_RMV	17.63

continued on next page

Study	Magnitude of perturbation	kappa	γ	variable	RMSE[%]
I	30	1	0.5	THETA2_RMV	16.26
I	30	1	0.2	THETA2_RMV	13.86
M	5	0	1	THETA2_RMV	13.13
M	5	0	0.5	THETA2_RMV	12.78
M	5	0	0.2	THETA2_RMV	12.97
M	5	1	1	THETA2_RMV	12.48
M	5	1	0.5	THETA2_RMV	12.48
M	5	1	0.2	THETA2_RMV	13.45
M	10	0	1	THETA2_RMV	15.58
M	10	0	0.5	THETA2_RMV	13.07
M	10	0	0.2	THETA2_RMV	12.95
M	10	1	1	THETA2_RMV	12.35
M	10	1	0.5	THETA2_RMV	11.84
M	10	1	0.2	THETA2_RMV	12.6
M	15	0	1	THETA2_RMV	19.25
M	15	0	0.5	THETA2_RMV	15.17
M	15	0	0.2	THETA2_RMV	13.8
M	15	1	1	THETA2_RMV	13.46
M	15	1	0.5	THETA2_RMV	13.33

continued on next page

Study	Magnitude of perturbation	kappa	γ	variable	RMSE[%]
M	15	1	0.2	THETA2_RMV	12.78
M	30	0	1	THETA2_RMV	32.29
M	30	0	0.5	THETA2_RMV	22.01
M	30	0	0.2	THETA2_RMV	15.74
M	30	1	1	THETA2_RMV	23.34
M	30	1	0.5	THETA2_RMV	19.96
M	30	1	0.2	THETA2_RMV	15.04
S	5	0	1	THETA2_RMV	18.93
S	5	0	0.5	THETA2_RMV	17.96
S	5	0	0.2	THETA2_RMV	17.82
S	5	1	1	THETA2_RMV	17.93
S	5	1	0.5	THETA2_RMV	17.02
S	5	1	0.2	THETA2_RMV	17.49
S	10	0	1	THETA2_RMV	17.29
S	10	0	0.5	THETA2_RMV	15.95
S	10	0	0.2	THETA2_RMV	15.93
S	10	1	1	THETA2_RMV	17.72
S	10	1	0.5	THETA2_RMV	15.57
S	10	1	0.2	THETA2_RMV	15.87

continued on next page

Study	Magnitude of perturbation	kappa	γ	variable	RMSE[%]
S	15	0	1	THETA2_RMV	16.04
S	15	0	0.5	THETA2_RMV	10.97
S	15	0	0.2	THETA2_RMV	12.92
S	15	1	1	THETA2_RMV	19.09
S	15	1	0.5	THETA2_RMV	15.78
S	15	1	0.2	THETA2_RMV	15.66
S	30	0	1	THETA2_RMV	18.02
S	30	0	0.5	THETA2_RMV	8.26
S	30	0	0.2	THETA2_RMV	11.89
S	30	1	1	THETA2_RMV	27.96
S	30	1	0.5	THETA2_RMV	20.38
S	30	1	0.2	THETA2_RMV	16.32
I	5	0	1	THETA3_RMKa	11.56
I	5	0	0.5	THETA3_RMKa	11.17
I	5	0	0.2	THETA3_RMKa	11.12
I	5	1	1	THETA3_RMKa	9.9
I	5	1	0.5	THETA3_RMKa	10.38
I	5	1	0.2	THETA3_RMKa	11.2
I	10	0	1	THETA3_RMKa	13.36

continued on next page

Study	Magnitude of perturbation	kappa	γ	variable	RMSE[%]
I	10	0	0.5	THETA3_RMKa	12.27
I	10	0	0.2	THETA3_RMKa	11.48
I	10	1	1	THETA3_RMKa	9.44
I	10	1	0.5	THETA3_RMKa	9.02
I	10	1	0.2	THETA3_RMKa	9.9
I	15	0	1	THETA3_RMKa	16.97
I	15	0	0.5	THETA3_RMKa	14.55
I	15	0	0.2	THETA3_RMKa	12.58
I	15	1	1	THETA3_RMKa	9.18
I	15	1	0.5	THETA3_RMKa	9.09
I	15	1	0.2	THETA3_RMKa	9.49
I	30	0	1	THETA3_RMKa	26.72
I	30	0	0.5	THETA3_RMKa	21.96
I	30	0	0.2	THETA3_RMKa	15.84
I	30	1	1	THETA3_RMKa	12.62
I	30	1	0.5	THETA3_RMKa	12.83
I	30	1	0.2	THETA3_RMKa	11.08
M	5	0	1	THETA3_RMKa	10.4
M	5	0	0.5	THETA3_RMKa	10.54

continued on next page

Study	Magnitude of perturbation	kappa	γ	variable	RMSE[%]
M	5	0	0.2	THETA3_RMKa	11.25
M	5	1	1	THETA3_RMKa	10.04
M	5	1	0.5	THETA3_RMKa	10.36
M	5	1	0.2	THETA3_RMKa	11.94
M	10	0	1	THETA3_RMKa	9.77
M	10	0	0.5	THETA3_RMKa	8.71
M	10	0	0.2	THETA3_RMKa	10.59
M	10	1	1	THETA3_RMKa	10.18
M	10	1	0.5	THETA3_RMKa	9
M	10	1	0.2	THETA3_RMKa	10.47
M	15	0	1	THETA3_RMKa	12.18
M	15	0	0.5	THETA3_RMKa	9.98
M	15	0	0.2	THETA3_RMKa	11.18
M	15	1	1	THETA3_RMKa	12.23
M	15	1	0.5	THETA3_RMKa	10.89
M	15	1	0.2	THETA3_RMKa	10.73
M	30	0	1	THETA3_RMKa	31.95
M	30	0	0.5	THETA3_RMKa	20.38
M	30	0	0.2	THETA3_RMKa	13.9

continued on next page

Study	Magnitude of perturbation	kappa	γ	variable	RMSE[%]
M	30	1	1	THETA3_RMKa	19.68
M	30	1	0.5	THETA3_RMKa	17.44
M	30	1	0.2	THETA3_RMKa	13.32
S	5	0	1	THETA3_RMKa	16.79
S	5	0	0.5	THETA3_RMKa	16.24
S	5	0	0.2	THETA3_RMKa	16.69
S	5	1	1	THETA3_RMKa	17.64
S	5	1	0.5	THETA3_RMKa	16.59
S	5	1	0.2	THETA3_RMKa	17.18
S	10	0	1	THETA3_RMKa	11.61
S	10	0	0.5	THETA3_RMKa	13.79
S	10	0	0.2	THETA3_RMKa	14.64
S	10	1	1	THETA3_RMKa	19.13
S	10	1	0.5	THETA3_RMKa	15.88
S	10	1	0.2	THETA3_RMKa	15.72
S	15	0	1	THETA3_RMKa	6.88
S	15	0	0.5	THETA3_RMKa	12.16
S	15	0	0.2	THETA3_RMKa	13.86
S	15	1	1	THETA3_RMKa	21.7

continued on next page

Study	Magnitude of perturbation	kappa	γ	variable	RMSE[%]
S	15	1	0.5	THETA3_RMKa	16.74
S	15	1	0.2	THETA3_RMKa	15.79
S	30	0	1	THETA3_RMKa	18.41
S	30	0	0.5	THETA3_RMKa	8.23
S	30	0	0.2	THETA3_RMKa	12.97
S	30	1	1	THETA3_RMKa	29.51
S	30	1	0.5	THETA3_RMKa	20.7
S	30	1	0.2	THETA3_RMKa	16.28
I	5	0	1	THETA4_RMQ	6.75
I	5	0	0.5	THETA4_RMQ	6.43
I	5	0	0.2	THETA4_RMQ	6.07
I	5	1	1	THETA4_RMQ	5.75
I	5	1	0.5	THETA4_RMQ	5.97
I	5	1	0.2	THETA4_RMQ	6.23
I	10	0	1	THETA4_RMQ	9.12
I	10	0	0.5	THETA4_RMQ	7.6
I	10	0	0.2	THETA4_RMQ	6.48
I	10	1	1	THETA4_RMQ	5.56
I	10	1	0.5	THETA4_RMQ	5.7

continued on next page

Study	Magnitude of perturbation	kappa	γ	variable	RMSE[%]
I	10	1	0.2	THETA4_RMQ	5.64
I	15	0	1	THETA4_RMQ	11.88
I	15	0	0.5	THETA4_RMQ	9.24
I	15	0	0.2	THETA4_RMQ	7.18
I	15	1	1	THETA4_RMQ	5.67
I	15	1	0.5	THETA4_RMQ	5.79
I	15	1	0.2	THETA4_RMQ	5.53
I	30	0	1	THETA4_RMQ	17.7
I	30	0	0.5	THETA4_RMQ	13.35
I	30	0	0.2	THETA4_RMQ	8.89
I	30	1	1	THETA4_RMQ	7.79
I	30	1	0.5	THETA4_RMQ	7.72
I	30	1	0.2	THETA4_RMQ	6.31
M	5	0	1	THETA4_RMQ	6.44
M	5	0	0.5	THETA4_RMQ	6.32
M	5	0	0.2	THETA4_RMQ	6.35
M	5	1	1	THETA4_RMQ	6.1
M	5	1	0.5	THETA4_RMQ	6.18
M	5	1	0.2	THETA4_RMQ	6.49

continued on next page

Study	Magnitude of perturbation	kappa	γ	variable	RMSE[%]
M	10	0	1	THETA4_RMQ	9.07
M	10	0	0.5	THETA4_RMQ	6.84
M	10	0	0.2	THETA4_RMQ	6.32
M	10	1	1	THETA4_RMQ	6.42
M	10	1	0.5	THETA4_RMQ	5.95
M	10	1	0.2	THETA4_RMQ	6.21
M	15	0	1	THETA4_RMQ	11.62
M	15	0	0.5	THETA4_RMQ	8.37
M	15	0	0.2	THETA4_RMQ	6.77
M	15	1	1	THETA4_RMQ	7.27
M	15	1	0.5	THETA4_RMQ	6.74
M	15	1	0.2	THETA4_RMQ	6.38
M	30	0	1	THETA4_RMQ	18.66
M	30	0	0.5	THETA4_RMQ	11.65
M	30	0	0.2	THETA4_RMQ	7.43
M	30	1	1	THETA4_RMQ	10.01
M	30	1	0.5	THETA4_RMQ	9.3
M	30	1	0.2	THETA4_RMQ	6.96
S	5	0	1	THETA4_RMQ	14.29

continued on next page

Study	Magnitude of perturbation	kappa	γ	variable	RMSE[%]
S	5	0	0.5	THETA4_RMQ	12.99
S	5	0	0.2	THETA4_RMQ	12.6
S	5	1	1	THETA4_RMQ	12.31
S	5	1	0.5	THETA4_RMQ	12.42
S	5	1	0.2	THETA4_RMQ	12.91
S	10	0	1	THETA4_RMQ	18.73
S	10	0	0.5	THETA4_RMQ	14.02
S	10	0	0.2	THETA4_RMQ	11.51
S	10	1	1	THETA4_RMQ	11.18
S	10	1	0.5	THETA4_RMQ	11.79
S	10	1	0.2	THETA4_RMQ	12.45
S	15	0	1	THETA4_RMQ	12.62
S	15	0	0.5	THETA4_RMQ	9.28
S	15	0	0.2	THETA4_RMQ	10.27
S	15	1	1	THETA4_RMQ	11.6
S	15	1	0.5	THETA4_RMQ	12.4
S	15	1	0.2	THETA4_RMQ	12.81
S	30	0	1	THETA4_RMQ	18.57
S	30	0	0.5	THETA4_RMQ	19.28

continued on next page

Study	Magnitude of perturbation	kappa	γ	variable	RMSE[%]
S	30	0	0.2	THETA4_RMQ	14.14
S	30	1	1	THETA4_RMQ	26.67
S	30	1	0.5	THETA4_RMQ	21.01
S	30	1	0.2	THETA4_RMQ	16.3
I	5	0	1	THETA5_RMVp	5.47
I	5	0	0.5	THETA5_RMVp	5.28
I	5	0	0.2	THETA5_RMVp	5.22
I	5	1	1	THETA5_RMVp	4.86
I	5	1	0.5	THETA5_RMVp	5.01
I	5	1	0.2	THETA5_RMVp	5.36
I	10	0	1	THETA5_RMVp	6.4
I	10	0	0.5	THETA5_RMVp	5.83
I	10	0	0.2	THETA5_RMVp	5.39
I	10	1	1	THETA5_RMVp	4.79
I	10	1	0.5	THETA5_RMVp	4.69
I	10	1	0.2	THETA5_RMVp	4.84
I	15	0	1	THETA5_RMVp	7.74
I	15	0	0.5	THETA5_RMVp	6.74
I	15	0	0.2	THETA5_RMVp	5.84

continued on next page

Study	Magnitude of perturbation	kappa	γ	variable	RMSE[%]
I	15	1	1	THETA5_RMVp	4.79
I	15	1	0.5	THETA5_RMVp	4.8
I	15	1	0.2	THETA5_RMVp	4.77
I	30	0	1	THETA5_RMVp	11.14
I	30	0	0.5	THETA5_RMVp	9.34
I	30	0	0.2	THETA5_RMVp	6.99
I	30	1	1	THETA5_RMVp	6.63
I	30	1	0.5	THETA5_RMVp	6.62
I	30	1	0.2	THETA5_RMVp	5.36
M	5	0	1	THETA5_RMVp	4.92
M	5	0	0.5	THETA5_RMVp	4.96
M	5	0	0.2	THETA5_RMVp	5.24
M	5	1	1	THETA5_RMVp	4.93
M	5	1	0.5	THETA5_RMVp	4.94
M	5	1	0.2	THETA5_RMVp	5.51
M	10	0	1	THETA5_RMVp	5.52
M	10	0	0.5	THETA5_RMVp	4.58
M	10	0	0.2	THETA5_RMVp	4.98
M	10	1	1	THETA5_RMVp	5.37

continued on next page

Study	Magnitude of perturbation	kappa	γ	variable	RMSE[%]
M	10	1	0.5	THETA5_RMVp	4.67
M	10	1	0.2	THETA5_RMVp	5.11
M	15	0	1	THETA5_RMVp	6.77
M	15	0	0.5	THETA5_RMVp	5.24
M	15	0	0.2	THETA5_RMVp	5.31
M	15	1	1	THETA5_RMVp	6.01
M	15	1	0.5	THETA5_RMVp	5.66
M	15	1	0.2	THETA5_RMVp	5.21
M	30	0	1	THETA5_RMVp	12.29
M	30	0	0.5	THETA5_RMVp	7.83
M	30	0	0.2	THETA5_RMVp	5.63
M	30	1	1	THETA5_RMVp	8.76
M	30	1	0.5	THETA5_RMVp	7.85
M	30	1	0.2	THETA5_RMVp	5.87
S	5	0	1	THETA5_RMVp	9.97
S	5	0	0.5	THETA5_RMVp	9.44
S	5	0	0.2	THETA5_RMVp	9.56
S	5	1	1	THETA5_RMVp	10.08
S	5	1	0.5	THETA5_RMVp	9.96

continued on next page

Study	Magnitude of perturbation	kappa	γ	variable	RMSE[%]
S	5	1	0.2	THETA5_RMVp	10.31
S	10	0	1	THETA5_RMVp	11.44
S	10	0	0.5	THETA5_RMVp	9.3
S	10	0	0.2	THETA5_RMVp	8.59
S	10	1	1	THETA5_RMVp	10.16
S	10	1	0.5	THETA5_RMVp	9.75
S	10	1	0.2	THETA5_RMVp	9.89
S	15	0	1	THETA5_RMVp	8.98
S	15	0	0.5	THETA5_RMVp	6.75
S	15	0	0.2	THETA5_RMVp	8.6
S	15	1	1	THETA5_RMVp	10.83
S	15	1	0.5	THETA5_RMVp	10.32
S	15	1	0.2	THETA5_RMVp	10.1
S	30	0	1	THETA5_RMVp	8.45
S	30	0	0.5	THETA5_RMVp	10
S	30	0	0.2	THETA5_RMVp	10.47
S	30	1	1	THETA5_RMVp	17.8
S	30	1	0.5	THETA5_RMVp	14.01
S	30	1	0.2	THETA5_RMVp	11.39

continued on next page

Study	Magnitude of perturbation	kappa	γ	variable	RMSE[%]
I	5	0	1	OMEGA(1,1)_RMOM	5.94
I	5	0	0.5	OMEGA(1,1)_RMOM	5.86
I	5	0	0.2	OMEGA(1,1)_RMOM	5.84
I	5	1	1	OMEGA(1,1)_RMOM	5.8
I	5	1	0.5	OMEGA(1,1)_RMOM	5.79
I	5	1	0.2	OMEGA(1,1)_RMOM	5.9
I	10	0	1	OMEGA(1,1)_RMOM	6.45
I	10	0	0.5	OMEGA(1,1)_RMOM	6.12
I	10	0	0.2	OMEGA(1,1)_RMOM	5.97
I	10	1	1	OMEGA(1,1)_RMOM	5.73
I	10	1	0.5	OMEGA(1,1)_RMOM	5.73
I	10	1	0.2	OMEGA(1,1)_RMOM	5.85
I	15	0	1	OMEGA(1,1)_RMOM	7.01
I	15	0	0.5	OMEGA(1,1)_RMOM	6.45
I	15	0	0.2	OMEGA(1,1)_RMOM	6.14
I	15	1	1	OMEGA(1,1)_RMOM	5.67
I	15	1	0.5	OMEGA(1,1)_RMOM	5.73
I	15	1	0.2	OMEGA(1,1)_RMOM	5.79
I	30	0	1	OMEGA(1,1)_RMOM	7.71

continued on next page

Study	Magnitude of perturbation	kappa	γ	variable	RMSE[%]
I	30	0	0.5	OMEGA(1,1)_RMOM	6.82
I	30	0	0.2	OMEGA(1,1)_RMOM	6.28
I	30	1	1	OMEGA(1,1)_RMOM	5.76
I	30	1	0.5	OMEGA(1,1)_RMOM	5.77
I	30	1	0.2	OMEGA(1,1)_RMOM	5.81
M	5	0	1	OMEGA(1,1)_RMOM	5.65
M	5	0	0.5	OMEGA(1,1)_RMOM	5.53
M	5	0	0.2	OMEGA(1,1)_RMOM	5.54
M	5	1	1	OMEGA(1,1)_RMOM	5.48
M	5	1	0.5	OMEGA(1,1)_RMOM	5.45
M	5	1	0.2	OMEGA(1,1)_RMOM	5.45
M	10	0	1	OMEGA(1,1)_RMOM	6.43
M	10	0	0.5	OMEGA(1,1)_RMOM	5.85
M	10	0	0.2	OMEGA(1,1)_RMOM	5.65
M	10	1	1	OMEGA(1,1)_RMOM	5.37
M	10	1	0.5	OMEGA(1,1)_RMOM	5.37
M	10	1	0.2	OMEGA(1,1)_RMOM	5.47
M	15	0	1	OMEGA(1,1)_RMOM	7.5
M	15	0	0.5	OMEGA(1,1)_RMOM	6.39

continued on next page

Study	Magnitude of perturbation	kappa	γ	variable	RMSE[%]
M	15	0	0.2	OMEGA(1,1)_RMOM	5.86
M	15	1	1	OMEGA(1,1)_RMOM	5.33
M	15	1	0.5	OMEGA(1,1)_RMOM	5.36
M	15	1	0.2	OMEGA(1,1)_RMOM	5.43
M	30	0	1	OMEGA(1,1)_RMOM	8.69
M	30	0	0.5	OMEGA(1,1)_RMOM	7.13
M	30	0	0.2	OMEGA(1,1)_RMOM	6.1
M	30	1	1	OMEGA(1,1)_RMOM	5.48
M	30	1	0.5	OMEGA(1,1)_RMOM	5.52
M	30	1	0.2	OMEGA(1,1)_RMOM	5.49
S	5	0	1	OMEGA(1,1)_RMOM	7.04
S	5	0	0.5	OMEGA(1,1)_RMOM	6.74
S	5	0	0.2	OMEGA(1,1)_RMOM	6.69
S	5	1	1	OMEGA(1,1)_RMOM	6.71
S	5	1	0.5	OMEGA(1,1)_RMOM	6.67
S	5	1	0.2	OMEGA(1,1)_RMOM	6.77
S	10	0	1	OMEGA(1,1)_RMOM	8.37
S	10	0	0.5	OMEGA(1,1)_RMOM	7.49
S	10	0	0.2	OMEGA(1,1)_RMOM	6.85

continued on next page

Study	Magnitude of perturbation	kappa	γ	variable	RMSE[%]
S	10	1	1	OMEGA(1,1)_RMOM	6.9
S	10	1	0.5	OMEGA(1,1)_RMOM	6.91
S	10	1	0.2	OMEGA(1,1)_RMOM	6.93
S	15	0	1	OMEGA(1,1)_RMOM	7.85
S	15	0	0.5	OMEGA(1,1)_RMOM	7.7
S	15	0	0.2	OMEGA(1,1)_RMOM	7.01
S	15	1	1	OMEGA(1,1)_RMOM	7.18
S	15	1	0.5	OMEGA(1,1)_RMOM	7.17
S	15	1	0.2	OMEGA(1,1)_RMOM	7.13
S	30	0	1	OMEGA(1,1)_RMOM	6.93
S	30	0	0.5	OMEGA(1,1)_RMOM	7.37
S	30	0	0.2	OMEGA(1,1)_RMOM	7.09
S	30	1	1	OMEGA(1,1)_RMOM	7.91
S	30	1	0.5	OMEGA(1,1)_RMOM	7.35
S	30	1	0.2	OMEGA(1,1)_RMOM	7.18
I	5	0	1	OMEGA(2,2)_RMOM	14.1
I	5	0	0.5	OMEGA(2,2)_RMOM	14
I	5	0	0.2	OMEGA(2,2)_RMOM	13.47
I	5	1	1	OMEGA(2,2)_RMOM	12.66

continued on next page

Study	Magnitude of perturbation	kappa	γ	variable	RMSE[%]
I	5	1	0.5	OMEGA(2,2)_RMOM	13.17
I	5	1	0.2	OMEGA(2,2)_RMOM	13.2
I	10	0	1	OMEGA(2,2)_RMOM	18.47
I	10	0	0.5	OMEGA(2,2)_RMOM	15.73
I	10	0	0.2	OMEGA(2,2)_RMOM	15.14
I	10	1	1	OMEGA(2,2)_RMOM	16.86
I	10	1	0.5	OMEGA(2,2)_RMOM	14.14
I	10	1	0.2	OMEGA(2,2)_RMOM	13.56
I	15	0	1	OMEGA(2,2)_RMOM	27.4
I	15	0	0.5	OMEGA(2,2)_RMOM	18.6
I	15	0	0.2	OMEGA(2,2)_RMOM	16.6
I	15	1	1	OMEGA(2,2)_RMOM	19.85
I	15	1	0.5	OMEGA(2,2)_RMOM	15.59
I	15	1	0.2	OMEGA(2,2)_RMOM	13.66
I	30	0	1	OMEGA(2,2)_RMOM	31.76
I	30	0	0.5	OMEGA(2,2)_RMOM	26.08
I	30	0	0.2	OMEGA(2,2)_RMOM	19.34
I	30	1	1	OMEGA(2,2)_RMOM	21.96
I	30	1	0.5	OMEGA(2,2)_RMOM	20.05

continued on next page

Study	Magnitude of perturbation	kappa	γ	variable	RMSE[%]
I	30	1	0.2	OMEGA(2,2)_RMOM	15.18
M	5	0	1	OMEGA(2,2)_RMOM	19.98
M	5	0	0.5	OMEGA(2,2)_RMOM	19.5
M	5	0	0.2	OMEGA(2,2)_RMOM	18.51
M	5	1	1	OMEGA(2,2)_RMOM	17.37
M	5	1	0.5	OMEGA(2,2)_RMOM	18.82
M	5	1	0.2	OMEGA(2,2)_RMOM	18.64
M	10	0	1	OMEGA(2,2)_RMOM	25.76
M	10	0	0.5	OMEGA(2,2)_RMOM	19.75
M	10	0	0.2	OMEGA(2,2)_RMOM	19.42
M	10	1	1	OMEGA(2,2)_RMOM	17.81
M	10	1	0.5	OMEGA(2,2)_RMOM	18.24
M	10	1	0.2	OMEGA(2,2)_RMOM	17.59
M	15	0	1	OMEGA(2,2)_RMOM	34.13
M	15	0	0.5	OMEGA(2,2)_RMOM	24.81
M	15	0	0.2	OMEGA(2,2)_RMOM	22.03
M	15	1	1	OMEGA(2,2)_RMOM	20.4
M	15	1	0.5	OMEGA(2,2)_RMOM	21.74
M	15	1	0.2	OMEGA(2,2)_RMOM	17.05

continued on next page

Study	Magnitude of perturbation	kappa	γ	variable	RMSE[%]
M	30	0	1	OMEGA(2,2)_RMOM	42.45
M	30	0	0.5	OMEGA(2,2)_RMOM	30.67
M	30	0	0.2	OMEGA(2,2)_RMOM	24.24
M	30	1	1	OMEGA(2,2)_RMOM	24.05
M	30	1	0.5	OMEGA(2,2)_RMOM	25.74
M	30	1	0.2	OMEGA(2,2)_RMOM	21.45
S	5	0	1	OMEGA(2,2)_RMOM	38.05
S	5	0	0.5	OMEGA(2,2)_RMOM	32.29
S	5	0	0.2	OMEGA(2,2)_RMOM	32.01
S	5	1	1	OMEGA(2,2)_RMOM	40.07
S	5	1	0.5	OMEGA(2,2)_RMOM	37.72
S	5	1	0.2	OMEGA(2,2)_RMOM	37.47
S	10	0	1	OMEGA(2,2)_RMOM	53.46
S	10	0	0.5	OMEGA(2,2)_RMOM	38.64
S	10	0	0.2	OMEGA(2,2)_RMOM	32.54
S	10	1	1	OMEGA(2,2)_RMOM	43.46
S	10	1	0.5	OMEGA(2,2)_RMOM	37.73
S	10	1	0.2	OMEGA(2,2)_RMOM	36.6
S	15	0	1	OMEGA(2,2)_RMOM	55.53

continued on next page

Study	Magnitude of perturbation	kappa	γ	variable	RMSE[%]
S	15	0	0.5	OMEGA(2,2)_RMOM	39.82
S	15	0	0.2	OMEGA(2,2)_RMOM	30.79
S	15	1	1	OMEGA(2,2)_RMOM	44.92
S	15	1	0.5	OMEGA(2,2)_RMOM	40.21
S	15	1	0.2	OMEGA(2,2)_RMOM	37.57
S	30	0	1	OMEGA(2,2)_RMOM	47.2
S	30	0	0.5	OMEGA(2,2)_RMOM	30.45
S	30	0	0.2	OMEGA(2,2)_RMOM	29.96
S	30	1	1	OMEGA(2,2)_RMOM	55.47
S	30	1	0.5	OMEGA(2,2)_RMOM	46.16
S	30	1	0.2	OMEGA(2,2)_RMOM	39.01
I	5	0	1	OMEGA(3,3)_RMOM	22.97
I	5	0	0.5	OMEGA(3,3)_RMOM	20.48
I	5	0	0.2	OMEGA(3,3)_RMOM	18.81
I	5	1	1	OMEGA(3,3)_RMOM	18.57
I	5	1	0.5	OMEGA(3,3)_RMOM	18.36
I	5	1	0.2	OMEGA(3,3)_RMOM	19.37
I	10	0	1	OMEGA(3,3)_RMOM	34.59
I	10	0	0.5	OMEGA(3,3)_RMOM	25.23

continued on next page

Study	Magnitude of perturbation	kappa	γ	variable	RMSE[%]
I	10	0	0.2	OMEGA(3,3)_RMOM	20.79
I	10	1	1	OMEGA(3,3)_RMOM	21
I	10	1	0.5	OMEGA(3,3)_RMOM	17.7
I	10	1	0.2	OMEGA(3,3)_RMOM	18.12
I	15	0	1	OMEGA(3,3)_RMOM	47.03
I	15	0	0.5	OMEGA(3,3)_RMOM	30.26
I	15	0	0.2	OMEGA(3,3)_RMOM	22.76
I	15	1	1	OMEGA(3,3)_RMOM	22.87
I	15	1	0.5	OMEGA(3,3)_RMOM	19.29
I	15	1	0.2	OMEGA(3,3)_RMOM	18.18
I	30	0	1	OMEGA(3,3)_RMOM	83.45
I	30	0	0.5	OMEGA(3,3)_RMOM	50.77
I	30	0	0.2	OMEGA(3,3)_RMOM	29.24
I	30	1	1	OMEGA(3,3)_RMOM	31.77
I	30	1	0.5	OMEGA(3,3)_RMOM	27
I	30	1	0.2	OMEGA(3,3)_RMOM	20.83
M	5	0	1	OMEGA(3,3)_RMOM	30.52
M	5	0	0.5	OMEGA(3,3)_RMOM	26.23
M	5	0	0.2	OMEGA(3,3)_RMOM	23.86

continued on next page

Study	Magnitude of perturbation	kappa	γ	variable	RMSE[%]
M	5	1	1	OMEGA(3,3)_RMOM	23.08
M	5	1	0.5	OMEGA(3,3)_RMOM	24.1
M	5	1	0.2	OMEGA(3,3)_RMOM	23.89
M	10	0	1	OMEGA(3,3)_RMOM	57.94
M	10	0	0.5	OMEGA(3,3)_RMOM	43.24
M	10	0	0.2	OMEGA(3,3)_RMOM	27.83
M	10	1	1	OMEGA(3,3)_RMOM	23.89
M	10	1	0.5	OMEGA(3,3)_RMOM	24.14
M	10	1	0.2	OMEGA(3,3)_RMOM	22.08
M	15	0	1	OMEGA(3,3)_RMOM	81.14
M	15	0	0.5	OMEGA(3,3)_RMOM	58
M	15	0	0.2	OMEGA(3,3)_RMOM	33
M	15	1	1	OMEGA(3,3)_RMOM	26.92
M	15	1	0.5	OMEGA(3,3)_RMOM	25.34
M	15	1	0.2	OMEGA(3,3)_RMOM	23.02
M	30	0	1	OMEGA(3,3)_RMOM	132.51
M	30	0	0.5	OMEGA(3,3)_RMOM	85.74
M	30	0	0.2	OMEGA(3,3)_RMOM	42.36
M	30	1	1	OMEGA(3,3)_RMOM	36.06

continued on next page

Study	Magnitude of perturbation	kappa	γ	variable	RMSE[%]
M	30	1	0.5	OMEGA(3,3)_RMOM	39.16
M	30	1	0.2	OMEGA(3,3)_RMOM	27.44
S	5	0	1	OMEGA(3,3)_RMOM	51.76
S	5	0	0.5	OMEGA(3,3)_RMOM	40.56
S	5	0	0.2	OMEGA(3,3)_RMOM	35.95
S	5	1	1	OMEGA(3,3)_RMOM	45.02
S	5	1	0.5	OMEGA(3,3)_RMOM	43.97
S	5	1	0.2	OMEGA(3,3)_RMOM	42.31
S	10	0	1	OMEGA(3,3)_RMOM	95.03
S	10	0	0.5	OMEGA(3,3)_RMOM	59.23
S	10	0	0.2	OMEGA(3,3)_RMOM	39.03
S	10	1	1	OMEGA(3,3)_RMOM	48.54
S	10	1	0.5	OMEGA(3,3)_RMOM	47.26
S	10	1	0.2	OMEGA(3,3)_RMOM	44.89
S	15	0	1	OMEGA(3,3)_RMOM	111.74
S	15	0	0.5	OMEGA(3,3)_RMOM	52.8
S	15	0	0.2	OMEGA(3,3)_RMOM	35.7
S	15	1	1	OMEGA(3,3)_RMOM	51.08
S	15	1	0.5	OMEGA(3,3)_RMOM	52.56

continued on next page

Study	Magnitude of perturbation	kappa	γ	variable	RMSE[%]
S	15	1	0.2	OMEGA(3,3)_RMOM	49.74
S	30	0	1	OMEGA(3,3)_RMOM	123.79
S	30	0	0.5	OMEGA(3,3)_RMOM	45.71
S	30	0	0.2	OMEGA(3,3)_RMOM	35.54
S	30	1	1	OMEGA(3,3)_RMOM	50.97
S	30	1	0.5	OMEGA(3,3)_RMOM	51.11
S	30	1	0.2	OMEGA(3,3)_RMOM	50
I	5	0	1	OMEGA(4,4)_RMOM	25.12
I	5	0	0.5	OMEGA(4,4)_RMOM	22.61
I	5	0	0.2	OMEGA(4,4)_RMOM	20.55
I	5	1	1	OMEGA(4,4)_RMOM	20.14
I	5	1	0.5	OMEGA(4,4)_RMOM	19.89
I	5	1	0.2	OMEGA(4,4)_RMOM	19.22
I	10	0	1	OMEGA(4,4)_RMOM	46.44
I	10	0	0.5	OMEGA(4,4)_RMOM	34.42
I	10	0	0.2	OMEGA(4,4)_RMOM	24.88
I	10	1	1	OMEGA(4,4)_RMOM	20.35
I	10	1	0.5	OMEGA(4,4)_RMOM	20.08
I	10	1	0.2	OMEGA(4,4)_RMOM	19.17

continued on next page

Study	Magnitude of perturbation	kappa	γ	variable	RMSE[%]
I	15	0	1	OMEGA(4,4)_RMOM	66.34
I	15	0	0.5	OMEGA(4,4)_RMOM	47.51
I	15	0	0.2	OMEGA(4,4)_RMOM	30.48
I	15	1	1	OMEGA(4,4)_RMOM	20.74
I	15	1	0.5	OMEGA(4,4)_RMOM	20.5
I	15	1	0.2	OMEGA(4,4)_RMOM	19.25
I	30	0	1	OMEGA(4,4)_RMOM	78.04
I	30	0	0.5	OMEGA(4,4)_RMOM	57.93
I	30	0	0.2	OMEGA(4,4)_RMOM	35.97
I	30	1	1	OMEGA(4,4)_RMOM	24.46
I	30	1	0.5	OMEGA(4,4)_RMOM	20.8
I	30	1	0.2	OMEGA(4,4)_RMOM	19.28
M	5	0	1	OMEGA(4,4)_RMOM	21.6
M	5	0	0.5	OMEGA(4,4)_RMOM	19.28
M	5	0	0.2	OMEGA(4,4)_RMOM	18.62
M	5	1	1	OMEGA(4,4)_RMOM	18.48
M	5	1	0.5	OMEGA(4,4)_RMOM	18.19
M	5	1	0.2	OMEGA(4,4)_RMOM	18.2
M	10	0	1	OMEGA(4,4)_RMOM	45.08

continued on next page

Study	Magnitude of perturbation	kappa	γ	variable	RMSE[%]
M	10	0	0.5	OMEGA(4,4)_RMOM	27.34
M	10	0	0.2	OMEGA(4,4)_RMOM	20.98
M	10	1	1	OMEGA(4,4)_RMOM	18.56
M	10	1	0.5	OMEGA(4,4)_RMOM	18.08
M	10	1	0.2	OMEGA(4,4)_RMOM	18.03
M	15	0	1	OMEGA(4,4)_RMOM	70.26
M	15	0	0.5	OMEGA(4,4)_RMOM	43.35
M	15	0	0.2	OMEGA(4,4)_RMOM	25.81
M	15	1	1	OMEGA(4,4)_RMOM	18.83
M	15	1	0.5	OMEGA(4,4)_RMOM	18.62
M	15	1	0.2	OMEGA(4,4)_RMOM	17.97
M	30	0	1	OMEGA(4,4)_RMOM	80.9
M	30	0	0.5	OMEGA(4,4)_RMOM	52.49
M	30	0	0.2	OMEGA(4,4)_RMOM	30.87
M	30	1	1	OMEGA(4,4)_RMOM	19.48
M	30	1	0.5	OMEGA(4,4)_RMOM	20.71
M	30	1	0.2	OMEGA(4,4)_RMOM	18.54
S	5	0	1	OMEGA(4,4)_RMOM	39.74
S	5	0	0.5	OMEGA(4,4)_RMOM	40.79

continued on next page

Study	Magnitude of perturbation	kappa	γ	variable	RMSE[%]
S	5	0	0.2	OMEGA(4,4)_RMOM	42.53
S	5	1	1	OMEGA(4,4)_RMOM	50.93
S	5	1	0.5	OMEGA(4,4)_RMOM	51.21
S	5	1	0.2	OMEGA(4,4)_RMOM	50.08
S	10	0	1	OMEGA(4,4)_RMOM	82.56
S	10	0	0.5	OMEGA(4,4)_RMOM	58.69
S	10	0	0.2	OMEGA(4,4)_RMOM	40.44
S	10	1	1	OMEGA(4,4)_RMOM	53.79
S	10	1	0.5	OMEGA(4,4)_RMOM	57.07
S	10	1	0.2	OMEGA(4,4)_RMOM	54.4
S	15	0	1	OMEGA(4,4)_RMOM	99.82
S	15	0	0.5	OMEGA(4,4)_RMOM	92.47
S	15	0	0.2	OMEGA(4,4)_RMOM	61.55
S	15	1	1	OMEGA(4,4)_RMOM	54.56
S	15	1	0.5	OMEGA(4,4)_RMOM	60.62
S	15	1	0.2	OMEGA(4,4)_RMOM	59.42
S	30	0	1	OMEGA(4,4)_RMOM	99.94
S	30	0	0.5	OMEGA(4,4)_RMOM	97.47
S	30	0	0.2	OMEGA(4,4)_RMOM	72.03

continued on next page

Study	Magnitude of perturbation	kappa	γ	variable	RMSE[%]
S	30	1	1	OMEGA(4,4)_RMOM	82.44
S	30	1	0.5	OMEGA(4,4)_RMOM	76.94
S	30	1	0.2	OMEGA(4,4)_RMOM	65.74
I	5	0	1	OMEGA(5,5)_RMOM	11.66
I	5	0	0.5	OMEGA(5,5)_RMOM	11.93
I	5	0	0.2	OMEGA(5,5)_RMOM	11.91
I	5	1	1	OMEGA(5,5)_RMOM	11.71
I	5	1	0.5	OMEGA(5,5)_RMOM	12.07
I	5	1	0.2	OMEGA(5,5)_RMOM	12.11
I	10	0	1	OMEGA(5,5)_RMOM	11.12
I	10	0	0.5	OMEGA(5,5)_RMOM	11.61
I	10	0	0.2	OMEGA(5,5)_RMOM	11.82
I	10	1	1	OMEGA(5,5)_RMOM	12.1
I	10	1	0.5	OMEGA(5,5)_RMOM	12.17
I	10	1	0.2	OMEGA(5,5)_RMOM	11.95
I	15	0	1	OMEGA(5,5)_RMOM	12.47
I	15	0	0.5	OMEGA(5,5)_RMOM	11.85
I	15	0	0.2	OMEGA(5,5)_RMOM	11.89
I	15	1	1	OMEGA(5,5)_RMOM	12.36

continued on next page

Study	Magnitude of perturbation	kappa	γ	variable	RMSE[%]
I	15	1	0.5	OMEGA(5,5)_RMOM	12.63
I	15	1	0.2	OMEGA(5,5)_RMOM	12.02
I	30	0	1	OMEGA(5,5)_RMOM	12.87
I	30	0	0.5	OMEGA(5,5)_RMOM	13.03
I	30	0	0.2	OMEGA(5,5)_RMOM	12.68
I	30	1	1	OMEGA(5,5)_RMOM	14.68
I	30	1	0.5	OMEGA(5,5)_RMOM	14.55
I	30	1	0.2	OMEGA(5,5)_RMOM	12.74
M	5	0	1	OMEGA(5,5)_RMOM	12.59
M	5	0	0.5	OMEGA(5,5)_RMOM	13.07
M	5	0	0.2	OMEGA(5,5)_RMOM	13.08
M	5	1	1	OMEGA(5,5)_RMOM	12.98
M	5	1	0.5	OMEGA(5,5)_RMOM	13.21
M	5	1	0.2	OMEGA(5,5)_RMOM	13.38
M	10	0	1	OMEGA(5,5)_RMOM	13.81
M	10	0	0.5	OMEGA(5,5)_RMOM	12.18
M	10	0	0.2	OMEGA(5,5)_RMOM	12.74
M	10	1	1	OMEGA(5,5)_RMOM	13.48
M	10	1	0.5	OMEGA(5,5)_RMOM	13.09

continued on next page

Study	Magnitude of perturbation	kappa	γ	variable	RMSE[%]
M	10	1	0.2	OMEGA(5,5)_RMOM	13.06
M	15	0	1	OMEGA(5,5)_RMOM	18.6
M	15	0	0.5	OMEGA(5,5)_RMOM	14.03
M	15	0	0.2	OMEGA(5,5)_RMOM	13.45
M	15	1	1	OMEGA(5,5)_RMOM	13.99
M	15	1	0.5	OMEGA(5,5)_RMOM	13.78
M	15	1	0.2	OMEGA(5,5)_RMOM	13.23
M	30	0	1	OMEGA(5,5)_RMOM	19.02
M	30	0	0.5	OMEGA(5,5)_RMOM	13.76
M	30	0	0.2	OMEGA(5,5)_RMOM	13.55
M	30	1	1	OMEGA(5,5)_RMOM	19.18
M	30	1	0.5	OMEGA(5,5)_RMOM	16.65
M	30	1	0.2	OMEGA(5,5)_RMOM	13.92
S	5	0	1	OMEGA(5,5)_RMOM	16.96
S	5	0	0.5	OMEGA(5,5)_RMOM	16.26
S	5	0	0.2	OMEGA(5,5)_RMOM	16.12
S	5	1	1	OMEGA(5,5)_RMOM	18.86
S	5	1	0.5	OMEGA(5,5)_RMOM	19.37
S	5	1	0.2	OMEGA(5,5)_RMOM	19.13

continued on next page

Study	Magnitude of perturbation	kappa	γ	variable	RMSE[%]
S	10	0	1	OMEGA(5,5)_RMOM	40.5
S	10	0	0.5	OMEGA(5,5)_RMOM	30.1
S	10	0	0.2	OMEGA(5,5)_RMOM	17.87
S	10	1	1	OMEGA(5,5)_RMOM	20.23
S	10	1	0.5	OMEGA(5,5)_RMOM	21.35
S	10	1	0.2	OMEGA(5,5)_RMOM	21.05
S	15	0	1	OMEGA(5,5)_RMOM	79.21
S	15	0	0.5	OMEGA(5,5)_RMOM	55.02
S	15	0	0.2	OMEGA(5,5)_RMOM	30.53
S	15	1	1	OMEGA(5,5)_RMOM	20.85
S	15	1	0.5	OMEGA(5,5)_RMOM	23.2
S	15	1	0.2	OMEGA(5,5)_RMOM	23.97
S	30	0	1	OMEGA(5,5)_RMOM	92.02
S	30	0	0.5	OMEGA(5,5)_RMOM	71.09
S	30	0	0.2	OMEGA(5,5)_RMOM	39.34
S	30	1	1	OMEGA(5,5)_RMOM	23.25
S	30	1	0.5	OMEGA(5,5)_RMOM	23.5
S	30	1	0.2	OMEGA(5,5)_RMOM	23.4
I	5	0	1	SIGMA(1,1)_RMR	9.53

continued on next page

Study	Magnitude of perturbation	kappa	γ	variable	RMSE[%]
I	5	0	0.5	SIGMA(1,1)_RMR	5.93
I	5	0	0.2	SIGMA(1,1)_RMR	3.92
I	5	1	1	SIGMA(1,1)_RMR	3.62
I	5	1	0.5	SIGMA(1,1)_RMR	3.63
I	5	1	0.2	SIGMA(1,1)_RMR	3.5
I	10	0	1	SIGMA(1,1)_RMR	40.79
I	10	0	0.5	SIGMA(1,1)_RMR	22.09
I	10	0	0.2	SIGMA(1,1)_RMR	9.59
I	10	1	1	SIGMA(1,1)_RMR	3.67
I	10	1	0.5	SIGMA(1,1)_RMR	3.59
I	10	1	0.2	SIGMA(1,1)_RMR	3.59
I	15	0	1	SIGMA(1,1)_RMR	78
I	15	0	0.5	SIGMA(1,1)_RMR	42.19
I	15	0	0.2	SIGMA(1,1)_RMR	18.02
I	15	1	1	SIGMA(1,1)_RMR	3.98
I	15	1	0.5	SIGMA(1,1)_RMR	3.66
I	15	1	0.2	SIGMA(1,1)_RMR	3.64
I	30	0	1	SIGMA(1,1)_RMR	121.63
I	30	0	0.5	SIGMA(1,1)_RMR	65.62

continued on next page

Study	Magnitude of perturbation	kappa	γ	variable	RMSE[%]
I	30	0	0.2	SIGMA(1,1)_RMR	27.92
I	30	1	1	SIGMA(1,1)_RMR	12.46
I	30	1	0.5	SIGMA(1,1)_RMR	7.2
I	30	1	0.2	SIGMA(1,1)_RMR	4.57
M	5	0	1	SIGMA(1,1)_RMR	8.92
M	5	0	0.5	SIGMA(1,1)_RMR	5
M	5	0	0.2	SIGMA(1,1)_RMR	4.4
M	5	1	1	SIGMA(1,1)_RMR	4.52
M	5	1	0.5	SIGMA(1,1)_RMR	4.71
M	5	1	0.2	SIGMA(1,1)_RMR	4.59
M	10	0	1	SIGMA(1,1)_RMR	45.98
M	10	0	0.5	SIGMA(1,1)_RMR	20.32
M	10	0	0.2	SIGMA(1,1)_RMR	8.46
M	10	1	1	SIGMA(1,1)_RMR	4.91
M	10	1	0.5	SIGMA(1,1)_RMR	5.15
M	10	1	0.2	SIGMA(1,1)_RMR	5.12
M	15	0	1	SIGMA(1,1)_RMR	94.63
M	15	0	0.5	SIGMA(1,1)_RMR	45.3
M	15	0	0.2	SIGMA(1,1)_RMR	18.36

continued on next page

Study	Magnitude of perturbation	kappa	γ	variable	RMSE[%]
M	15	1	1	SIGMA(1,1)_RMR	4.98
M	15	1	0.5	SIGMA(1,1)_RMR	5.34
M	15	1	0.2	SIGMA(1,1)_RMR	5.45
M	30	0	1	SIGMA(1,1)_RMR	139.16
M	30	0	0.5	SIGMA(1,1)_RMR	69.96
M	30	0	0.2	SIGMA(1,1)_RMR	28.73
M	30	1	1	SIGMA(1,1)_RMR	10.02
M	30	1	0.5	SIGMA(1,1)_RMR	6.2
M	30	1	0.2	SIGMA(1,1)_RMR	4.84
S	5	0	1	SIGMA(1,1)_RMR	11.67
S	5	0	0.5	SIGMA(1,1)_RMR	8.25
S	5	0	0.2	SIGMA(1,1)_RMR	8.28
S	5	1	1	SIGMA(1,1)_RMR	20.27
S	5	1	0.5	SIGMA(1,1)_RMR	19.57
S	5	1	0.2	SIGMA(1,1)_RMR	19.83
S	10	0	1	SIGMA(1,1)_RMR	82.82
S	10	0	0.5	SIGMA(1,1)_RMR	49.21
S	10	0	0.2	SIGMA(1,1)_RMR	18.9
S	10	1	1	SIGMA(1,1)_RMR	28.57

continued on next page

Study	Magnitude of perturbation	kappa	γ	variable	RMSE[%]
S	10	1	0.5	SIGMA(1,1)_RMR	26.96
S	10	1	0.2	SIGMA(1,1)_RMR	24.87
S	15	0	1	SIGMA(1,1)_RMR	174.29
S	15	0	0.5	SIGMA(1,1)_RMR	107.94
S	15	0	0.2	SIGMA(1,1)_RMR	49.11
S	15	1	1	SIGMA(1,1)_RMR	32.55
S	15	1	0.5	SIGMA(1,1)_RMR	31.45
S	15	1	0.2	SIGMA(1,1)_RMR	30.15
S	30	0	1	SIGMA(1,1)_RMR	229.03
S	30	0	0.5	SIGMA(1,1)_RMR	143.57
S	30	0	0.2	SIGMA(1,1)_RMR	66.59
S	30	1	1	SIGMA(1,1)_RMR	22.98
S	30	1	0.5	SIGMA(1,1)_RMR	26.19
S	30	1	0.2	SIGMA(1,1)_RMR	26.45

Appendix C

Evaluation of Bias in Weighted Residual Calculations

Figure C.1: Represent the average of residuals for scenario 1. Panel A represents the SUBSET model, and panel B represents the M3 method.

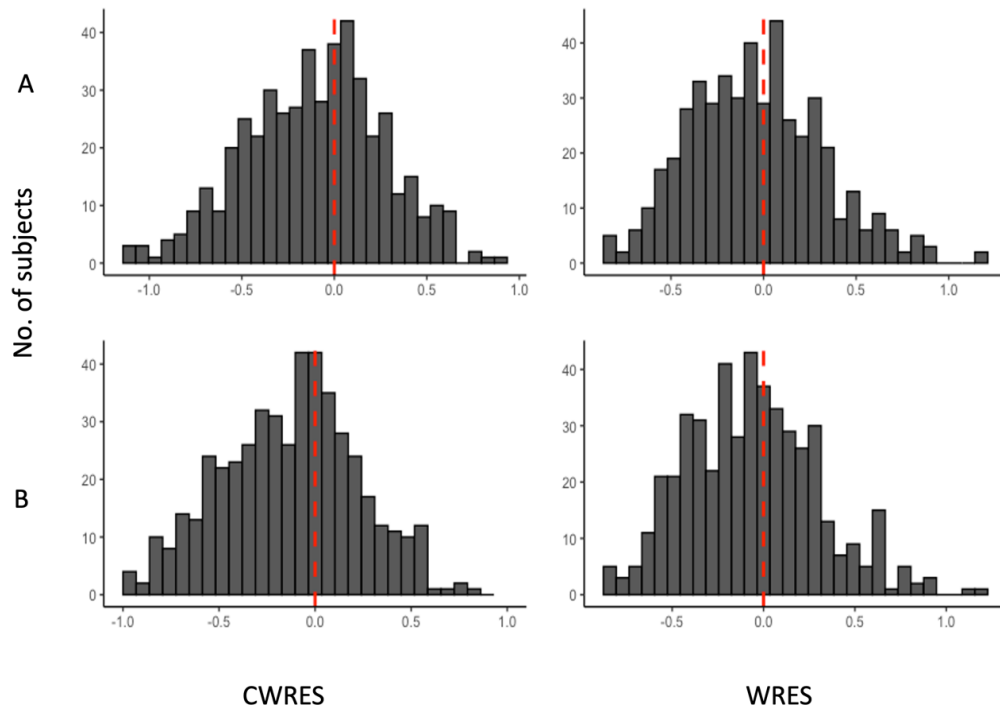


Figure C.2: Represent the average sum of residuals for scenario 2. Panel A represents the SUBSET model, and panel B represents the M3 method.

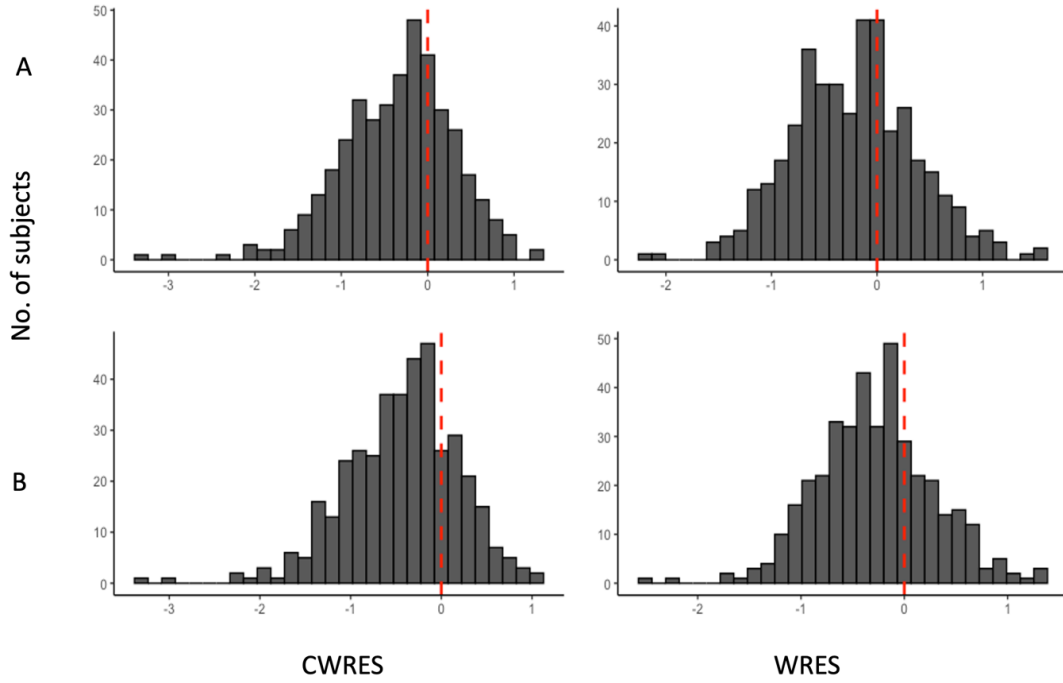


Figure C.3: Average deviation bias evaluation by individual; Scenario 1

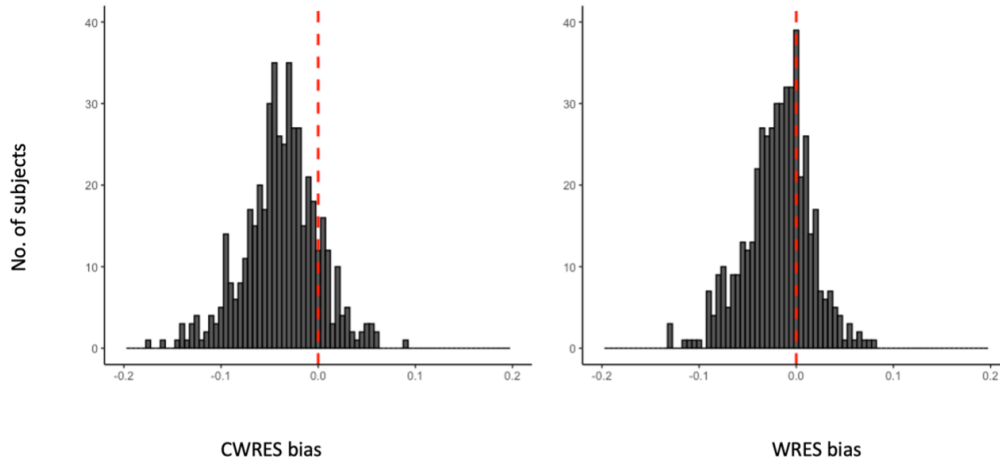
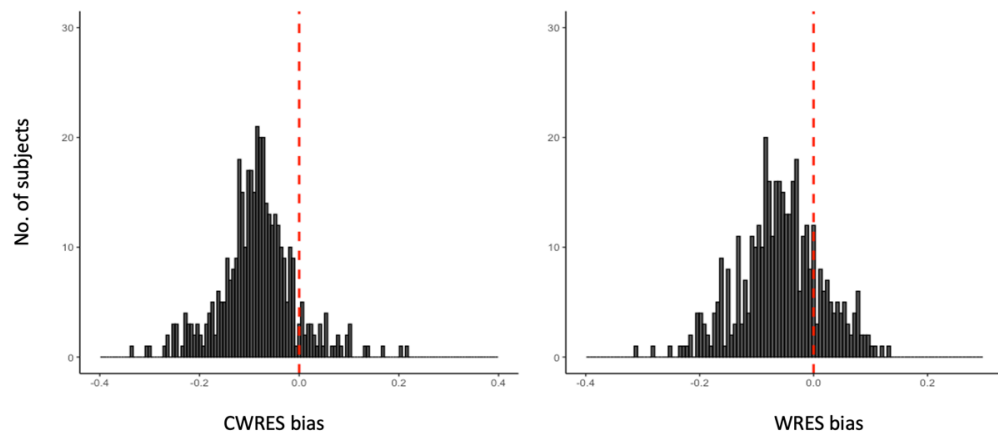


Figure C.4: Average deviation bias evaluation by individual; Scenario 2



```

[ PROB ]
Simulation for a one compartment model
Intensive sampling
[ SET ] end = 12, delta=0.1

[CMT] GUT CENT

[ PARAM ]
TVCL = 8 // CLEARANCE (L/HR)
TVV  = 25 // VOLUME (L)
TVKA = 1.5 // RATE CONSTANT (1/HR)
WT   = 70 // WT (KG)

[ MAIN ]

double CL = TVCL*pow((WT/70), 0.75) * exp(ETA(1));
double V  = TVV*pow((WT/70), 1) * exp(ETA(2));
double KA = TVKA * exp(ETA(3));

[ OMEGA ] 0.04 0.0625 0.09

[ SIGMA ] 0.0225

[ ODE ]

dxdt_GUT = -KA * GUT;
dxdt_CENT = KA * GUT - (CL/V)* CENT;

```

[TABLE]

```
double CP = (CENT/V) * (1 + EPS(1));
```

[CAPTURE] CP

Estimation script

```
$PROB original model - Scenario 1
$INPUT  C ID TIME DV AMT CMT MDV BLQ WT
$DATA blq.csv ignore=@
$SUB ADVAN2 TRANS2

$COV
$PK

TVCL = THETA(1)*(WT/70)**.75
CL   = TVCL * EXP(ETA(1))

TVV  = THETA(2)*(WT/70)
V    = TVV * EXP(ETA(2))

TVKA = THETA(3)
KA   = TVKA * EXP(ETA(3))

S2 = V
```

\$ERROR

PROP = THETA(4)*F

W = SQRT(PROP*PROP)

Y = F + W*ERR(1)

IPRE = F

\$THETA (0, 5) ; [CL]

(0, 21) ; [V]

(0, 1.5) ; [KA]

(0, 0.1) ; [Prop SD]

\$OMEGA 0.1 ; [BSV CL]

0.1 ; [BSV V]

0.1 ; [BSV KA]

\$SIGMA 1 FIX

\$EST METH=1 MAXEVAL=9999 NOABORT PRINT=5 INTER

Estimation 2

\$PROBLEM M3 model-Scenario 1

\$INPUT C ID TIME DV AMT CMT MDV BLQ WT

\$DATA blq.csv ignore=@

\$SUB ADVAN2 TRANS2

\$COV

\$PK

TVCL = THETA(1)*(WT/70)**.75

CL = TVCL * EXP(ETA(1))

TVV = THETA(2)*(WT/70)

V = TVV * EXP(ETA(2))

TVKA = THETA(3)

KA = TVKA * EXP(ETA(3))

S2 = V

\$ERROR

PROP = THETA(4)*F

W = SQRT(PROP*PROP)

LLOQ = 0.1

IF(BLQ.EQ.1) THEN

F_FLAG = 0

Y = F + W*ERR(1)

ELSE

F_FLAG = 1

Y = PHI((LLOQ - F)/W)

MDVRES = 1

ENDIF

IF(COMACT.EQ.1) PREDV = F

IPRE = F

```
$THETA (0,8.12796) ; [CL]
(0,25.0844) ; [V]
(0,1.4539) ; [KA]
(0,0.150632) ; [Prop SD]
$OMEGA 0.0388201 ; [BSV CL]
0.0680018 ; [BSV V]
0.0861074 ; [BSV KA]
$SIGMA 1 FIX
$EST METH=1 MAXEVAL=9999 LAPLACE NOABORT PRINT=5 INTER
```

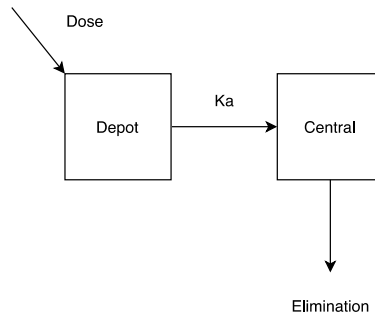
Appendix D

Individualized absorption models

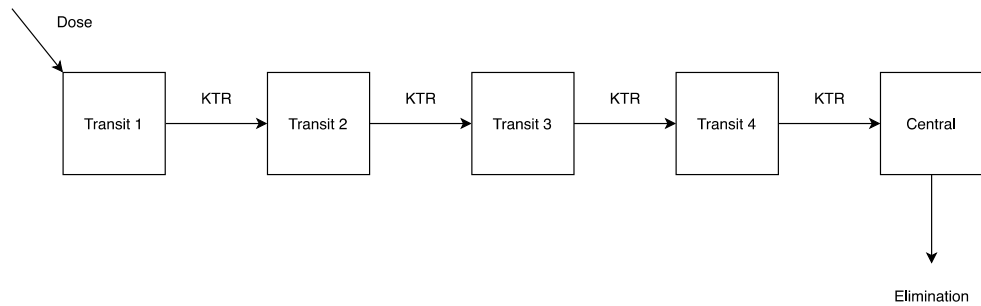
Figure D.1: structural Pharmacokinetic models; (a) First-order absorption; (b) Erlang distributive delay; and (c) shoulder models

Supplementary information (Figure S1)

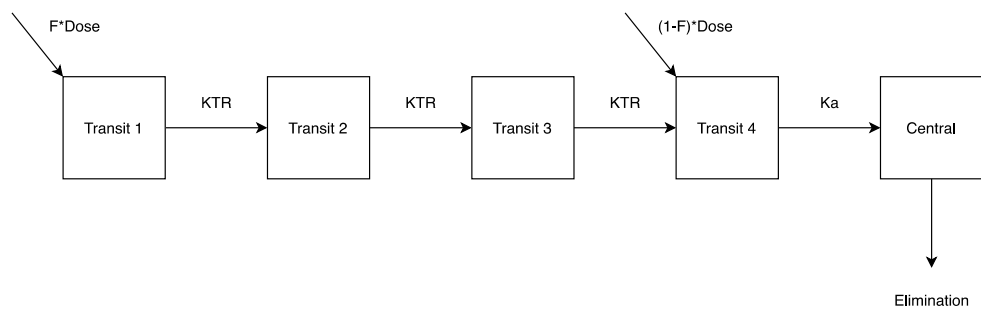
A. First order model



B. Erlang model



C. Shoulder model



Appendix E

Application of Deep Neural Networks in Pharmacokinetic Analysis

NONMEM code

```
$PROB Hydrocortisone PK
;; Individualized absorption model for Hydrocortisone
;; The model has 3 absorption shapes
;; Abs 1: First order
;; Abs 2: Erlang distribution
;; Abs 3: Mixed first/Erlang distribution
;; Author: Mutaz Jaber <jaber038@umn.edu>
$INPUT C ID TIME TAD AMT DV CMTD CMT MDV MDV17 MDVD4 WT DX FLAG
$DATA data.csv
$SUBR ADVAN13 TOL12
$EST  METH=1 NOABORT PRINT=5 INTER MAX=10000
$COVR  UNCOND
```

```

$MODEL  NCOMP=7

$PK

TVCL    =    LOG(THETA(1)) + .75*LOG(WT/70)

MU_1    =    TVCL

CL      =    EXP(MU_1 + ETA(1))

TVV     =    LOG(THETA(2)) + LOG(WT/70)

MU_2    =    TVV

V       =    EXP(MU_2 + ETA(2))

TVKA    =    LOG(THETA(3))

IF(FLAG==3) TVKA    = LOG(THETA(4))

MU_3    =    TVKA

KA      =    EXP(MU_3 + ETA(3))

TVKTR   =    LOG(THETA(5))

IF(FLAG==3) TVKTR   = LOG(THETA(6))

MU_4    =    TVKTR

KTR     =    EXP(MU_4 + ETA(4))

FR      =    1

IF(FLAG==3) THEN

    TVF    =    THETA(7)

    LGT    =    LOG(TVF/(1-TVF))

    FR     =    EXP(LGT+ETA(7))/(1 + EXP(LGT+ETA(7)))

    F1     =    FR

    F5     =    1 - FR

ENDIF

IF(FLAG==2) F1 = 1

IF(FLAG==1) F5 = 1

```

```

IF(DX==1) THEN
    TVCORT = LOG(THETA(8)) + 0.75*LOG(WT/70)
ELSE
    TVCORT = LOG(THETA(9)) + 0.75*LOG(WT/70)
ENDIF
MU_6      = TVCORT
CORT_IN   = EXP(MU_6 + ETA(6))
TVIC50    = LOG(THETA(10))
MU_5      = TVIC50
IC50      = EXP(MU_5 + ETA(5))
GAM       = 3
KEL       = CL/V
S2        = V/100
;; Fourier coefficient
A0        = 1.311
A1        = 0.35
A2        = 0.004036
B1        = 0.2445
B2        = -0.04736
KELA     = 0.2467
PI       = 3.141592653
A00      = A0*KELA
A01      = A1*KELA + (B1*2*PI/24)
A02      = A2*KELA + (B2*2*PI/12)
B01      = B1*KELA - (A1*2*PI/24)
B02      = B2*KELA - (B2*2*PI/12)

```

```

$DES
N1      =   A01*COS(2*PI*T/24) + B01*SIN(2*PI*T/24)
N2      =   A02*COS(2*PI*T/12) + B02*SIN(2*PI*T/12)
R_IN    =   A00 + N1 + N2
IF(R_IN <= 0) R_IN = 1E-5
CC      =   A(2)/S2
IF(CC <= 0) CC = 1E-5
EFF     =   CC**GAM/(CC**GAM + IC50**GAM)
INH     =   R_IN*(1-EFF)
DADT(1) =   -KTR * A(1)
DADT(2) =   KA*A(5) + KTR*A(6) - KEL * A(2)
DADT(3) =   KTR * (A(1) - A(3))
DADT(4) =   KTR * (A(3) - A(4))
DADT(6) =   KTR * (A(4) - A(6))
DADT(5) =   -KA * A(5)
DADT(7) =   CORT_IN*INH - KEL*A(7)
$ERROR
IPRE    =   A(2)/S2 + A(7)
Y       =   IPRE *(1+EPS(1)) + EPS(2)
$THETA
(0, 22.6) ; CL
(0, 38.8) ; V
(0, 3.31) ; KA F
(0, 7.6)  ; KA S
(0, 8.17) ; KTR E
(0, 5.2) ; KTR S
(0, 0.7, 1) ; F

```

(0, 1.15) ; CORT SW

(0, 3.26) ; CORT SV

(0, 1.55) ; IC50

\$OMEGA

0.184 ; IIV CL

0.441 ; IIV V

0.237 ; IIV KA

0.05 ; IIV KTR

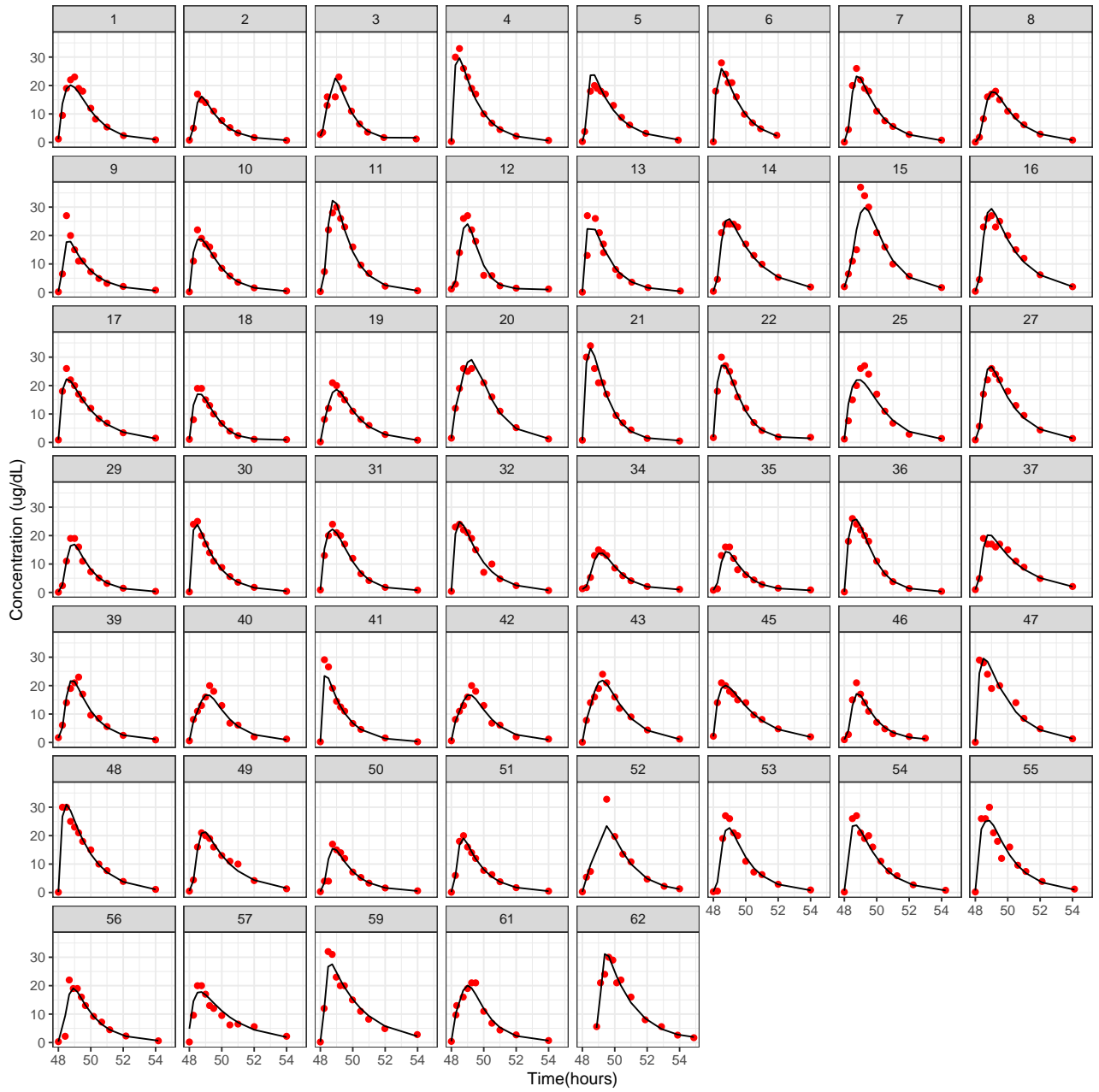
0.1 ; IIV IC50

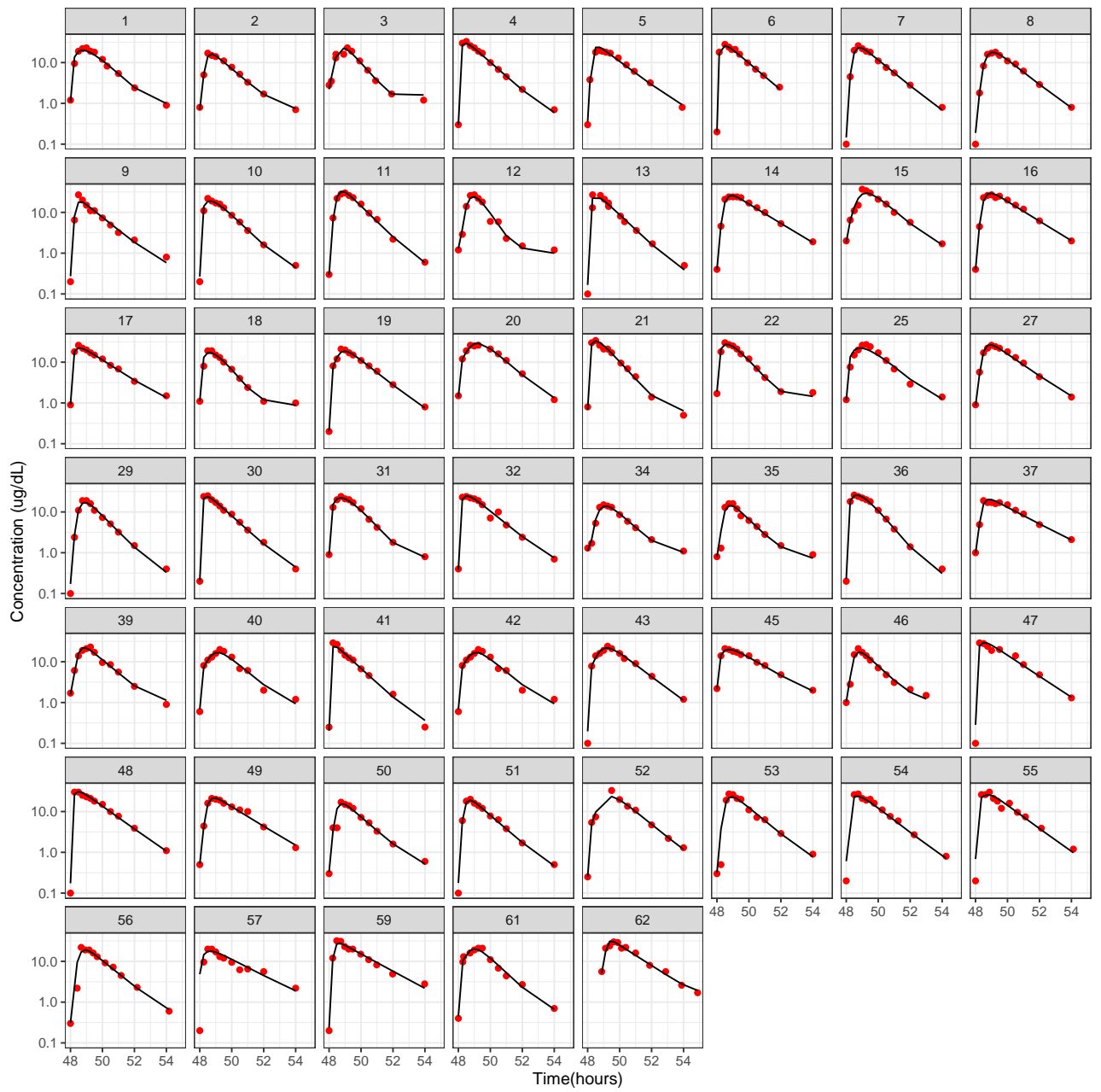
0.98 ; CORT IN

0.7 ; F

\$SIGMA 0.027 0.015

Individual Prediction





R code for creating model

```
# DNN algorithm

library(tensorflow)
library(keras)
library(tidyverse)
library(splitstackshape)

# dt is the simulated data
# df is the real data

class_df <- df %>%
  filter(TAD==0) %>%
  select(ABS0) %>%
  as_vector() %>%
  unname()

df_norm <- df %>%
  group_by(id) %>%
  summarise(MIN=min(DV),
            MAX=max(DV),
            DVN = (DV-MIN)/(MAX-MIN)) %>%
  ungroup()
```

```

class_df <- if_else(class_df==1, 0, if_else(class_df==2, 1, 2))

lc <- list()

for (i in 1:62) {
  lc[[paste("subj",i)]] <- df_norm %>%
    filter(id==i) %>%
    select(DVN) %>%
    as_vector() %>%
    unname()
}

f <- function(data) {
  nCol <- max(vapply(data, length, 0))
  data <- lapply(data, function(row) c(row, rep(NA, nCol-length(row))))
  data <- matrix(unlist(data), nrow=length(data), ncol=nCol, byrow=TRUE)
  data.frame(data)
}

df_x$class <- class_df
df_x <- df_x[complete.cases(df_x),]

x_eval <- df_x %>% select(contains("X")) %>% as.matrix()

```

```

y_eval <- df_x %>% pull(class) %>% to_categorical(3)

x <- dt %>% select(contains("X")) %>% as.matrix()
y <- dt %>% pull(FLAG) %>% to_categorical(3)

DNN <- keras_model_sequential() %>%
  layer_dense(units = 12, activation = 'relu', input=12) %>%
  layer_dense(units = 64, activation = 'relu') %>%
  layer_dense(units = 24, activation = 'relu') %>%
  layer_dense(units = 3, activation = 'softmax')

DNN %>%
  compile(
  optimizer = "adam",
  loss = "categorical_crossentropy",
  metrics= c("accuracy"))

NN_TRAIN <- fit(DNN, x,y, validation.split=0.3, batch_size=32,epochs=100)

```